

การศึกษาการกำจัดอะลูมิเนียมของซีโอไลต์ Y

นางสาวชุตินา ทองเกษม

วิทยานิพนธ์นี้เป็นส่วนหนึ่งของการศึกษาตามหลักสูตรปริญญาวิทยาศาสตรมหาบัณฑิต
สาขาวิชาเคมี
มหาวิทยาลัยเทคโนโลยีสุรนารี
ปีการศึกษา 2549

DEALUMINATION STUDY OF ZEOLITE Y

Chutima Thongkasam

A Thesis Submitted in Partial Fulfillment of the Requirements for the

Degree of Master of Science in Chemistry

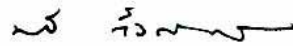
Suranaree University of Technology

Academic Year 2006

DEALUMINATION STUDY OF ZEOLITE Y

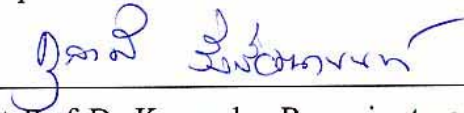
Suranaree University of Technology has approved this thesis submitted in partial fulfillment of the requirements for a Master's Degree.

Thesis Examining Committee



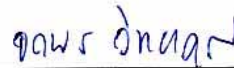
(Assoc. Prof. Dr. Malee Tangsathitkulchai)

Chairperson



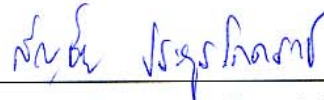
(Asst. Prof. Dr. Kunwadee Rangriwatananon)

Member (Thesis Advisor)



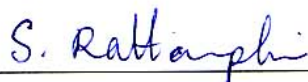
(Assoc. Prof. Dr. Jatuporn Wittayakun)

Member



(Dr. Sanchai Prayoonpokarach)

Member



(Assoc. Prof. Dr. Saowanee Rattanaphani)

Vice Rector for Academic Affairs



(Assoc. Prof. Dr. Sompong Thammathaworn)

Dean of Institute of Science

CHUTIMA THONGKASAM : DEALUMINATION STUDY OF ZEOLITE Y
THESIS ADVISOR : ASST. PROF. KUNWADEE RANGSRIWATANANON,
Ph.D. 122 PP.

ZEOLITE Y/DEALUMINATION/HYDROCHLORIC/AMMONIUM
HEXAFLUOROSILICATE/SILICON TETRACHLORIDE/ION EXCHANGE

In this work, the study of modification of synthesized zeolite Y ($4.6\text{Na}_2\text{O}:\text{Al}_2\text{O}_3:10\text{SiO}_2:180\text{H}_2\text{O}$; Si/Al ratio = 3.7) by dealumination was examined. The factors affecting on each step of dealumination methods such as reaction temperature, time, concentration and type of reagents, cation and anion were investigated. The comparison between different dealumination methods of hydrochloric (HCl), ammonium hexafluorosilicate (NH_4SiF_6) and silicon tetrachloride (SiCl_4) was also demonstrated. It was found that the ammonium hexafluorosilicate method produced the highest Si/Al mole ratio in the range of 5.2-11.3 and it remained the crystallinity about 99-21%. The Si/Al mole ratio could be increased with increasing $\text{NH}_4\text{SiF}_6/\text{NH}_4\text{OAc}$. The presence of ammonium acetate (NH_4OAc) was found to be necessary in the dealumination with NH_4SiF_6 , in order to remain high percentage of crystallinity. In addition, the Na form is suitable for dealumination with NH_4SiF_6 more than Li and K form. It may depend on cationic size. In the case of HCl dealumination method, which included the effect of Cl^- , the calcination temperature for removing NH_3 and HCl concentration, it gave Si/Al ratio about 3.9-4.4 and crystallinity about 64-16%. Moreover, the strong acid (HCl and HNO_3) was found to be more suitable for dealumination than weak acid (CH_3COOH). Under the studied

conditions, the result of SiCl_4 dealumination showed the amount of Si/Al ratio about 5.8 and crystallinity about 73%.

School of Chemistry

Academic Year 2006

Student's Signature _____

Advisor's Signature David R. ...

ACKNOWLEDGEMENTS

First, I would like to thank my advisor, Assistant Professor Dr. Kunwadee Rangsriwatananon, for her continuous support in the M.Sc. program. She was always there to listen and to give advice. She taught me how to ask questions and express my ideas. She showed me different ways to approach a research problem and the need to be persistent to accomplish any goal. I also thank all my thesis committee members Associate Professor Dr. Jatuporn Wittayakun and Dr. Sanchai Prayoonpokarach for their valuable and grateful direction, suggestion and criticism. My thanks go to the Chairman of School of Chemistry, Associate Professor Dr. Malee Tangsathitkulchai for serving as the chairperson of the committee and all lecturers at the School of Chemistry for their suggestions and encouragement. I would like to thank all the staffs at the Center of Scientific and Technological Equipment for their service and helpful suggestions. I wish to thank Zeolite's group and all my friends at the Suranaree University of Technology for their kindness and help. Also thanks to Mr. Thanakorn Pluangklang for understanding and encouragement.

I wish to express my special thanks to the Nakhon Ratchasima Rajabhat University for the main offering the scholarship during the course of this work, Institute of Research and Development at Suranaree University of Technology for the support on my thesis, Center for International Affairs (CIA) at Suranaree University of Technology for providing a visiting scholarship at the Mie University, Japan.

Last, but not least, I thank my family: my parents, Mali and Lamai Thongkasam, for their love, for giving my life in the first place, for educating me with aspects from both arts and sciences, for unconditional support and encouragement to pursue my interests, my sister and my brother, Supatra and Jackapong Thongkasam, for listening to my complaints and frustrations, and for believing in me. I would like to adore Buddha for my life guide though anywhere and time.

Chutima Thongkasam

CONTENTS

	Page
ABSTRACT IN THAI	I
ABSTRACT IN ENGLISH	II
ACKNOWLEDGEMENTS	III
CONTENTS	VI
LIST OF TABLES	X
LIST OF FIGURES	XII
LIST OF ABBREVIATIONS	XVI
CHAPTER	
I INTRODUCTION	1
1.1 Modifications and Formulation	6
1.1.1 Ion Exchange.....	6
1.1.2 Dealumination	9
1.2 Characterization techniques	10
1.2.1 Powder X-ray diffraction	10
1.2.2 Fourier transform infrared spectroscopy.....	11
1.2.3 Scanning electron microscope	12
1.2.4 Simultaneous thermogravimetry-differential thermal analysis.....	13
1.2.5 Brunauer-Emmett-Teller (BET)	14
1.2.6 Particle size analysis.....	15

CONTENTS (Continued)

	Page
1.2.7 Inductively coupled plasma mass spectrometry (ICP-MS).....	16
1.3 Research objectives	17
II LITERATURE REVIEWS	18
III MATERIALS, INSTRUMENTATION AND EXPERIMENTAL	
PROCEDURES	25
3.1 Material lists	25
3.1.1 Chemical and materials	25
3.1.2 Glasswares	26
3.1.3 Apparatus	27
3.2 Instrumentation	27
3.2.1 X-ray powder diffraction	27
3.2.2 Fourier transform infrared spectroscopy	28
3.2.3 Scanning electron microscope	29
3.2.4 Thermogravimetric analysis	29
3.2.5 Particle size analysis	30
3.2.6 Brunauer-Emmett-Teller (BET)	30
3.2.7 Inductively coupled plasma mass spectrometry (ICP-MS).....	30
3.3 Experimental methods	31
3.3.1 Sample preparation of zeolite Y	31
3.3.2 Study of the dealumination method	31

CONTENTS (Continued)

	Page
3.3.2.1 Dealumination by hydrochloric (HCl) method	31
3.3.2.2 Dealumination by ammonium hexafluorosilicate (NH ₄) ₂ SiF ₆ method	33
3.3.2.3 Dealumination by silicon tetrachloride (SiCl ₄) method	34
3.3.3 Effect of different exchangeable cations (Li ⁺ , Na ⁺ and K ⁺) and anions (Cl ⁻ and NO ₃ ⁻) on dealumination	37
3.3.4 Physical and chemical characterization of the dealuminated zeolite Y..	38
IV RESULTS AND DISCUSSION	40
4.1 Synthesis of zeolite NaY	40
4.2 Dealumination with HCl treatment	42
4.2.1 Effect of anions on NH ₄ ⁺ exchange processes	42
4.2.2 Effect of concentration of NH ₄ NO ₃	44
4.2.3 Effect of calcination temperature on transformation of NH ₄ Y to HY form.....	48
4.2.4 Effect of concentration of HCl, temperature and time on dealumination	52
4.2.5 Comparison between organic and inorganic acid affecting dealumination	62
4.3 Dealumination with ammonium hexafluorosilicate (AHFS) treatment	66

CONTENTS (Continued)

	Page
4.3.1 Effect of the presence and absence of NH_4OAc on dealumination with AHFS	66
4.3.2 Effect of AHFS and NH_4OAc concentration on AHFS dealumination.....	68
4.4 The effect of cation and anion on dealumination with ammonium hexafluorosilicate (AHFS).....	76
4.5 Dealumination with Silicon tetrachloride (SiCl_4) treatment	83
4.5.1 Effect of dehydration on SiCl_4 dealumination	84
4.5.2 Effect of concentration of SiCl_4 vapor and flowing N_2 on dealumination...	87
4.5.3 Effect of reaction temperatures on SiCl_4 dealumination	90
4.5.4 Effect of reaction times on SiCl_4 dealumination	91
V CONCLUSION	93
REFERENCES	96
APPENDICES	102
Appendix A Simulated XRD powder patterns for zeolites.....	103
Appendix B Atlas of zeolite structure types	110
Appendix C Adsorption Isotherms	113
Appendix D Particle size analysis	119
CURRICULUM VITAE	122

LIST OF TABLES

Table	Page
3.1 The dealumination of zeolite NaY by HCl treatment under various conditions.....	32
3.2 The dealumination of zeolite NaY by AHFS treatment under various conditions.....	33
3.3 The dealumination of zeolite NaY by SiCl ₄ treatment under various conditions.....	36
3.4 The effect of cation and anion on dealumination of zeolite NaY by AHFS treatment under various conditions.....	37
4.1 Wavenumbers of the zeolite NaY before and after the ion exchange with NH ₄ NO ₃ at various concentrations and followed with calcinations at 500°C for 6 hours.....	47
4.2 The wavenumbers of the HCl dealumination for zeolite Y at various concentrations of HCl.....	56
4.3 The amount of Si/Al ratio and percent crystallinity of dealuminated zeolite Y with HCl at various conditions.....	57
4.4 The average particle size of zeolite NaY before and after dealumination with HCl method.....	59
4.5 The dealumination of zeolite NaY by AHFS treatment under various conditions.....	67

LIST OF TABLES (Continued)

Table	Page
4.6 The wave numbers, %crystallinity and Si/Al mole ratio of zeolite Y with AHFS dealumination.....	71
4.7 The effect of mole ratio of cation:Na ⁺ on dealumination of zeolite NaY by AHFS treatment under various conditions	77
4.8 The wavenumbers of zeolite Y with AHFS dealumination.....	79
4.9 The surface area, micropore volume and pore size were recorded before and after different dealuminations.....	82
4.10 The amount of Si/Al ratio and percent crystallinity of dealuminated zeolite Y by the SiCl ₄ at various conditions.....	83
4.11 The %crystallinity and Si/Al mole ratio of dealuminated zeolite NaY with SiCl ₄ vapor depending on the concentration of SiCl ₄ and flowing N ₂	88
4.11 The %crystallinity and Si/Al mole ratio of dealuminated zeolite NaY with SiCl ₄ vapor depending on the flowing N ₂ after reaction for removing residual.	88
4.13 The %crystallinity and Si/Al mole ratio of dealuminated zeolite NaY with SiCl ₄ vapor depending on temperatures.....	90
4.14 The %crystallinity and Si/Al mole ratio of dealuminated zeolite NaY with SiCl ₄ vapor depending on reaction times	91

LIST OF FIGURES

Figure	Page
1.1 The structure of Zeolite Y	4
1.2 Potential initiation mechanism for acid dealumination.....	5
1.3 The mechanism for steam dealumination of a zeolite resulting in a silanol (hydroxyl) nest and Al(OH) ₃	5
1.4 The mechanism for dealumination by phosgene.....	6
4.1 XRD pattern of zeolite NaY.....	41
4.2 Morphology of the zeolite NaY.....	41
4.3 XRD patterns of synthesizedzeolite NaY (a) before and (b-c) after exchanging with (b) 1M NH ₄ NO ₃ , (c) 1M NH ₄ Cl	43
4.4 Percent crystallinity of zeolite NaY after ion exchanging with 1M NH ₄ NO ₃ and 1M NH ₄ Cl.....	44
4.5 XRD patterns of zeolite NaY (a) before and (b-d) after exchanging with different concentration of NH ₄ NO ₃ and followed calcination at 500°C for 6 hours. (b) exchanging with 1M NH ₄ NO ₃ ; (c) exchanging with 3M NH ₄ NO ₃ ; (d) exchanging with 7M NH ₄ NO ₃	45
4.6 IR spectra of zeolite NaY (a) before and (b-d) after exchanging with different concentration of NH ₄ NO ₃ and followed with calcination at 500°C for 6 hours. (b) exchanging with 1M NH ₄ NO ₃ ; (c) exchanging with 3M NH ₄ NO ₃ ; (d) exchanging with 7M NH ₄ NO ₃	46

LIST OF FIGURES (Continued)

Figure	Page
4.7	Relationship between the Si/Al ratio and concentration of NH_4NO_3 (M)47
4.8	Thermogram of NH_4NaY exchanged with 1M NH_4NO_349
4.9	Thermogram of NH_4NaY calcined at 500°C50
4.10	XRD patterns of synthesized zeolite NaY (a) before and (b-c) after exchanging with 1M NH_4NO_3 and followed with calcination at different temperatures for 6 hours. (b) calcination at 500°C ; (c) calcination at 650°C51
4.11	IR spectra of synthesized zeolite NaY (a); NH_4NaY calcined at 500°C (b) and NH_4NaY (c)52
4.12	XRD patterns of zeolite NaY (a) before and (b-f) after dealumination with HCl method. (b) Exchanging with 1M NH_4NO_3 and followed with calcination at 500°C for 6 hours (HY); (c) HY dealuminated at 0.01M HCl for 30 min; (d) 0.05M HCl; (e) 0.1M HCl; (f) 0.2M HCl.....53
4.13	XRD patterns of zeolite NaY (a) before and (b-f) after dealumination with HCl method. (b) Exchanging with 2M NH_4NO_3 and followed with calcination at 500°C for 6 hours (HY); (c) HY dealuminated at 0.1M HCl for 2 hours; (d) 0.2M HCl; (e) 0.3M HCl; (f) more than 0.3M HCl54
4.14	Plot of Si/Al ratio and HCl concentration.....58
4.15	Morphology of the zeolite NaY before (a) and after dealumination with HCl method (b)59

LIST OF FIGURES (Continued)

Figure	Page
4.16 Mechanism of dealumination of zeolite by HCl	61
4.17 IR spectra of zeolite NaY and dealuminated NaY with HCl	62
4.18 XRD patterns of HY dealuminated at various concentrations of acetic acid (CH ₃ COOH) at 60°C for 2 hours; (a) zeolite HY; (b) HY dealuminated at 0.1 M CH ₃ COOH; (c) 0.2 M CH ₃ COOH; (d) 0.3 M CH ₃ COOH	63
4.19 XRD patterns of HY dealuminated at various concentrations of nitric acid (HNO ₃) at 60°C for 2 hours. (a) zeolite HY; (b) HY dealuminated at 0.1 M HNO ₃ ; (c) 0.2 M HNO ₃ ; (d) 0.3 M HNO ₃	64
4.20 Plot of Si/Al ratio, %crystallinity and acid concentration	65
4.21 IR spectra of synthesized zeolite NaY (a) before and (b) after dealuminated of zeolite NaY with AHFS	70
4.22 Plot of Si/Al ratio and AHFS/NH ₄ OAc mole ratio	72
4.23 Plot of percent crystallinity and AHFS/NH ₄ OAc mole ratio	73
4.24 Relation of between %crystallinity and Si/Al ratio of dealuminated NaY by AHFS method	75
4.25 %crystallinity related to with Si/Al ratio for dealuminated LiY and KY by AHFS	80
4.26 %crystallinity related to Si/Al ratio for dealumination of zeoliteY with AHFS and HCl, the effect of cation and anion on dealuminated zeoliteY by AHFS and ion exchange	81

LIST OF FIGURES (Continued)

Figure		Page
4.27	XRD patterns of NaY and dehydrated NaY at 200°C for 2 hours.....	85
4.28	XRD patterns of dealuminated NaY with SiCl ₄ (a) NaY dealuminated from hydrated zeolite NaY; (b) NaY dealuminated from dehydrated zeolite NaY.....	86
4.29	XRD patterns of dealumination of NaY with SiCl ₄ vapor.....	89

LIST OF ABBREVIATIONS

BET	Brunauer-Emmett-Teller
FT-IR	Fourier transforms infrared spectrophotometer
SEM	Scanning electron microscope
XRD	X-ray diffractometer
DTA	Differential Thermal analysis
TGA	Thermogravimetric analysis
ICP-MS	Inductively Coupled Plasma Mass Spectrometry
AHFS	Ammonium hexafluorosilicate
BBK	Barrer, Barri and Klinowski equation
°C	Degree celcius
Å	Angstrom
% T	Percent transmittance
cm ⁻¹	Per centimeter
MAS NMR	Magic-angle spin nuclear magnetic resonances
M	Molar
K	Degree Kelvin
kV	Kilovolt
mA	Milliampere
µm	Micrometer
g	Gram

LIST OF ABBREVIATIONS (Continued)

mg	Milligram
L	Liter
ML	Milliliter
min ⁻¹	Per minute
PMMA	Polymethyl metaacrylate
%cry	Percent crystallinity

CHAPTER I

INTRODUCTION

Zeolites are microporous crystalline solid with well-defined structures. Generally, they contain silicon, aluminium and oxygen in their framework and cations, water and other molecules within their pores. Many zeolites occur naturally as minerals, and are extensively mined in many parts of the world. Others are synthetic, and are made commercially for specific uses, or produced by research scientists trying to understand more about their chemistry (Breck, 1974). In 1756 the Swedish mineralogist, Cronstedt who discovered zeolites, named them for the Greek roots means “boiling stones” for their peculiar bubbling characteristic (Dryer, 1988; Cheetham and Day, 1992). Since that time, about 50 different natural species have been recognized, and at least 150 species have been synthesized in the laboratory. Zeolites consisting of three dimensional framework structure were composed of TO_4 tetrahedra where T = Si, Al (framework of $[SiO_4]^{4-}$ and $[AlO_4]^{5-}$ tetrahedra). Zeolites have the general chemical formula (Roland and Kleinschmit, 1998):



When formula (1.1) expression enclosed in the square brackets shows the composition of the anionic framework in the crystallographic unit cell M; represents the

nonframework metal cation; n is its charge; z is the number of water molecules per unit cell; x and y are the total number of tetrahedra per unit cell and the ratio y/x usually has values of 1 - 5. Formula (1.2) occurs frequently in the literature and unlike formula (1.1), where y' is 2 to 10, n is the cation (M) valence, and z' represents the water contained in the voids of the zeolite. The frameworks are open containing channels and cavities where cations and water molecules are located. Zeolites have an uniform pore size (0.3 nm to 1.0 nm), which is uniquely determined by the unit structure of the crystal. The various zeolite structures differ not only in the type and dimensionality of their pore systems, but also in the size of the pore apertures. Narrow-pore, medium-pore, and wide-pore zeolites have different pore apertures formed by rings of 8, 10 or 12 T atoms, corresponding to crystallographic diameters of 0.35 - 0.45, 0.45 - 0.60, and 0.60 - 0.80 nm, respectively (Breck, 1974). Zeolite Y was first synthesized in the sodium form in 1964 by Union Carbide. It exhibits the FAU (faujasite) structure shown in the Fig. 1.1. Zeolite Y was a 3-dimensional pore structure with pores running perpendicular to each other in the x , y , and z planes similar to LTA, and is made of secondary building units 4, 6, and 6-6. The pore diameter is large at 7.4\AA , since the aperture is defined by a 12 member oxygen ring, and leads into a larger cavity of diameter 12\AA . The cavity is surrounded by ten sodalite cages (truncated octahedral) connected on their hexagonal faces. The unit cell is cubic ($a = 24.7\text{\AA}$) with $Fd-3m$ symmetry. Zeolite Y has a void volume fraction of 0.48, with a Si/Al ratio of 2.43. It thermally decomposes at 793°C (Herrerros, www, 2001, Meier, www, 2001 and Bhatia, 1990). Zeolite Y, like zeolite X, is synthesized in a gelling process. Sources of alumina (sodium aluminate) and silica (sodium silicate) are mixed in alkaline (NaOH) aqueous solution to give a gel. The gel is then

usually heated to 70 - 300°C to crystallize the zeolite. The zeolite is present in Na⁺ form and can be converted to acid form through NH₄⁺ form before being converted to acidic form (Bhatia, 1990). The most important use of zeolite Y is as a cracking catalyst. It is used in acidic form in petroleum refinery catalytic cracking units to increase the yield of gasoline and diesel fuel from crude oil feedstock by cracking heavy paraffins into gasoline grade naphtha. Zeolite Y has superseded zeolite X in this use because it is both more active and more stable at high temperatures due to the higher Si/Al ratio. It is also used in the hydrocracking units as a platinum/palladium support to increase aromatic content of reformulated refinery products (Bhatia, 1990; Ribeiro *et al.*, 1984).

The removal of solvents, dioxins and elemental mercury from moist water-air and exhaust-gas streams by hydrophobic and high-silica zeolites such as dealuminated Y zeolite, is a relatively new field. Compared with other adsorbents, these materials have the advantage of high thermal capacity, catalytic activity, nonflammability and pronounced hydrophobic properties. Regeneration is possible even if the compounds adsorbed have high boiling points or can form polymers as the zeolite adsorbent can be treated at high temperatures. Moreover, they are structurally stable in the presence of acidic components, such as SO₂ and HCl in incineration off-gases (Dyer, 1998).

The catalytic and hydrophobic properties of zeolites are strongly influenced by the SiO₂/Al₂O₃ ratio, whose variation is a frequent goal of zeolite research, either through direct synthesis or through post-synthesis dealumination methods. Dealumination USY zeolites form the basis of most fluidized cracking catalysts, and highly dealuminated mordenite has also shown remarkable catalytic properties (Bartl and Hölderich, 2000).

The dealumination of the zeolitic framework is widely used for the production of high-silica or hydrophobic zeolites Y and different types of dealumination procedures have been applied in the past, such as treatment with steam at elevated temperatures, with SiCl_4 vapor at moderate temperature, with ammonium hexafluorosilicate (AHFS) and with chelating agents, such as ethylenediamine tetra acetic acid (EDTA), at relatively low temperatures (Triantafillidis, Vlessidis, and Evmirds, 2000). The different mechanisms of dealumination showed in the Figs. 1.2-1.4.

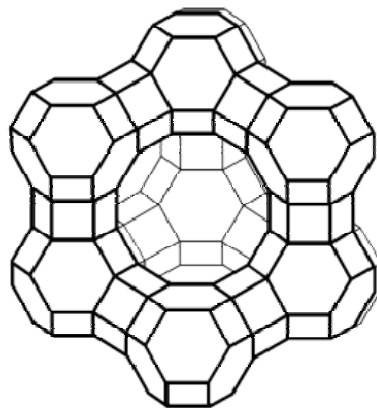


Figure 1.1 The structure of Zeolite Y. (Grey, Poshni, Gualtieri, Norby, Hanson, and Corbin, 1997).

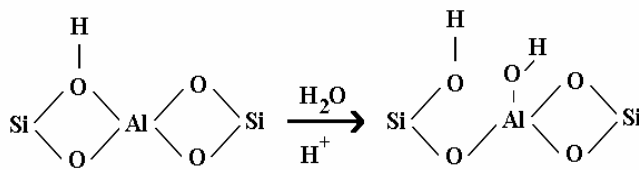


Figure 1.2 Potential initiation mechanism for acid dealumination.

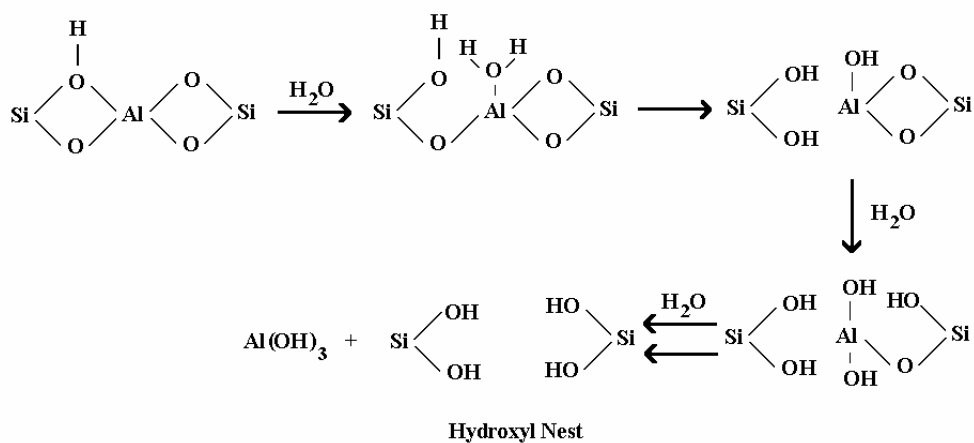


Figure 1.3 The mechanism for steam dealumination of a zeolite resulting in a silanol (hydroxyl) nest and $\text{Al}(\text{OH})_3$.

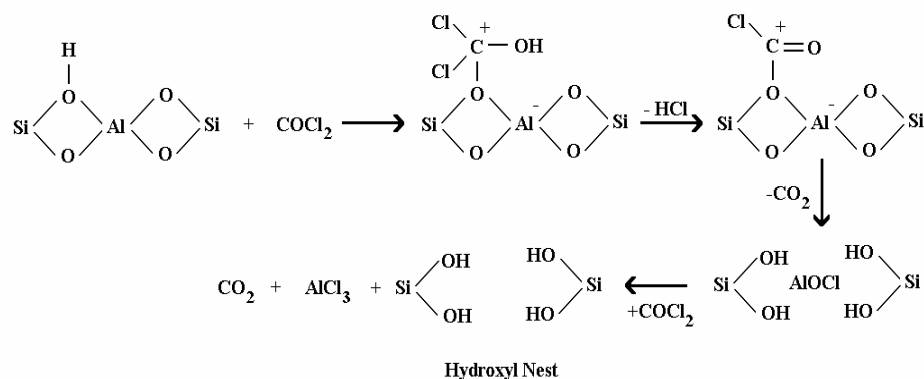


Figure 1.4 The mechanism for dealumination by phosgene.

1.1 Modifications and Formulation

For use as a catalyst or adsorbent, zeolite properties must be fine tuned. This is mainly performed by ion exchange and dealumination.

1.1.1 Ion Exchange

Zeolite has very attractive features to use as models for ion exchange because the silicon ion has a charge of +4 ($\text{Si}^{4+}/4\text{O}^-$) and aluminium +3 ($\text{Al}^{3+}/4\text{O}^-$). Therefore, a negative charge is in the aluminium atom, the number of Na^+ ions required for charge equalization is equal to the number of aluminium ions (Farrauto, 1997). The AlO_4^- tetrahedral in the structure determines the framework charge. This is balanced by cations (for instance, K^+ , Ca^{2+} or NH_4^+) that occupy nonframework positions (Szostak, 1998). The regularity and openness of zeolitic structures confers properties that have become of considerable industrial and fundamental research interest. Zeolite also has the ability to exchange cations, which are positively charged ions. This substitution of ions enables zeolites to selectively adsorb certain harmful or unwanted elements from soil, water and air, for example, zeolite exchanges sodium

ions for calcium ions, which results in soft water. Zeolite also has a strong affinity for certain harmful heavy metals such as mercury, lead and chromium (Bell, www, 2001).

The maximum ion exchange capacity is determined by the framework Si/Al ratio, although the actual capacity may be lower if a proportion of the cations are sited within small, inaccessible cages (Cheetham and Day, 1992). To simply represent the structure of ion exchange, the exchangeable cations are placed near AlO_4^- tetrahedra, because the negative charges are predominantly located there.

The selectivity factors of ion exchange may be dependent on framework topology, ion size, shape, charge density on anionic framework, and ion valency and electrolyte concentration in the aqueous phase.

Framework topology, ion size and shape often determine whether a given ion can fit readily into the framework and stability of the product. The more open zeolite structures are regularly observed in the thermodynamic affinity sequences (Vaughan, 1978). Most common ions will exchange readily into zeolites. However, the ion-sieving effect is observed with the zeolites having the smallest pore openings and with the largest cations.

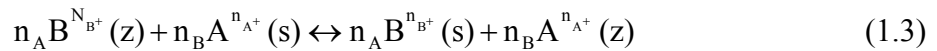
Charge density for both of synthetic and natural zeolites is possible to vary the $\text{SiO}_2:\text{Al}_2\text{O}_3$ ratio of a given framework. The higher $\text{SiO}_2:\text{Al}_2\text{O}_3$ ratio represents a large charge density which could affect the selectivity of the ion pair. For the exchange of a pair of ions between the alumina (high charge) and silica (low charge) forms of the given zeolite, the larger ion was preferred by the low charge form and the smaller ion was preferred by the high charge one (Vaghan, 1978).

The exchange process for the univalent ions, concentration of electrolyte has no large effect upon its selectivity. However, when the ions have different

charges, the situation becomes more complex. Selectivity is greater for the ion of higher valence in the dilute exchanging solution.

Zeolites have rigid, strong frameworks, stable at high temperatures, oxidation/reduction and ionizing radiation, not subject to physical attrition due to osmotic shock. The ion exchange properties of the zeolites are more constant and predictable over wide ranges of temperature and ionic strength than other ion exchanges. Zeolites are also stable at evaluated pH levels at which other inorganic ion exchange (Zirconium phosphates, etc) tend to lose functional group due to slow hydrolysis (Larsen and Vissers, 1960).

The ion exchange process can be represented by the following equation (Breck, 1974):



In general, the ion exchange reaction for two cations A and B with charges n_A and n_B is represented by this equation. The symbol (z) and (s) indicate whether the cation is in the zeolite phase or aqueous solution. The position of the equilibrium is a measure of the ion-exchange selectivity. The selectivity for given cations is determined by the electric fields of the coordinating anionic locations in the zeolite framework. Thus, for each zeolite type there is a specific selectivity series with the cations arranged in order of increasing exchangeability (Dyer, 1998).

In the production of zeolitic adsorbents, the most important techniques for increasing or decreasing the apparent pore diameter (pore-size engineering) are those involving ion exchange (Dyer, 1998).

Ion exchange is also important in the synthesis of zeolite catalysis. The aim is usually to produce Brønsted acid sites, as zeolites act as solid acids in catalysis. For certain intermediate-silica and high-silica zeolites, the necessary ion exchange can be achieved by treatment with mineral acids. Therefore, an indirect route via an ion exchange with ammonium salt solution must be followed. This produces the ammonium form, which is calcinations to liberate ammonia and give the hydrogen form. In the case of zeolite Y, an acid form is also obtained by incorporating polyvalent cations, especially of rare earth metals, by ion exchange.

In the most widely used ion-exchange process, zeolite is treated with aqueous solutions that contain the cation to be introduced. Solid-state ion exchange in which the zeolite, usually in the ammonium or hydrogen form, are heated with crystalline salts, is as yet rarely used in industry (Dyer, 1998). Ion exchange also occurs on impregnating zeolites with solutions of metal salts.

1.1.2 Dealumination

Dealumination increases the $\text{SiO}_2/\text{Al}_2\text{O}_3$ ratio of zeolites. The term is understood to mean the removal of aluminum from the zeolite framework, even where the overall composition of the material is unaltered or only slightly altered because the aluminum removed from the framework remains in the channels and cavities (Dyer, 1998).

Dealumination is mainly carried out on zeolites with an intermediate $\text{SiO}_2/\text{Al}_2\text{O}_3$ ratio that cannot be directly produced in a high-silica form and have sufficient stability to survive the sometimes drastic treatment without appreciable loss of crystallinity. The prototype for the development of dealumination methods was zeolite Y, as both its hydrothermal stability can be considerably increased and its

catalytic activity for use in FCC catalysts can be modified by dealumination. The catalytic properties of high-silica materials synthesized by dealumination are expected to differ from those of zeolites with the same $\text{SiO}_2/\text{Al}_2\text{O}_3$ ratio produced directly, as the dealumination of the structure can lead to the production of crystal defects, creation of a secondary pore system and formation of nonframework aluminum.

The simplest method is to extract aluminum with a mineral acid. This is often carried out with a mineral acid. Depending on the reactions conditions, a high-silica material with low cation content is obtained.

1.2 Characterization techniques

1.2.1 Powder X-ray diffraction

X-ray diffraction (XRD) is a powerful technique used to uniquely identify the crystalline phases present in materials and to measure the structural properties (strain state, grain size, phase composition, preferred orientation and defect structure) of these phases. The X-ray region is normally considered to be the part of the electromagnetic spectrum lying between 0.1 and 100 Å bounded by the X-ray region to the short-wavelength side and the vacuum ultraviolet region to the long-wavelength side. In terms of energy, the X-ray region covers the range from about 0.1 to 100 keV. An X-ray diffraction has been used in two main areas; the fingerprint characterization of crystalline materials and the determination of their structures. Each crystalline solid has its unique characteristic X-ray powder pattern, which may be used as a “fingerprint” for its identification. Once the material has been identified, an X-ray crystallography may be used to determine its structure, i.e. how the atoms packed together in the crystalline state and what the inter-atomic distance and angle

are. These unique properties make X-ray diffraction one of the most important characterization tools used in solid state chemistry and material science.

An important equation for X-ray diffraction is Bragg's equation, which shows the relationship between X-ray wavelength (λ) with lattice point distance (d) and incident diffraction angle (θ).

$$n\lambda = 2d \sin\theta \quad (1.4)$$

The different crystal plane in the crystal will diffract X-ray at different angles according to the Bragg's equation. Therefore, by rotating the sample plane with respect to the incident X-ray, the diffracted angles can be recorded by a detector and the diffraction pattern is obtained. The identification of the sample structure can be done by comparing the spectrum with the pattern stored in the database.

1.2.2 Fourier transform infrared spectroscopy

Fourier transform infrared (FT-IR) spectroscopy is a characterization method about the infrared radiation, which is passed through a sample. FT-IR techniques may be used for qualitative observations or quantitative measurements if used in conjunction with the Beer-Lambert relationship. The atoms in a molecule constantly oscillate around average positions. Bond length and bond angles are continuously changed due to this vibration. A molecule absorbs on infrared radiation when the vibration of the atoms in the molecule produces an oscillating electric field with the same frequency as the incident IR radiation when they are in resonance. Each molecule has its own characteristic spectrum. The bands that appear depend on the types of bonds and the structure of the molecule. FT-IR spectroscopy measures

dominantly vibrations of functional groups and highly polar bonds. Thus, these chemical fingerprints are made up of the vibration features of all the sample components. FT-IR spectrometer records the interaction of the IR radiation with experimental samples, measuring the frequencies at which the sample absorbs the radiation and the intensities of the absorptions. Determining these frequencies allows the identification of the sample's chemical makeup, since chemical functional groups are known to absorb light at specific frequencies.

Samples may be prepared in a solid, liquid or gas form. The nature of the sample determines which technique should be used. A common sample preparation method includes: the salt pellet technique (sample powder is diluted in an IR-transparent salt like KBr); Nujol Mull method (sample powder is diluted in an IR-transparent oil); thin sample technique; attenuated total reflectance (the sample is sandwiched between two IR-transparent crystals); and diffuse reflectance infrared FT (optics focus beam on the top surface of the sample)

1.2.3 Scanning electron microscope

Scanning electron microscope (SEM) is a type of microscope that uses electrons rather than light to form an image. There are many advantages to use SEM instead of a light microscope. SEM has a large depth of field, which allows a large amount of sample to be in focus at one time. SEM also produces images of high resolution, which means that small spaced features can be examined at a high magnification. The preparation of samples is relatively easy since most SEM instruments only require the sample to be conductive. The combination of higher magnification, larger depth of focus, greater resolution and ease of sample

observation make SEM one of the most heavily used instruments in present-day research.

By using the wave-particle duality, SEM creates the magnified images by using electrons instead of light waves. The SEM shows very detailed 3-dimensional images at a much higher magnification than is possible with a light microscope. The images created without light waves are rendered black and white. By the nature of an electron beam, the vacuum is required during the operation; therefore, the sample has to be prepared carefully to withstand the vacuum inside the microscope. The samples must be a conductive material in order to be able to interact with an electron; SEM samples are coated with a very thin layer of gold by a machine called a sputter coater. The sample is placed inside the microscope's vacuum column through an airtight door. After the air is pumped out of the column, an electron gun emits a beam of high energy electrons. This beam travels downward through a series of magnetic lenses designed to focus the electrons to a very fine spot. Near the bottom, a set of scanning coils moves the focused beam back and forth across the specimen, row by row. As the electron beam hits each spot on the sample, the secondary electrons and the back scattered electrons are knocked loose from its surface. A detector counts these electrons and sends the signals to an amplifier. The final image is built up from the number of electrons emitted from each spot on the sample. By this way, the morphology of the sample can be seen directly from the micrograph.

1.2.4 Simultaneous thermogravimetry-differential thermal analysis

TGA and DTA have been the two most common techniques for thermal analysis for many years. TG is a technique in which a change in the weight of a

substance is recorded as a function of temperature or time. DTA measures the temperature difference between a substance and a reference material as a function of temperature whilst the substance and reference are subjected to a controlled temperature program. Simultaneous thermal analysis (STA) techniques are two or more types of measurement, which are made at the same time on a single sample. Modern TG-DTA instruments are capable in general of a TG resolution of around 1 μg , using samples typically from 5 mg to 100 mg, which can give sensitive and quantitative DTA performance when the head is of the appropriate type i.e. there is a heat flow link between sample and reference (Haines, 2002).

1.2.5 Brunauer-Emmett-Teller (BET)

In 1938, The first developed the BET theory for a flat surface and there is no limit in the number of layers that can be accommodated on the surface. The surface is energetically homogeneous (adsorption energy does not change with the progress of adsorption in the same layer) and there is no interaction among adsorbed molecules.

$$\frac{V}{V_m} = \frac{1}{(1 - P/P_0)} \quad (1.5)$$

Equation 1.5 is the famous BET equation, and it is used extensively for the determination of area because once the monolayer coverage V_m is known and if the area occupied by one molecule is known the surface area of the solid can be calculated. To conveniently determine V_m , the BET equation can be cast into the form, which is amenable for a linear plot as follows:

$$\frac{P}{V(P_0 - P)} = \frac{1}{V_m C} + \left(\frac{C-1}{V_m C}\right) \frac{P}{P_0} \quad (1.6)$$

The pressure range of validity of the BET equation is $P/P_0 = 0.05-0.3$. For relative pressures above 0.3, there exists capillary condensation, which is not amenable to multilayer analysis. A plot of $(P/(V(P_0-P)))$ versus P/P_0 would yield a straight line with a slope $((C-1)/CV_m)$ and an intercept $(1/CV_m)$. Usually the value of C is very large because the adsorption energy of the first layer is larger than the heat of liquid fraction, the slope is then simply the inverse of the monolayer coverage, and the intercept is effectively the origin of such plot. Therefore, very often only one point is sufficient for the first estimate of the surface area.

Once V_m (mole/g) is obtained from the slope, the surface area is calculated from:

$$A = V_m N_A a_m \quad (1.7)$$

Where N_A is the Avogadro number and a_m is the molecular project area (nitrogen = $16 \text{ \AA}^2/\text{molecule}$ at 77 K) (Do, 1998).

1.2.6 Partical size analysis

In recent years particle sizing using the laser diffraction techniques has become the dominant method of choice. Laser diffraction units do not measure particle size distributions but carry out light scattering experiments. The relationship between the light scattered by the particles and the final particle size distribution

reported depends critically upon assumptions made about the optical properties of the material under study. While the previous sentences are statements of the obvious, misleading results continue to be published due to the potential influence of time pressure, psychology and lack of formal training in optics.

Laser diffraction instruments usually report the volume (rather than the number) of particles that have a given size because the light scattering signal is proportional to D^2 . Discriminating the tiny scattering pattern from a single small particle in the presence of the huge scattering signal from a single large particle is very difficult. If enough small particles are present to equal the volume of the single large particle the scattering of the small particles can be discriminated (separated out) and analyzed. This is why laser diffraction units usually report the volume of particles in each size class.

Calculations using Mie theory require an input of the following parameters: wavelength of illumination, the polarisation state of the illumination, the refractive index both real and imaginary of both particle and the medium, the diameter of the particle, the angle of observation relative to the incident illumination (In both azimuthal planes).

The output value returned is the intensity of the scattered light from a single spherical particle viewed at the selected angle from the incident illumination. For each diameter the scattered intensity may be divided by the cube of the diameter to give the scattering intensity per unit volumes of particles for that diameter.

1.2.7 Inductively Coupled Plasma Mass Spectrometry (ICP-MS)

It is a very powerful tool for *trace* (ppb-ppm) and *ultra-trace* (ppq-ppb) elemental analysis. ICP-MS is rapidly becoming the technique of choice in many

analytical laboratories for the accurate and precise measurements needed for today's demanding applications.

In ICP-MS, a plasma or gas consisting of ions, electrons and neutral particles is formed from Argon gas. The plasma is used to atomize and ionize the elements in a sample. The resulting ions are then passed through a series of apertures (cones) into the high vacuum mass analyzer. The isotopes of the elements are identified by their mass-to-charge ratio (m/e) and the intensity of a specific peak in the mass spectrum is proportional to the amount of that isotope (element) in the original sample.

1.3 Research objectives

1. To prepare zeolite Y with different ratio of Si/Al by using dealumination methods.
2. To characterize physical and chemical properties of the dealuminated zeolite Y samples.
3. To compare the results from the different dealumination methods.
4. To study the effect of others cations (Li^+ and K^+) in zeolite Y on the dealumination.

CHAPTER II

LITERATURE REVIEWS

The dealumination is assumed to mean that tetrahedral Al leaves the silicon-aluminium-oxygen framework. It is very important to increase the Si/Al ratio for changes in the properties of the zeolite, for example the thermal stability adsorption and catalytic properties. So the dealumination of zeolite in different types of dealumination procedures is interesting.

In the past, it studied dealumination zeolite with acid solutions. Barrer and Makki (1964) were the first to observe that after treatment of the Na-form of clinoptilolite with HCl solutions at 100°C the, $\text{SiO}_2/\text{Al}_2\text{O}_3$ ratio is increased with increasing in the acid concentration. The dealumination products remain crystalline. Losses in crystallinity are shown as a certain decrease in the intensity of the lines on the X-ray patterns, observed only after removing 65% of the Al from the crystals. It was show that crystals of erionite (Zhdanov and Novikov, 1966) and mordenite (Belenkaya and Dubinin, 1967) could be dealuminated to different degree of dealumination by treatment with HCl solution. In the case of erionite it was noted that the positions and intensities of all the main lines on the X-ray diffraction patterns were unaltered for a specimen dealuminated by 40%, while highly dealuminated specimens of mordenite kept their crystallinity. In addition, Bronsted and Lewis acid sites in dealuminated ZSM-12 and β zeolite were researched by Zhang *et al.* (2000).

Dealumination of zeolites was treated with different concentrations of HCl at 90°C for 4 hours. The bulk Si/Al ratio was determined with inductively-coupled plasma (ICP) spectroscopy, Fourier transforms infrared spectrophotometer (FT-IR) and Magic-angle-spinning nuclear magnetic resonance (MAS NMR), and also NH₃-Stepwise Temperature-Program Desorption (STPD) was used for characterization of acid sites in zeolites. It was found that, the aluminum of ZSM-12 remains as the framework species and ZSM-12 high level of crystallinity even under severe dealumination conditions (5N HCl). In addition, the increase of extent of dealumination results in an increase of the acid strength in the case of β zeolite but a decrease of the acid strength for ZSM-12. Strong organic acid has been shown to be also reliable dealumination agents; however, treatments with these acids generally result in a significant loss of crystallinity. Some of the structural degradation can be prevented through the addition of structure directing agents during dealumination process. Shitinskaya *et al.* (1971) and Ermolenko *et al.* (1984) showed that significant dealumination of synthetic L zeolites and erionite can be achieved also by repeated treatment of the crystals with solutions of organic acids (benzoic, o- and m-nitrobenzoic, anthranilic, and salicylic). In specific cases (in fivefold treatment with salicylic acid and o-nitrobenzoic acid) the degree of dealumination was as much as 70 - 80% for L zeolites and 53 - 68% for erionite. In contrast to this, according to Belenkaya *et al.* (1967), mordenite was dealuminated only slightly, even after fivefold treatment with 1.5 - 3.0 N acids. It was found that, the degree of dealuminations was not greater than 1%, while the decationation reached a value of 64 - 75%.

Chelating agents are essentially any compound that can be used to remove aluminum atom from zeolite framework. They act as a ligands to a metal ion. Dealumination occurs by strongly coordinating with the aluminum in the framework, while acidity breaks the framework bonds. Kerr (1967) showed that Y zeolites dealuminated to different extents could be obtained by treatment of the Na form with specific amounts of a diluted solution of ethylenediaminetetraacetic acid (H₄-EDTA). The zeolites dealuminated by this reagent are much more heat resistant than the original Na form. The X-ray powder patterns show that the specimen crystallinity is retained even after removal of about 50% of the Al from the crystals and also the Na bonded to it. It can be seen that the proportion of Al removed from the crystals corresponds to the ratio of the number of gram moles of EDTA used to the number of gram atoms of Al in a weighed quantity of zeolite. It is important to note that, if the crystals are heated with specific quantities of EDTA, dealumination and decationation occur to an almost equivalent extent, and the degree of dealumination can be controlled easily by changing the ratio of the weighed quantity of zeolite to the quantity of EDTA.

Another common technique for the removal of aluminum eliminates the washing step by creating volatile aluminum compounds that can be removed from the zeolite. A number of compounds result in volatile aluminum species upon contact with a zeolite and a good summary of these can be found in Fejes *et al.* (1980). They discuss several cases of dealumination of zeolites, which were carried out by chemical treatment with several reagents (COCl₂, SOCl₂, NOCl, PCl₅, etc.), which were not use previously. Dealumination of the H-form of mordenite by treatment with these

reagents is accompanied by the removal of HCl and other volatile products. The dealumination takes place with the formation of intermediate surface compounds, which decompose during the final stages of the process. The reagents allow the possible appearance and existence of empty sites (empty nests) after Al leaves the framework when the zeolites are heated chemically. The accumulation of such nests in the framework destabilizes the structure and can lead to destruction of the framework structure. In treatment of the H-form of mordenite with PCl_5 , under specific conditions P atoms can be introduced into the Al vacancies and tetrahedral $[\text{PO}_2^+]$ formed in the frameworks of the dealuminated zeolites. The degree of dealumination of H-mordenite attained by treatment with COCl_2 over the temperature range 673-1073 K is significantly higher at all temperatures than that of Na-mordenite under the same conditions. Fejes *et al.* (1980) did not state what other zeolite apart from the H- and Na- mordenites were dealuminated in this work. However, they do state that in the case of H- mordenite the degree of dealumination can reach a level of 96% by treatment with COCl_2 without any significant loss in crystallinity.

Fluorosilicate salts such as ammonium fluorosilicate, $(\text{NH}_4)_2\text{SiF}_6$, have been shown to efficiently remove aluminum from the framework of zeolites through the formation of AlF_3 . Holmberg *et al.* (2004) attempted to produce acid resistant zeolite Y nanocrystals by both dealumination with ammonium hexafluorosilicate (AHFS) and by direct synthesis with lowered OH^- concentrations. As synthesized zeolite Y nanocrystals were found to be stable in acidic environments with pH greater than or equal to 3. Dealumination of zeolite Y nanocrystals with ammonium hexafluorosilicate did not increase the acid stability of the nanocrystals. Kao and

Chen (2003) interested the nature and type of aluminum fluoro-complexes, which were formed during the dealumination process, by using ^{27}Al and ^{19}F solid-state NMR in attempted to gain more insight into the dealumination mechanisms induced by AHFS. Dealumination of H- β zeolite by AHFS was carried out by Skeels and Breck (1983). After AHFS dealumination, extra framework aluminum species were predominating created in octahedral form. Complementary characterization with ^{19}F and ^{27}Al MAS NMR allows the detection of different dealumination processes, and thus provides a better insight into the dealumination mechanism.

In general, inorganic halides and oxyhalides in general are easily volatilized. The vapor of the halide or oxyhalide can be easily brought into contact with a zeolite, and it forms the more stable compounds and volatile dealuminum halide (Al_2Cl_6 , in the case of chloride reactants) which is continually removed from the zeolite via heat and carrier gas. This has been described by various authors (Beyer *et al.*, 1980; Fejes *et al.*, 1980; Lok *et al.*, 1982). The chemical basis of the method described by Beyer *et al.* (1980) is the interaction of the Al sites of the zeolite framework with SiCl_4 on heating. As noted by Bayer *et al.* (1980) the most convenient zeolite for dealumination by this method is Y zeolite. The reaction of the zeolite with SiCl_4 vapors must precede its dehydration at a temperature around 650 K in a current of dry nitrogen over 2 hs. The thickness of the layer of previously dehydrated zeolite in the quartz reactor should be about 3 cm. After dehydration under these conditions the nitrogen in the stream is saturated at room temperature with SiCl_4 vapors, and contact between the zeolite and SiCl_4 vapors is achieved at a constant and relatively slow rate of temperature increase in the reactor of 4 Kmin^{-1} to 730 - 830°C.

Treatment is kept up for 2 hours over this range of final temperatures. Dry nitrogen was then blown over the zeolite, followed by washing with water to complete extraction of the chlorides, and drying at about 400 K. After this treatment the Si/Al in the zeolite framework can be increased to high silica zeolite while retaining a high degree of crystallinity in the products. The degree of dealumination depends on the duration of the reaction and the final treatment temperature. The important factors for maintaining the crystalline structure of the dealuminated Y zeolites obtained by this method are the temperature of preliminary dehydration, the thickness of the layer of zeolite powder in the reactor, and the rate of temperature increase in the initial stages of reaction between the dehydrated zeolite and SiCl_4 are.

In addition, Bartl and Hölderich (2000) studied the dealumination methods for zeolite L with different method, such as treatment with SiCl_4 vapor, steam and $(\text{NH}_4)_2\text{SiF}_6$. The zeolite samples were characterized by FTIR, XRD, BET, ICP, and MAS. The effects of dealumination were measured by the change in the bulk of $\text{SiO}_2/\text{Al}_2\text{O}_3$ molar ratio and the shift in the wave numbers of the FTIR bands, especially the external symmetric stretch and the double-ring vibration. Shifts to higher wave numbers indicate the increase $\text{SiO}_2/\text{Al}_2\text{O}_2$ ratio in the framework. It has confirmed the limitations of dealumination of zeolite L through streaming and treatment with $(\text{NH}_4)_2\text{SiF}_6$. Treatment with SiCl_4 vapor is the method which delivers the highest degree of dealumination of zeolite L.

As mentioned earlier, many researchers have conducted the researches on the different dealumination methods of different zeolites. Some of them were investigated and prepared to be high silica-zeolites and also applied them in different purposes.

However, zeolite Y has gained more attention from the chemical industries. It has been used as catalysts and adsorbents. Therefore, an effort to increase adsorption capability of zeolite Y is of interest necessary. It is known that hydrophobicity or hydrophilicity of zeolite is dependent strongly on Si/Al ratio in the framework. Hence the purpose of this work is to prepare zeolites Y with varied Si/Al ratios through different dealumination procedures by removing different fractions of Al atoms in their frameworks. The treated samples are characterized by Powder X-ray diffractometer (XRD), Fourier transform infrared spectrophotometer (FT-IR), scanning electron microscopy (SEM) and differential thermal analyzer (DTA). As well as their surface areas and particle sizes are determined by Surface area analyzer (BET) and laser particle analyzer, respectively. Furthermore, the contents of silicon and aluminium after treatment are determined by inductively-coupled plasma-mass spectroscopy (ICP-MS).

CHAPTER III

MATERIALS, INSTRUMENTATION AND EXPERIMENTAL PROCEDURES

3.1. Material lists

3.1.1 Chemical and materials

- (a) Sodium silicate (Na_2SiO_3), Analytical reagent, Riedel-de Haën, Germany
- (b) Sodium aluminate (NaAl_2O_3), Analytical reagent, Riedel-de Haën,
Germany
- (c) Anhydrous sodium hydroxide pellets (NaOH), Analytical reagent, Merck,
Germany
- (d) Ammonium chloride (NH_4Cl), Analytical reagent, Fisher Scientific, UK
- (e) Ammonium nitrate (NH_4NO_3), Analytical reagent, Fisher Scientific, UK
- (f) Lithium chloride (LiCl), Analytical reagent, APS Ajax Finechem,
Australia
- (g) Lithium nitrate (LiNO_3), Analytical reagent, HIMEDIA, India
- (h) Sodium chloride (NaCl), Analytical reagent, Merck, Germany
- (i) Sodium Nitrate (NaNO_3), Analytical reagent, APS Ajax Finechem,
Australia
- (j) Potassium chloride (KCl), Analytical reagent, APS Ajax Finechem,
Australia

- (k) Potassium nitrate (KNO_3), Analytical reagent, APS Ajax Finechem, Australia
- (l) Hydrochloric acid 37% (HCl), Analytical reagent, Merck, Germany
- (m) Nitric acid 65% (HNO_3), Analytical reagent, BDH, UK
- (n) Acetic acid (CH_3COOH), Analytical reagent, BDH, UK
- (o) Ammonium acetate (NH_4OAc), Analytical reagent, BDH, UK
- (p) Ammonium hexafluorosilicate ($(\text{NH}_4)_2\text{SiF}_6$), Analytical reagent, Aldrich, USA
- (q) Silicon tetrachloride (SiCl_4), Analytical reagent, Riedel-de Haën, Germany
- (r) Hydrofluoric acid (HF), Analytical reagent, BDH, UK
- (s) Boric acid (H_3BO_4), 99.8%, Analytical reagent, APS Ajax Finechem, Australia
- (t) Potassium bromide (KBr), Analytical reagent, Merck, Germany

3.1.2 Glasswares

- (a) Watch glass
- (b) Utility clamp
- (c) Glass stirring rod
- (d) Breakers 50, 100, 250, 500, 1000 mL
- (e) Erlenmeyer flasks 125, 500 mL
- (f) Volumetric flasks 50, 100, 250, 500, 1000, 2000 mL
- (g) Mortar and pestle
- (h) Round bottom flask 250 mL
- (i) Condenser for reflux procedure
- (j) Porcelain crucible

- (k) Conical flask 125 mL
- (l) Volumetric pipets 1, 5, 10, 25, 50 mL

3.1.3 Apparatus

- (a) Thermometer
- (b) Heating mantle with stirrer (Horst)
- (c) Vacuum filtration apparatus (Gast)
- (d) Oven for drying sample (Memmert)
- (e) Furnace chamber (Carbolite CWF 12/23)
- (f) Desiccator
- (g) pH meter, (Mettler Delta 320)
- (h) Shaking water bath, (Maxi-Shake, Heto Lab Equipment, Denmark)
- (i) Standard sieve 230 mesh (63 μm), (Analysensieb, Retsch, USA)
- (j) Spatular
- (k) Analytical balance, (Model 250A, Precisa, Switzerland)
- (l) Sieve Shaker, (Octagon digital, Endecotts, England)
- (m) Glass microfiber filters, Whatman GF/C diameter 47 mm
- (n) Distilled water and deionised water

3.2 Instrumentation

3.2.1 X-ray powder diffraction

X-ray powder diffraction (XRD) is a popular technique used for the structural properties and the identifications of mineral in solid state and material science. The instrument used in the experiments of current research is Bruker D5005 powder X-ray diffractometer. The D5005 is equipped with a Ni filter in conjunction

with the Cu radiation (wavelength = 1.5406 Å). Prior to the measurement, each sample was prepared using a standard method for powder sample preparation. The procedure for powder XRD sample preparation was described as following: Dried the sample in oven at 110°C. Ground about 1.00 g of each solid sample to fine powder as homogeneous as possible, and then load into the polymethyl metaacrylate (PMMA) sample holder. Tapped the powder gently and evenly to uniformly cover the holder cavity. Gently pressed the powder sample into the cavity using a glass slide. Then gently lifted up glass slide to reveal the sample surface.

Each diffraction spectrum was recorded with the condition: 2θ angle of between 3° and 50°, Cu-target, 35 kV, 35 mA and scan speed of 0.4 degree/0.02 second. Typically, the data was expressed in the plot between intensity of diffraction peaks and 2θ angle. The positions of diffraction peaks were compared with a reference database and the identifications of compounds could be obtained. The %crystallite was calculated by equation 3.1 as follow:

$$\% \text{ cry} = \frac{(\text{total area of 10 strong peaks of sample})}{(\text{total area of 10 strong peaks of standard})} \times 100 \quad (3.1)$$

3.2.2 Fourier transforms infrared spectroscopy

Fourier transform infrared spectroscopy (FT-IR) is used to study structural features and examine the adsorption of many species. Spectroscopy is the study of the interaction of electromagnetic radiation with matter. Several spectroscopic techniques correspond to different regions in the electromagnetic radiation spectrum. Infrared spectroscopy studies the mid-infrared region (from 4000

to 370 cm^{-1}) where vibration and rotation bands are observed. The instrument used for this analysis was a Perkin -Elmer spectrum GX-FTIR Spectrophotometer with KBr pellet technique. The solid sample and KBr pellet were dried at 120°C for 12 hours before using. Approximately 0.004 mg of each sample was mixed with 0.2 g dried KBr powder and ground to very fine powder with a mortar and pestle. The ground powder was pressed to form a transparent disk by a hydraulic pressing machine with an equivalent weight of about 10 tons for 2 minute. The spectra were obtained by using an average of 10 scans with 4 cm^{-1} resolutions.

3.2.3 Scanning electron microscope

Morphology of the solid sample could be seen through the use of scanning electron microscope (SEM). Crystal shape and size of the crystalline solid phase could be identified from the micrograph. The observation was done by scanning electron microscope model JSM 6400. To prepare for the observation, the solid sample was placed on a brass stub sample holder using double stick carbon tape. Then, the sample was dried by using UV light for ten minutes. After that, the sample was coated with a layer of gold approximately 20 - 25 Å thick with a Balzer sputtering coater to make them conductive. The micrographs were recorded with an accelerating voltage of 10, 15, 20 kV and 500x - 10,000x magnification.

3.2.4 Thermogravimetric analysis

The thermogravimetric analysis (DTA/TGA) was used to measure the weight lost of solid samples at different temperatures and the temperature difference of sample and standard. The thermogravimetric analyses were carried out by Analyzer Simultaneous TGA-DTA Instrument model SDT-2960 at a heating rate of $10^{\circ}\text{C min}^{-1}$

under a flow of air of 120 mL min^{-1} with Al_2O_3 as a reference. The thermal analyses curves were recorded simultaneously along with temperature increment.

3.2.5 Particle size analyzer

Zeolite particle size distribution was measured by Malvern Mastersizer S Ver. 2.15 laser light-scattering-based particle sizer (for grain size determination of powder in suspension, ranging from 0.1 to $> 600 \text{ }\mu\text{m}$). For this purpose, the wet method of particle size distribution analysis was used. Water was used as the medium to disperse the samples. The solution was ultrasonicated for 45 min in order to break down the flocculates before the run was performed. All samples were run twice to ensure the accuracy of the measurements.

3.2.6 Brunauer-Emmett-Teller

Brunauer-Emmett-Teller (BET) is used to measure the surface area and pore size of zeolite. The Micromeritics ASAP 2010 analyzer contains two samples preparation ports and one analysis port. In line cold traps were located between the vacuum pump and the manifold in both the analysis and the degas systems. The sample saturation pressure tube is located next to the sample analysis port. The zeolite samples and sample tube were dried at 120°C for 12 hours before using. Approximately 0.2 g of each sample was added in the sample tube. For most reports and data entry, it can measure the pore diameter, pore size and surface area of the zeolite.

3.2.7 Inductively Coupled Plasma Mass Spectrometry

Inductively Coupled Plasma Mass Spectrometry (ICP-MS) is used to determine elemental compositions of zeolite. In an extension the work, an Agilent 7500 ICP-MS with Octopole Reaction System (ORS) is used to determine Na, Li, K,

Si, and Al in zeolite Y. The samples were prepared by digestion in PTFE vessel developed in the laboratory. Concentrated nitric acid (65% w/v), hydrofluoric acid, hydrochloric acid (37% w/v) and boric acid (4% w/v) were used for digestion and cleaning of the digestion tubes. Deionized water (Milli-Q ultrapure water) was used throughout.

3.3 Experimental methods

3.3.1 Synthesis of zeolite Y

The parent zeolite for all sample discussed in this study was Na-Y zeolite. Zeolite Y was synthesized hydrothermally reacted with mole ratio of starting reagent: $4.62\text{Na}_2\text{O} : \text{Al}_2\text{O}_3 : 10\text{SiO}_2 : 180\text{H}_2\text{O}$ (Ginter *et al.*, www, 2005). The solution was aged at room temperature for 1 day, then crystallize at 100°C for 7 hours, then washed with deionized water until the pH of filtrate became 7. To remove moisture in zeolite Y, each prepared product was dried overnight in the oven at 110°C before using in the next step.

3.3.2 Study of the dealumination method

The different dealumination methods for zeolite NaY were carried out as follows.

3.3.2.1 Dealumination by hydrochloric (HCl) method

Zeolite NaY was converted to zeolite NH_4Y form by ion exchanged with 1.0M NH_4Cl or 1.0 - 7.0 M NH_4NO_3 at room temperature. Then zeolite NH_4Y was converted to proton-exchanged form with heating rate at 10°Cmin^{-1} , followed by calcinations at 500°C and 650°C for 6 hours. Finally, the proton exchanged form was dealuminated by using 0.01 - 0.3 M of HCl, HNO_3 , and

CH₃COOH at 60°C for 30 min and 2 hours, then washed with deionized water until the pH of filtrate became 7. All the samples were represented in Table 3.1.

Table 3.1 The dealumination of zeolite NaY by HCl treatment under various conditions.

Sample	Concentration of NH₄NO₃ (M)	Concentration of HCl (M)	Temperature (°C) and Time (min)
HC11	1 M NH ₄ NO ₃	-	
HC12	1 M NH ₄ NO ₃	0.01 M HCl	60°C 30 min
HC13	1 M NH ₄ NO ₃	0.05 M HCl	60°C 30 min
HC14	1 M NH ₄ NO ₃	0.1 M HCl	60°C 30 min
HC15	1 M NH ₄ NO ₃	0.2 M HCl	60°C 30 min
HC16	2 M NH ₄ NO ₃	-	
HC17	2 M NH ₄ NO ₃	0.1 M HCl	60°C 30 min
HC18	2 M NH ₄ NO ₃	0.1 M HCl	60°C 120 min
HC19	2 M NH ₄ NO ₃	0.2 M HCl	60°C 30 min
HC110	2 M NH ₄ NO ₃	0.2 M HCl	60°C 120 min
HC111	2 M NH ₄ NO ₃	0.3 M HCl	60°C 120 min
HC112	3 M NH ₄ NO ₃	-	
HC113	3 M NH ₄ NO ₃	0.05 M HCl	60°C 30 min
HC114	3 M NH ₄ NO ₃	0.1 M HCl	60°C 30 min
HC115	7 M NH ₄ NO ₃	-	
HC116	7 M NH ₄ NO ₃	0.1 M HCl	60°C 30 min
HC117	7 M NH ₄ NO ₃	0.2 M HCl	60°C 30 min

3.3.2.2 Dealumination by ammonium hexafluorosilicate ($(\text{NH}_4)_2\text{SiF}_6$) method

The NaY zeolite was dealuminated by a modified method of ammonium hexafluorosilicate (AHFS) treatment. The concentration of AHFS from 0.05 - 1.0 M was added to stirred slurry of zeolite NaY in present and absence of 1.0 - 3.0 M ammonium acetate (NH_4OAc), which was used to buffer solution, and it was kept for 2 - 5 hours at 80°C. Then the hot suspension was filtered and the recovered zeolite was washed with hot deionized water (100°C). All the samples were represented in Table 3.2.

Table 3.2 The dealumination of zeolite NaY by AHFS treatment under various conditions.

Sample	Concentration of NH_4OAc (M)	Volume of NH_4OAc (ml)	Concentration of AHFS (M)	Volume of AHFS (ml)
AHFS1	-	-	0.05	15
AHFS2	1.0	50	0.05	15
AHFS3	1.0	50	0.25	15
AHFS4	1.0	50	0.5	15
AHFS5	1.0	100	-	-
AHFS6	1.0	100	0.05	15
AHFS7	1.0	100	0.25	15

Table 3.2 (continued)

Sample	Concentration of NH₄OAc (M)	Volume of NH₄OAc (ml)	Concentration of AHFS (M)	Volume of AHFS (ml)
AHFS8	1.0	100	0.5	15
AHFS9	1.0	100	0.75	15
AHFS10	1.0	100	1.0	15
AHFS11	1.0	150	0.05	15
AHFS12	1.0	150	0.25	15
AHFS13	1.0	150	0.5	15
AHFS14	3.0	100	-	-
AHFS15	3.0	100	0.25	15
AHFS16	3.0	100	0.5	15
AHFS17	3.0	100	0.75	15
AHFS18	3.0	100	1.0	15

3.3.2.3 Dealumination by silicon tetrachloride (SiCl₄) method

The NaY was first dried at 200°C for 2 hours under a nitrogen flow in reactor. Then, it was dealuminated with silicon tetrachloride vapor. In the case of silicon tetrachloride vapor was generated outside the reactor that showed in Fig. 3.1. The sample was dealuminated for various hours (2 - 10 hours) under the temperatures (room temperature and 200 - 500°C). After that the samples were treated further with a flow of dried nitrogen to remove the AlCl₃ for 2 hours and

without flow of dried nitrogen. In the other hand the silicon tetrachloride vapor was generated inside the reactor that showed in Fig. 3.1. The sample was dealuminated with silicon tetrachloride for various hours (24 - 96 hours) under the room temperatures. After that the samples were treated further with a flow of dried nitrogen and without flow of dried nitrogen during reaction. Finally, the treated samples were washed thoroughly with deionized water and dried at 110°C. All of the samples were represented in Table 3.3.

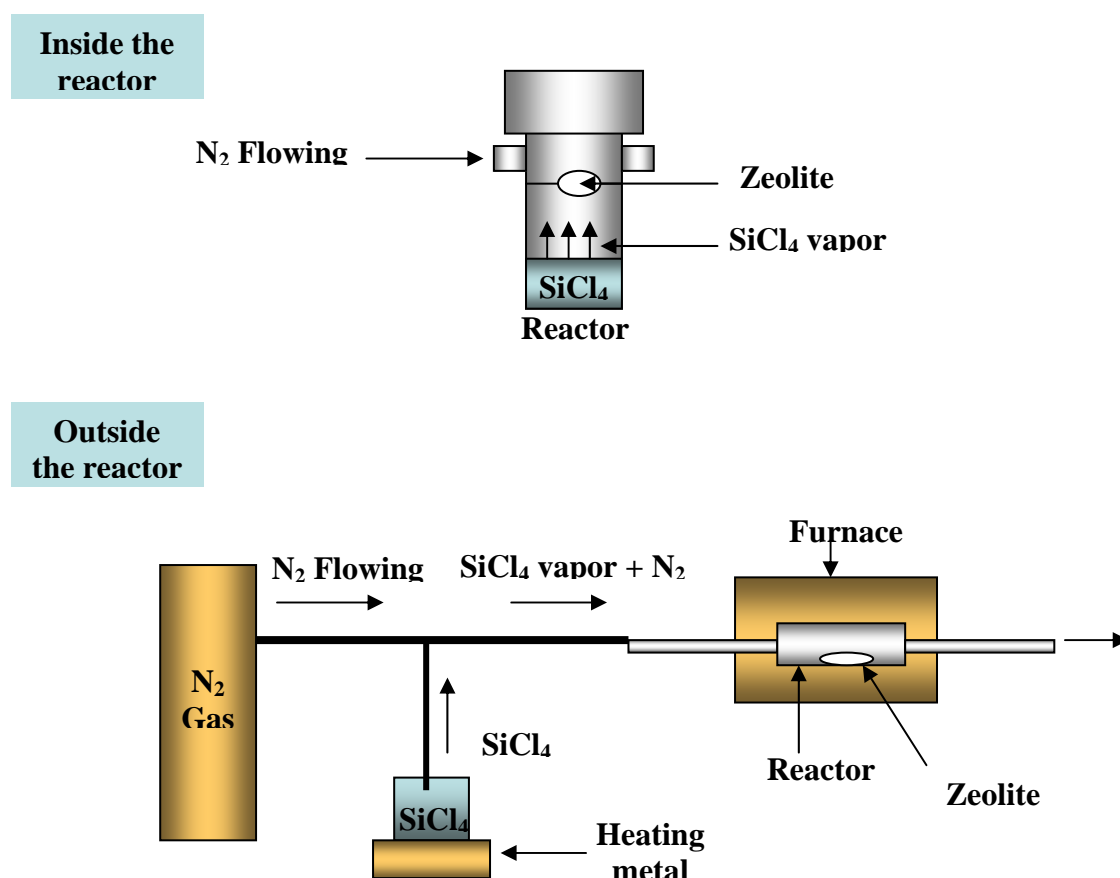


Figure 3.1 Diagram of the dealumination reactor.

Table 3.3 The dealumination of zeolite NaY by SiCl₄ treatment under various conditions.

Sample	Position of generated SiCl ₄		Temperature of generated SiCl ₄ (°C)	Reaction time (hours)	Reaction temperature (°C)	N ₂ Flow	
	Inside	Outside				During reaction	After reaction
	S1	✓	-	25	24	25	-
S2	✓	-	25	96	25	✓	-
S3	✓	-	25	96	25	-	-
S4	-	✓	25	6	500	✓	-
S5	-	✓	25	4	500	✓	✓
S6	-	✓	40	4	500	✓	✓
S7	-	✓	40	4	500	✓	-
S8	-	✓	25	4	500	✓	-
S9	-	✓	25	4	25	✓	✓
S10	-	✓	25	4	150	✓	✓
S11	-	✓	25	4	200	✓	✓
S12	-	✓	25	4	250	✓	✓
S13	-	✓	25	4	300	✓	✓
S14	-	✓	25	4	350	✓	✓
S15	-	✓	25	4	400	✓	✓
S16	-	✓	65	6	500	✓	✓
S17	-	✓	65	8	500	✓	✓
S18	-	✓	65	10	500	✓	✓

3.3.3 Effect of different exchangeable cations (Li^+ , Na^+ and K^+) and anion (Cl^- and NO_3^-) on dealumination

Cation-exchanged zeolite (i.e., zeolite LiY and KY) was prepared by an ion exchange method by using zeolite NaY exchanged three times with 0.25 - 1.0 M of LiCl, LiNO₃, KCl, KNO₃, NaCl, and NaNO₃ at room temperature for 24 hours. The products were washed several times with deionized water, followed by drying at 120°C for 1 hour. Zeolite LiY, NaY, and KY were further dealuminated by AHFS methods. The results obtained from the different exchangeable cations and anion (Cl^- and NO_3^-) affecting the dealumination of zeolite Y were compared. All the samples were represented in Table 3.4.

Table 3.4 The effect of cation and anion on dealumination of zeolite NaY by AHFS treatment under various conditions.

Sample	Cl^-		NO_3^-		Dealumination
	washing	no washing	washing	no washing	
LiY1	✓	-	-	-	-
LiY2	-	✓	-	-	-
LiY3	-	-	✓	-	-
LiY4	-	-	-	✓	-
LiY1D	✓	-	-	-	✓
LiY2D	-	✓	-	-	✓

Table 3.4 (continued)

Sample	Cl ⁻		NO ₃ ⁻		Dealumination
	washing	no washing	washing	no washing	
NaY1	✓	-	-	-	-
NaY2	-	✓	-	-	-
NaY3	-	-	✓	-	-
NaY4	-	-	-	✓	-
NaY1D	✓	-	-	-	✓
NaY2D	-	✓	-	-	✓
KY1	✓	-	-	-	-
KY2	-	✓	-	-	-
KY3	-	-	✓	-	-
KY4	-	-	-	✓	-
KY1D	✓	-	-	-	✓
KY2D	-	✓	-	-	✓

3.3.4 Physical and chemical characterization of the dealuminated zeolite Y.

The parent zeolite (NaY) and dealuminated zeolite samples were characterized by XRD, FT-IR, SEM, and DTA in order to determine structural transform and the percentage of crystallinity. Their surface areas and particle size were analyzed by nitrogen adsorption (BET) measurements and lazer particle size analyzer, respectively. Si and Al content were analyzed by ICP-MS. The SEM and

particle size analyzer were characterized before and after dealuminated zeolite with HCl method.

The results from different dealuminations in aspect of the crystalline dealuminated zeolite Y were compared and some correlations of Si/Al ratio with surface area and with particle size distribution were also considered.

CHAPTER IV

RESULTS AND DISCUSSION

4.1 Synthesis of zeolite NaY

The solids obtained from the synthesis experiments were identified using powder X-ray diffraction. Fig. 4.1 showed the XRD pattern of zeolite Y that were crystallized from a hydrothermal reaction with mole ratio of $4.62\text{Na}_2\text{O} : \text{Al}_2\text{O}_3 : 10\text{SiO}_2 : 180\text{H}_2\text{O}$. The solution was aged at room temperature for 1 day, then reacted at 100°C for 7 hours. XRD pattern exhibited the normal diffraction lines of synthesized zeolite NaY (e.g., the intense line at 2θ values of 6.1, 10.4, 12.12, 15.9, 20.6, 23.9, and 27.24). The BET surface area, pore volume and pore size of the zeolite NaY synthesized were determined. The value of observed surface area was $916 \text{ m}^2\text{g}^{-1}$. The pore volume and pore size were approximately average value of $0.44 \text{ cm}^3\text{g}^{-1}$ and 5.35 \AA , respectively. The particle size was $11.92 \text{ }\mu\text{m}$. The surface morphology of the zeolite NaY was observed by electron microscope (SEM) (see Fig. 4.2.). There were small sizes and octahedral shape crystals. The ratio of Si/Al of zeolite NaY was also determined by ICP-MS. It was about 3.7.

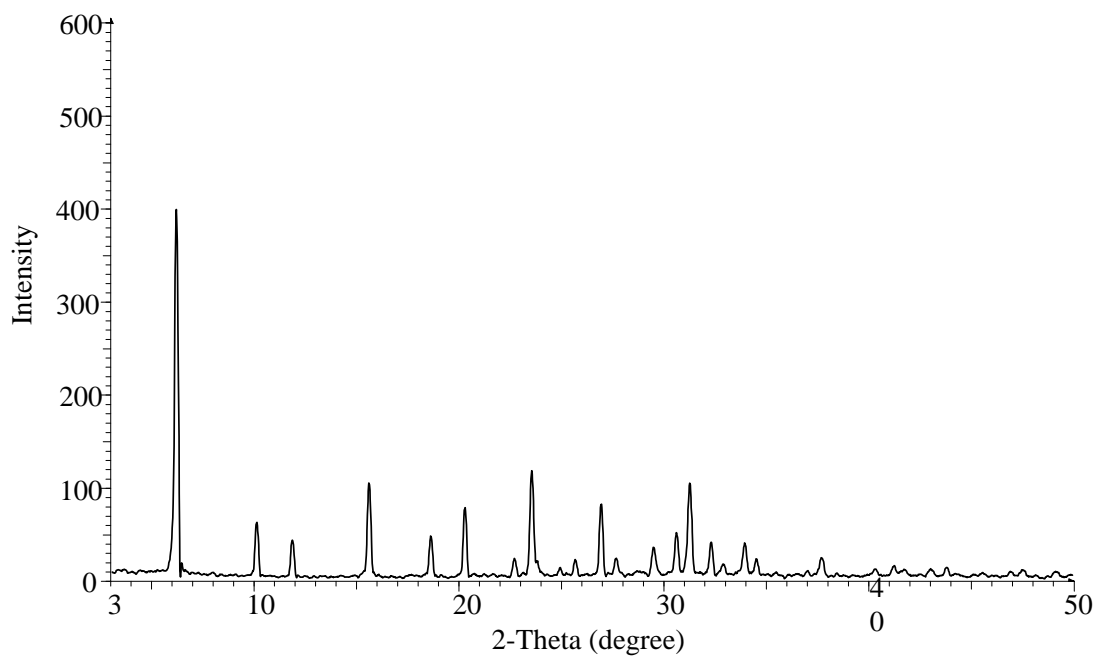


Figure 4.1 XRD pattern of synthesized zeolite NaY.

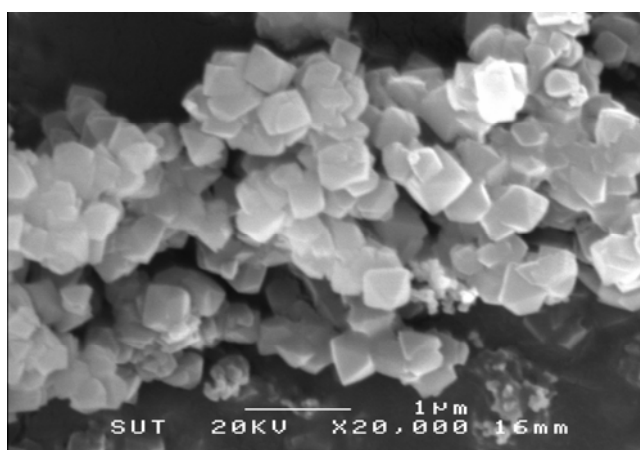


Figure 4.2 Morphology of synthesized zeolite NaY.

4.2 Dealumination with HCl treatment

The dealumination with HCl treatment of zeolite NaY carried out by ion exchange from a sodium form of zeolite into an ammonium form, followed by calcinations to convert the ammonium cations into gaseous ammonia and protons. Then HCl acid solution was used to dealuminate the zeolite HY. Different effects were investigated during the dealumination with HCl method such as effect of anions (NO_3^- , Cl^-) on NH_4^+ exchange process, temperature of calcination and concentration of HCl and NH_4NO_3 . The effects in each step of HCl dealumination method were studied as follows.

4.2.1 Effect of anions on NH_4^+ exchange processes

The XRD pattern of zeolite NaY exchanged with NH_4Cl and NH_4NO_3 were shown in Fig. 4.3. It showed that the main peak at position of $2\theta = 6.1$, corresponding to d-spacing at (111) reflections, shift to $2\theta = 6.2$ and 6.6 for exchange with NH_4NO_3 and NH_4Cl , respectively. The d-spacing value decreased from 14.37 to 14.12 in the case of exchanging with NH_4NO_3 and to 13.26 for exchanging with NH_4Cl . This indicates that the zeolite framework collapsed. Therefore, it affects the loss of crystallinity. Fig. 4.4 showed both of the samples contained 48% and 29% of crystallinity after exchanging with NH_4NO_3 and NH_4Cl , respectively. It indicated that NH_4Cl caused a change in the morphology of crystallite more than NH_4NO_3 . This effect is agreed to another research (Katada *et al.*, 2005).

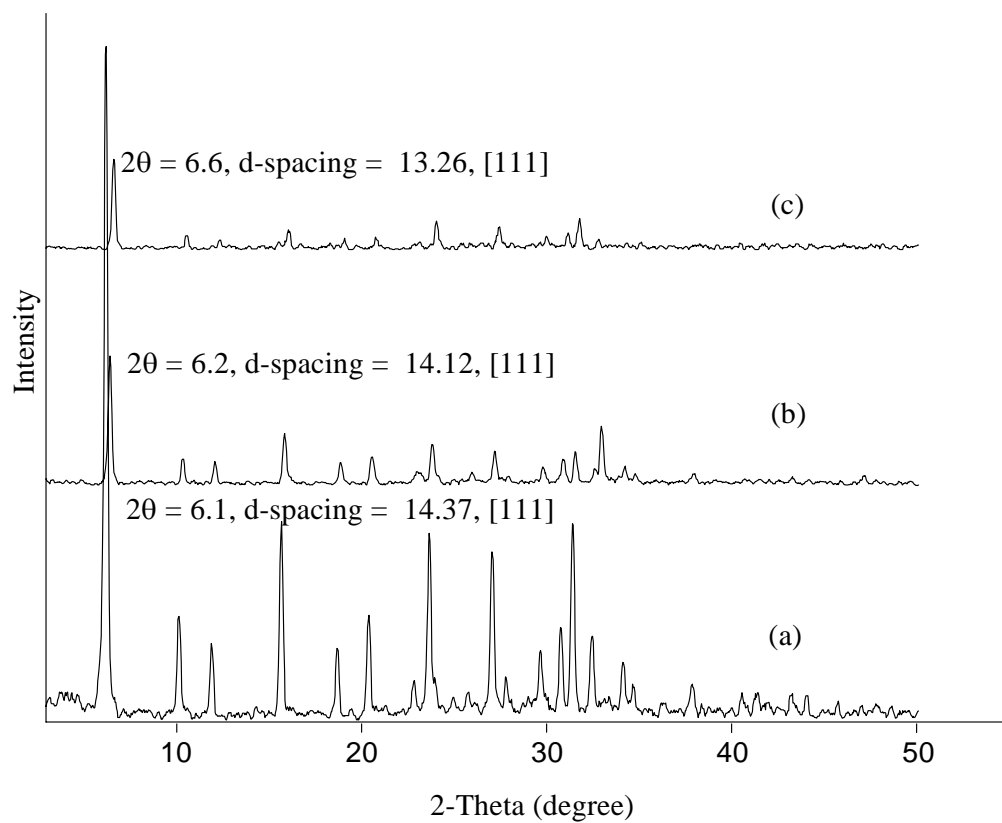


Figure 4.3 XRD patterns of synthesized zeolite NaY (a) before and (b-c) after exchanging with (b) 1M NH_4NO_3 , (c) 1M NH_4Cl .

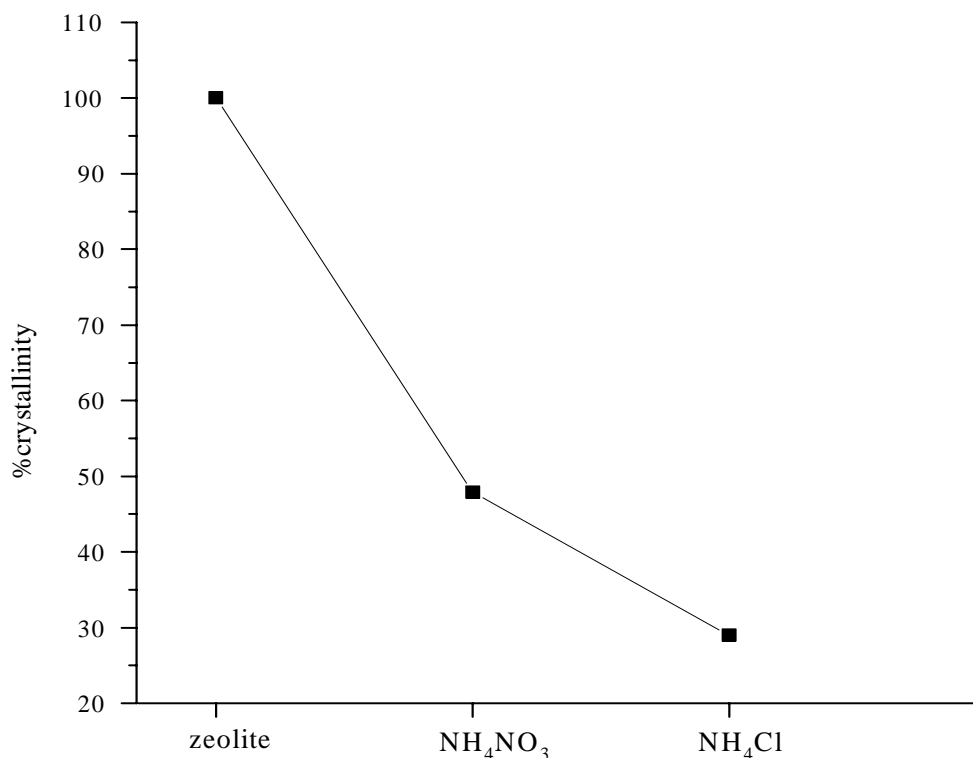


Figure 4.4 Percent crystallinity of zeolite NaY after ion exchanging with 1M NH₄NO₃ and 1M NH₄Cl.

4.2.2 Effect of concentration of NH₄NO₃

NH₄NO₃ solution was used to convert zeolite NaY to zeolite NH₄Y by ion exchange at room temperature. Then zeolite NH₄Y was further converted to proton-exchanged form by calcinations. The XRD patterns of the zeolite NaY were recorded before and after the ion exchange with various concentrations of NH₄NO₃ and followed with calcinations at 500°C for 6 hours. The observed crystallinity after NaY exchanged with NH₄NO₃ at 1, 3, and 7 M were 95%, 75%, and 33%, respectively (see Fig. 4.5). The crystalline structure of zeolite was almost completely destroyed with NH₄NO₃ concentration of 7M, because to at high concentration it

produces high amount of NH_4^+ and NO_3^- . Therefore, NO_3^- is more enough to damage the zeolite framework.

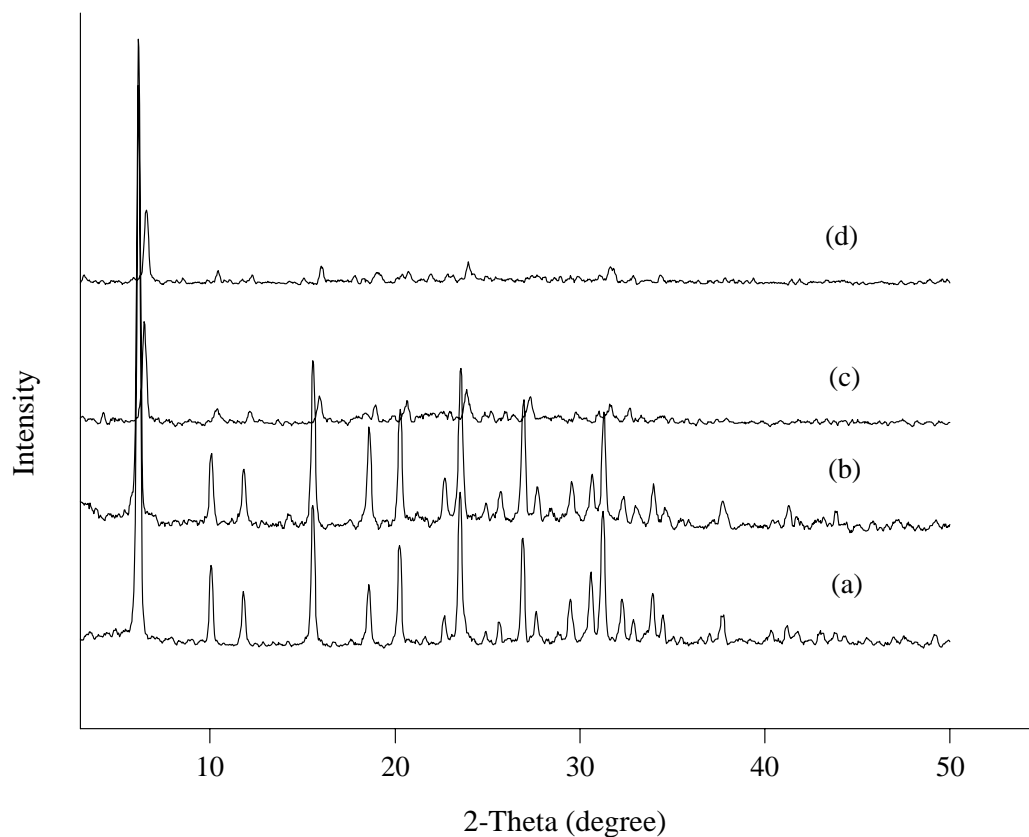


Figure 4.5 XRD patterns of zeolite NaY (a) before and (b-d) after exchanging with different concentration of NH_4NO_3 and followed calcination at 500°C for 6 hours. (b) exchanging with 1M NH_4NO_3 ; (c) exchanging with 3M NH_4NO_3 ; (d) exchanging with 7M NH_4NO_3 .

The IR spectra of the zeolite NaY exchanged with 1, 3, and 7M NH_4NO_3 for calcinations at 500°C were present in Fig. 4.6 and Table 4.1. This poorly resolved spectrum indicated that the zeolite had lost crystallinity and a higher Si/Al ratio upon increase of the concentration of NH_4NO_3 .

The HY form was analyzed by ICP-MS for quantitative determination of Si and Al. From this data the Si/Al mole ratio was determined. The ICP-MS results for the HY form given in the Fig. 4.7 showed the Si/Al ratio depending on NH_4NO_3 concentration. It was found that the Si/Al ratio of HY form increased with increasing concentration of NH_4NO_3 .

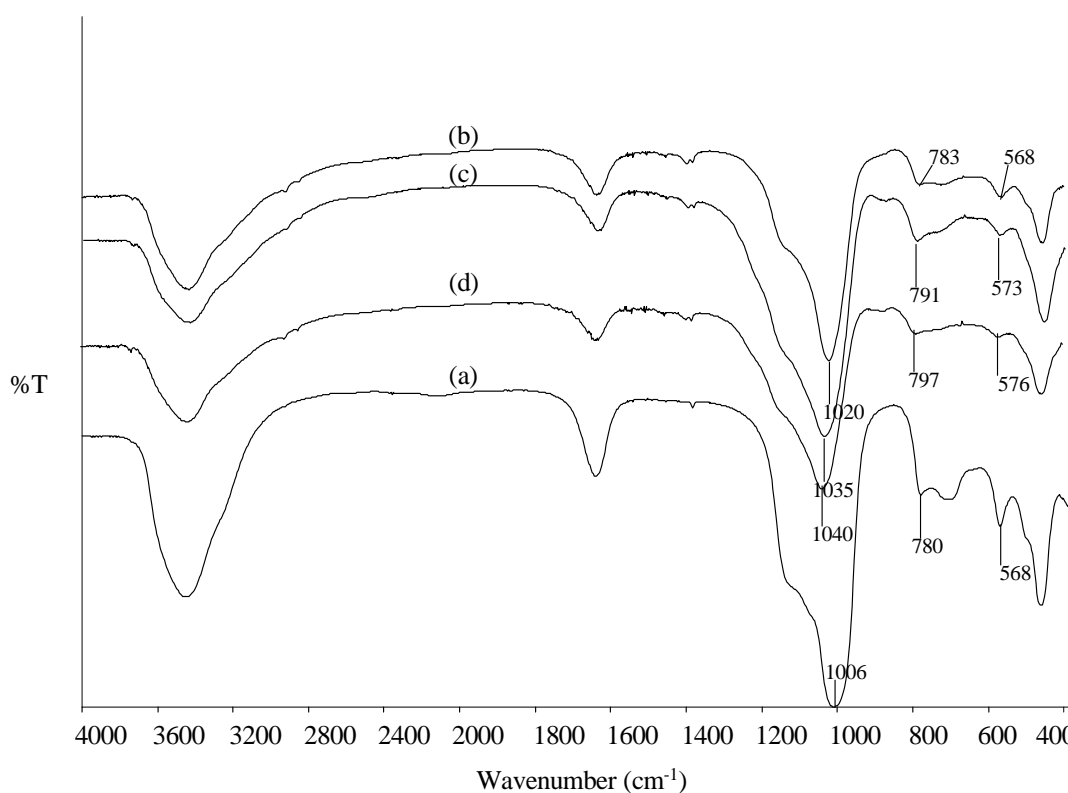


Figure 4.6 IR spectra of zeolite NaY (a) before and (b-d) after exchanging with different concentration of NH_4NO_3 and followed with calcination at 500°C for 6 hours. (b) exchanging with 1M NH_4NO_3 ; (c) exchanging with 3M NH_4NO_3 ; (d) exchanging with 7M NH_4NO_3 .

Table 4.1 Wavenumbers of the zeolite NaY before and after the ion exchange with NH_4NO_3 at various concentrations and followed with calcinations at 500°C for 6 hours.

Concentration of NH_4NO_3	Asymmetric stretch ($1050 - 1150 \text{ cm}^{-1}$)	Symmetric stretch ($750 - 820 \text{ cm}^{-1}$)	Double ring ($\sim 560 \text{ cm}^{-1}$)
Zeolite Y	1006	780	568
1M	1020	783	568
3M	1035	791	573
7M	1040	797	576

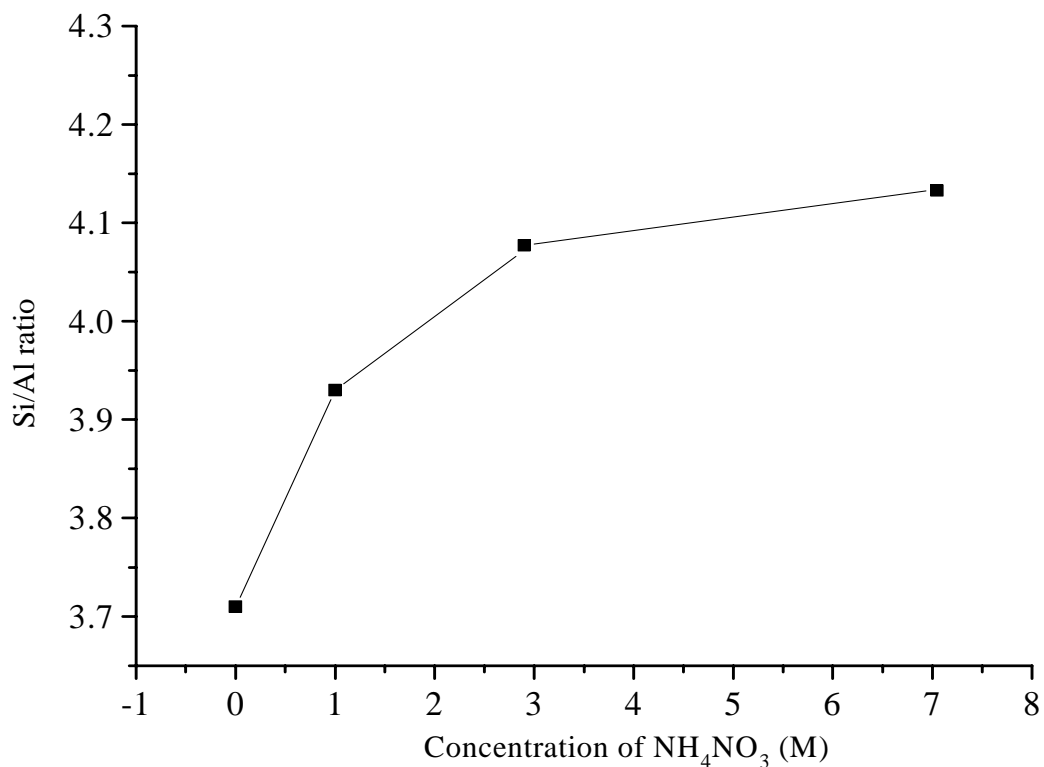


Figure 4.7 Relationship between the Si/Al ratio and concentration of NH_4NO_3 (M).

4.2.3 Effect of calcination temperature on transformation of NH_4Y to HY form

Thermograms of NH_4NaY presented in Figs. 4.8 and 4.9 showed an endothermic peak at 117°C and 108°C , respectively. It results from loss of water. A sharp endothermic peak at 668°C shown in Fig. 4.8 is attributed to dehydroxylation. An exothermic peak at 932°C may be result from phase transition. Loss of physically adsorbed water occurring between room temperature and 200°C while deammoniation overlaps with dehydroxylation between 300 and 700°C (Weeks and Bolton, 1975). The TGA was except as accepted from the lower ammonia content, the weight loss due to deammoniation was less. The thermograms of deammoniation for HY did not appear. It means that the calcinations at 500°C can remove NH_3 .

The XRD pattern of a single sample of NH_4NaY at various temperatures for calcinations was shown in Fig. 4.10. At 500 and 650°C the relative intensity of all the peaks decreased. At higher temperature of calcinations, amount of crystalline was destroyed. However, temperature at 500°C was selected for further calcinations because of percent crystallinity at 500°C higher than 650°C and able to remove NH_3 .

IR spectra between 400 and 4000 cm^{-1} of zeolite NaY was present in Fig. 4.11. Stretching vibration of adsorbed water forming H-bond appeared at $3444 - 3430\text{ cm}^{-1}$ bending vibration at $1634 - 1640\text{ cm}^{-1}$. An additional band of NH_4NaY at 1400 cm^{-1} attributed to vibration of ammonium as well as a band at 3167 cm^{-1} corresponded to stretching vibration of ammonium. After calcination at 500°C the peak of ammonium disappeared.

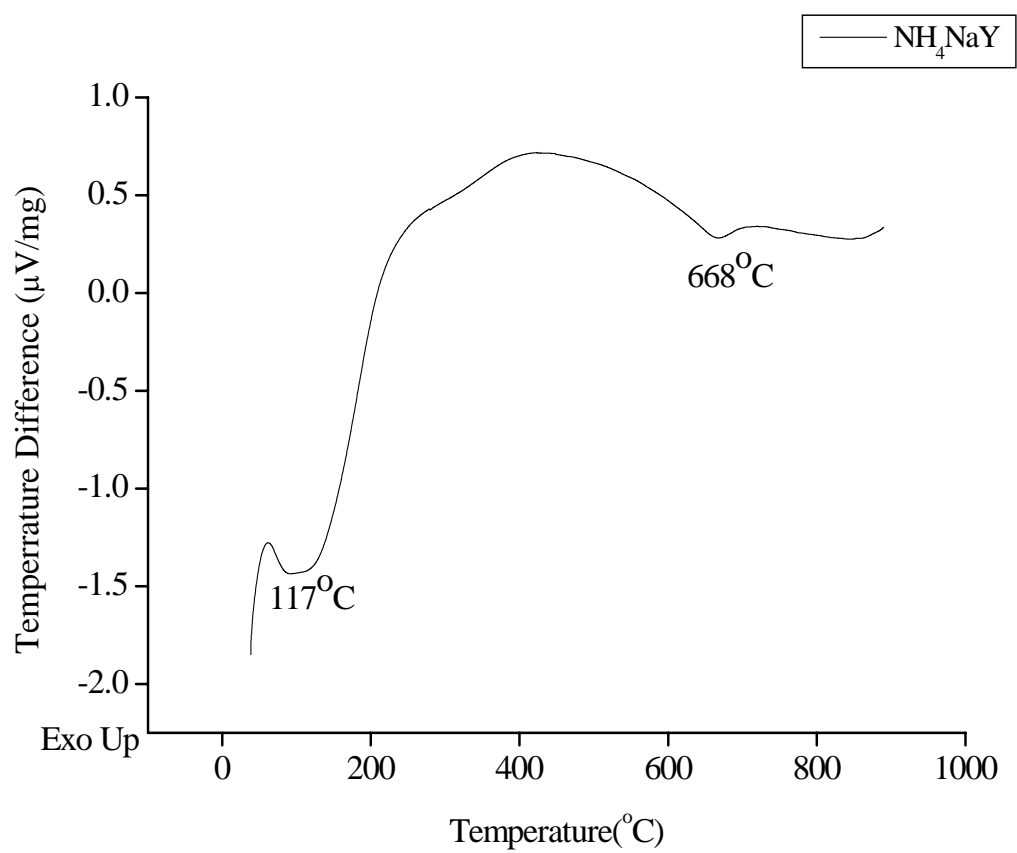


Figure 4.8 Thermogram of NH_4NaY exchanged with 1M NH_4NO_3 .

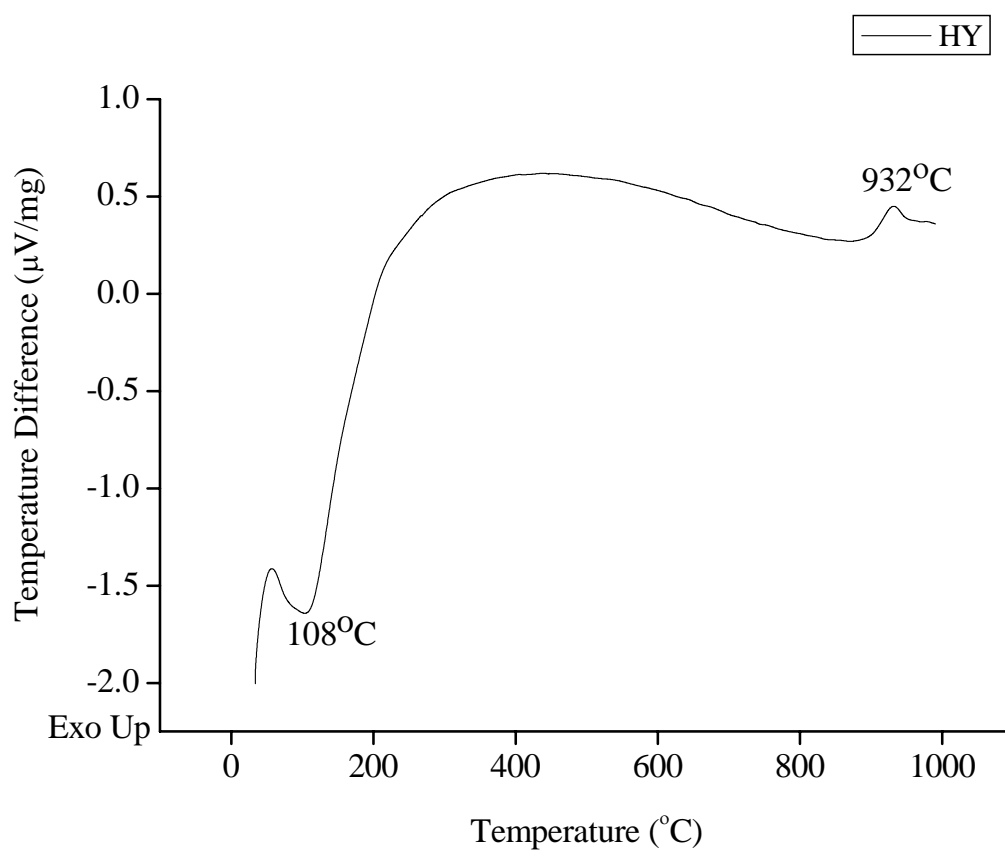


Figure 4.9 Thermogram of NH_4NaY calcined at 500°C .

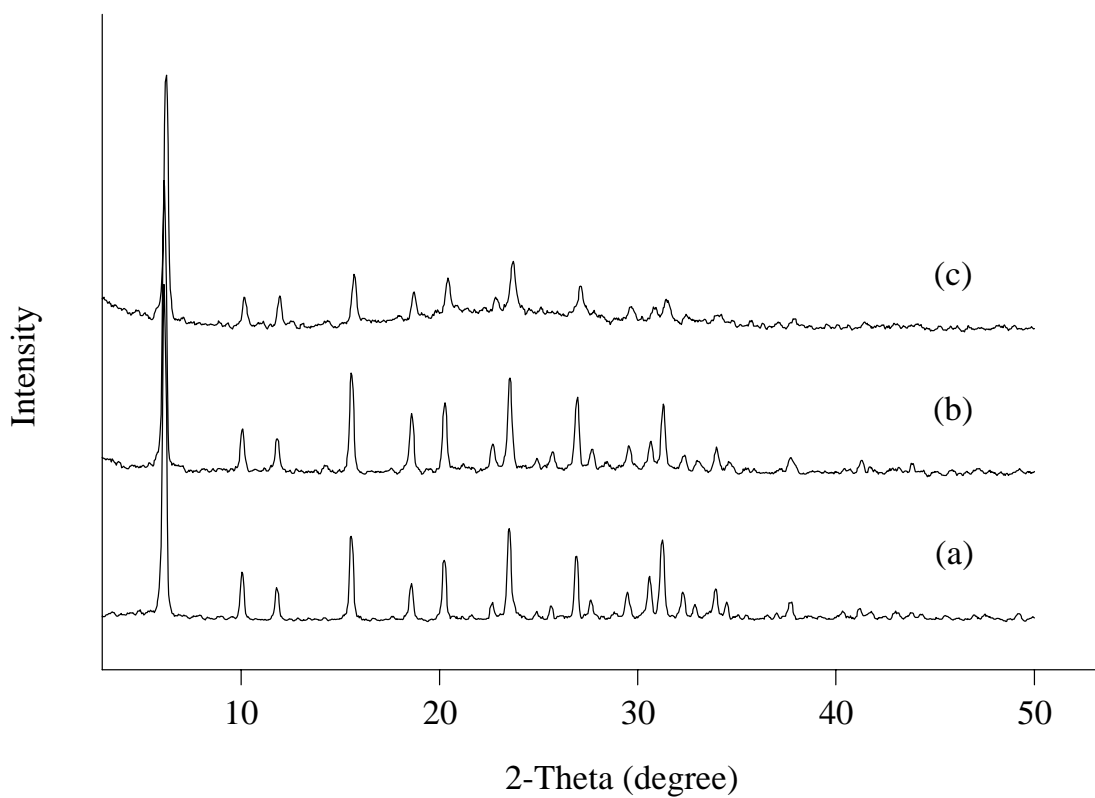


Figure 4.10 XRD patterns of synthesized zeolite NaY (a) before and (b-c) after exchanging with 1M NH_4NO_3 and followed with calcination at different temperatures for 6 hours. (b) calcination at 500°C; (c) calcination at 650°C.

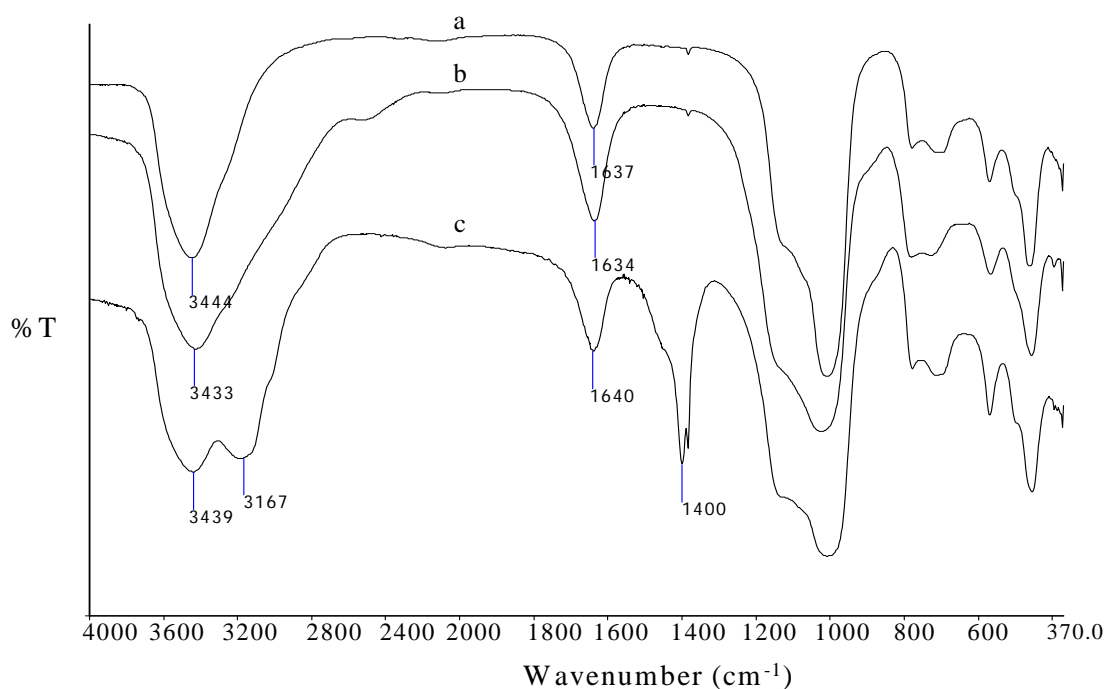


Figure 4.11 IR spectra of synthesized zeolite NaY (a); NH_4NaY calcined at 500°C (b) and NH_4NaY (c).

4.2.4 Effect of concentration of HCl, temperature and time on dealumination

For dealumination with HCl treatment, HY was treated in hydrochloric acid solution with 0.01 - 0.3M at 60°C for 30 minutes and 2 hours. XRD diffraction pattern were recorded before and after the treatments to determine the effect on the structure of the zeolite NaY. Figs. 4.12 and 4.13. At concentration higher than 0.2M, the structure of the zeolite began to breakdown. The 0.3 M HCl treatment almost completely destroyed the crystalline structure of the zeolite. Analysis of the XRD peak location was used to determine the unit cell parameter. Peak shifts to higher 2θ values parameters as a result of dealumination with treatment of increasing acid

strength (Holmberg *et al.*, 2004) and indicates smaller d-spacing and reduced unit cell parameters

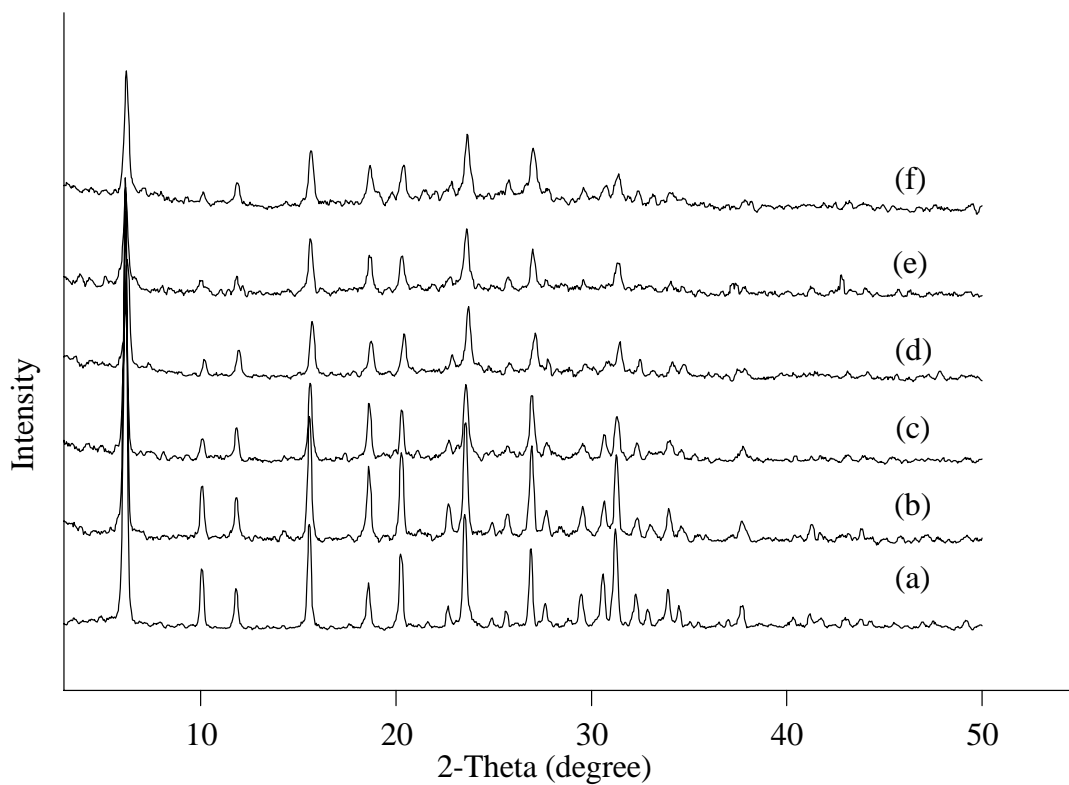


Figure 4.12 XRD patterns of zeolite NaY (a) before and (b-f) after dealumination with HCl method. (b) Exchanging with 1M NH_4NO_3 and followed with calcination at 500°C for 6 hours (HY); (c) HY dealuminated at 0.01M HCl for 30 min; (d) 0.05M HCl; (e) 0.1M HCl; (f) 0.2M HCl.

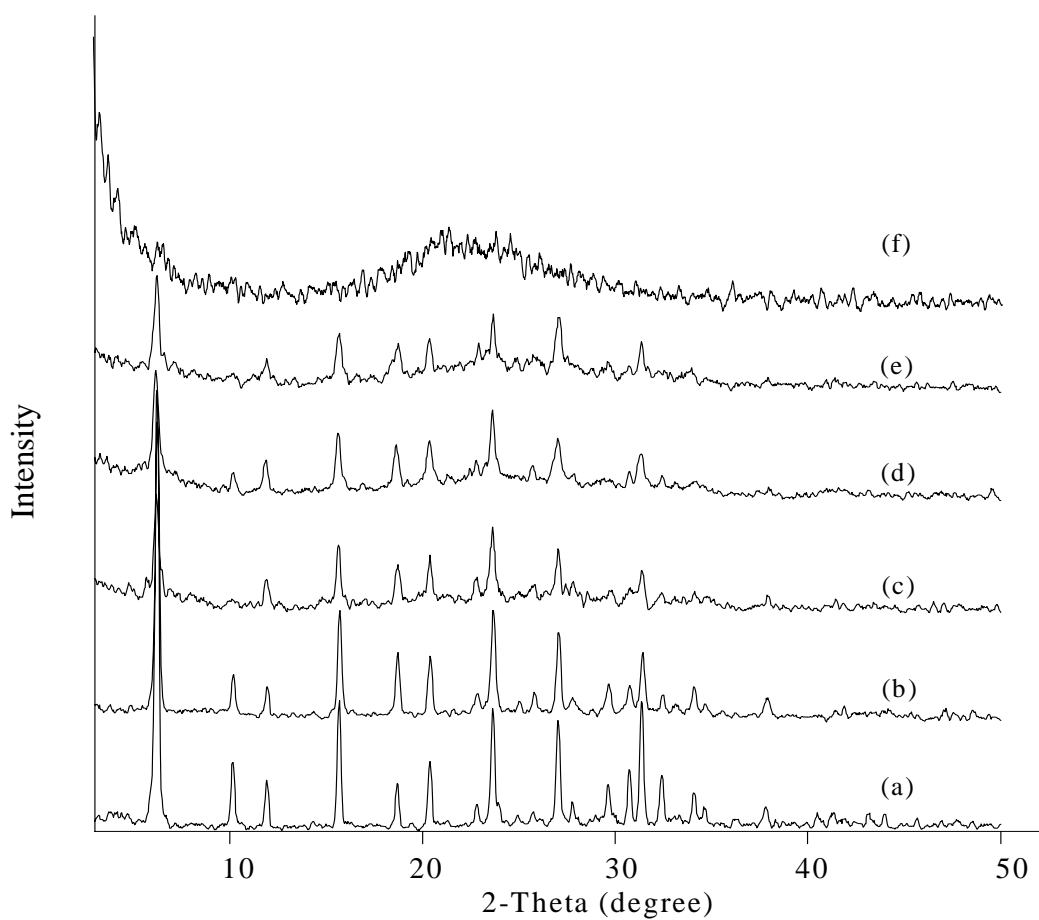


Figure 4.13 XRD patterns of zeolite NaY (a) before and (b-f) after dealumination with HCl method. (b) Exchanging with 2M NH_4NO_3 and followed with calcination at 500°C for 6 hours (HY); (c) HY dealuminated at 0.1M HCl for 2 hours; (d) 0.2M HCl; (e) 0.3M HCl; (f) more than 0.3M HCl.

The dealumination was also confirmed by FT-IR analyses. Shifts toward higher wavenumbers in the structure sensitive asymmetric stretch ($1050 - 1150 \text{ cm}^{-1}$), symmetric stretch ($750 - 820 \text{ cm}^{-1}$) and double ring ($\sim 560 \text{ cm}^{-1}$) regions of the FT-IR spectra of zeolite indicate a higher Si/Al ratio (Anderson, 1986; Skeels and Breck, 1983). Decreases in the intensity of the FT-IR spectrums, especially the double-ring vibration, are strong indications of intense crystallinity loss (Bartl *et al.*, 2000).

Mid-infrared spectroscopy is a very sensitive tool for investigating structural alterations of zeolitic frameworks. The wavenumber of the zeolite NaY treated with 0.01, 0.05, 0.1, 0.2, and 0.3M HCl was present in Table 4.2. It was found that asymmetric and symmetric stretch shifted towards higher frequencies from 1006 cm^{-1} to 1051 cm^{-1} for asymmetric stretch and $780, 703 \text{ cm}^{-1}$ to $785, 723 \text{ cm}^{-1}$ for symmetric stretch. It indicated that the zeolite had a higher Si/Al mole ratio upon increase of the concentration of HCl. It corresponds to the data in Table 4.3 and Fig. 4.14.

Table 4.3 showed Si/Al mole ratio from ICP-MS measurements and also %crystallinity from XRD results. It was found that with increasing the concentration of HCl and NH_4NO_3 amount of Si/Al ratio was increased, but % crystallinity was decreased.

Table 4.2 The wavenumbers of the HCl dealumination for zeolite Y at various concentrations of HCl.

Concentration of HCl(M)	asymmetric stretch (1050 – 1150 cm ⁻¹)	symmetric stretch (750 – 820 cm ⁻¹)	double ring (~560 cm ⁻¹)
NaY	1006	780, 703	570
HCl1	1018	785, 723	568
HCl2	1023	785, 723	568
HCl3	1026	788, 726	568
HCl4	1029	785, 723	568
HCl5	1035	788, 729	565
HCl6	1020	785, 726	570
HCl7	1035	785, 723	565
HCl9	1043	785, 723	565
HCl11	1051	785, 723	565

Notation of various concentrations of HCl was described in Table 3.1 (see page 32).

Table 4.3 The amount of Si/Al ratio and percent crystallinity of dealuminated zeolite Y with HCl at various conditions.

Sample				Si/Al ratio	% Cry
Zeolite NaY		NaY		3.7	100
1 M NH ₄ NO ₃	-	HCl1		3.9	64
	0.01 M HCl	HCl2	60°C 30 min	3.8	56
	0.05 M HCl	HCl3	60°C 30 min	3.7	39
	0.1 M HCl	HCl4	60°C 30 min	3.9	34
	0.2 M HCl	HCl5	60°C 30 min	4.1	28
2 M NH ₄ NO ₃	-	HCl6		3.9	66
	0.1 M HCl	HCl7	60°C 30 min	4.1	32
	0.1 M HCl	HCl8	60°C 2 hours	4.2	30
	0.2 M HCl	HCl9	60°C 30 min	4.4	21
	0.2 M HCl	HCl10	60°C 2 hours	4.4	23
	0.3 M HCl	HCl11	60°C 2 hours	4.4	15
3 M NH ₄ NO ₃	-	HCl12		4.1	31
	0.05 M HCl	HCl13	60°C 30 min	4.0	30
	0.1 M HCl	HCl14	60°C 30 min	4.1	30
7 M NH ₄ NO ₃	-	HCl15		4.1	14
	0.1 M HCl	HCl16	60°C 30 min	4.2	28
	0.2 M HCl	HCl17	60°C 30 min	4.2	16

Notation of various concentrations of HCl was described in Table 3.1 (see page 32).

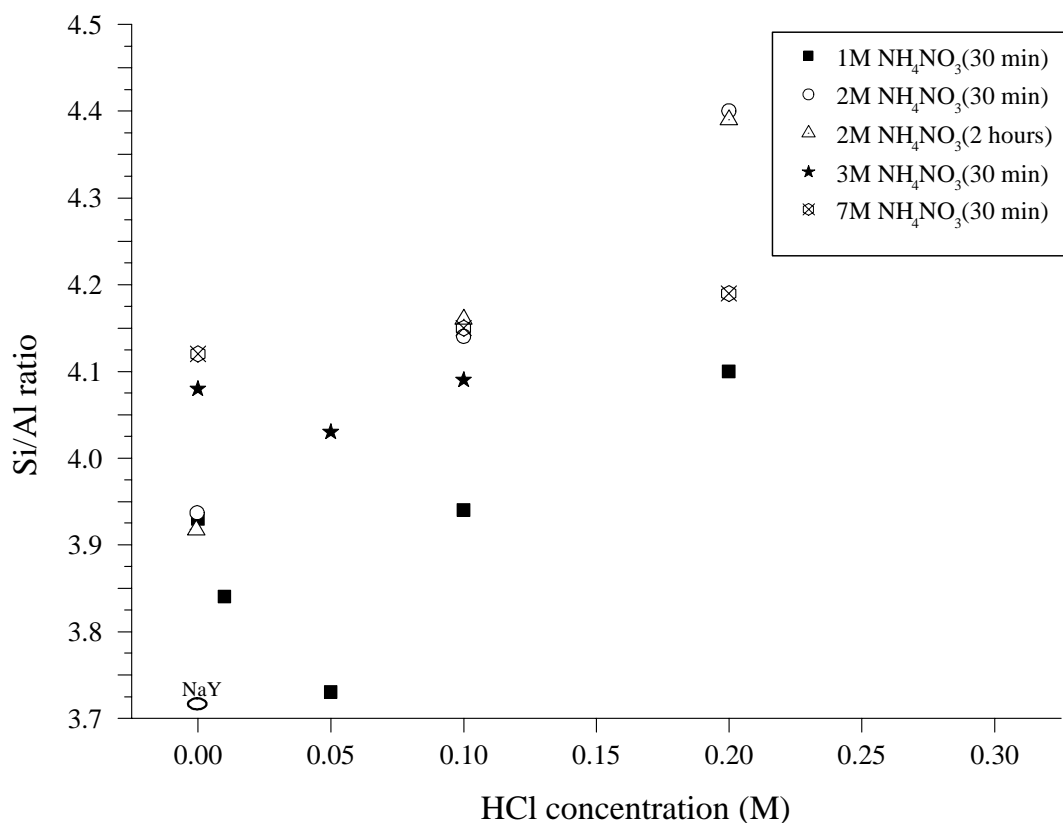
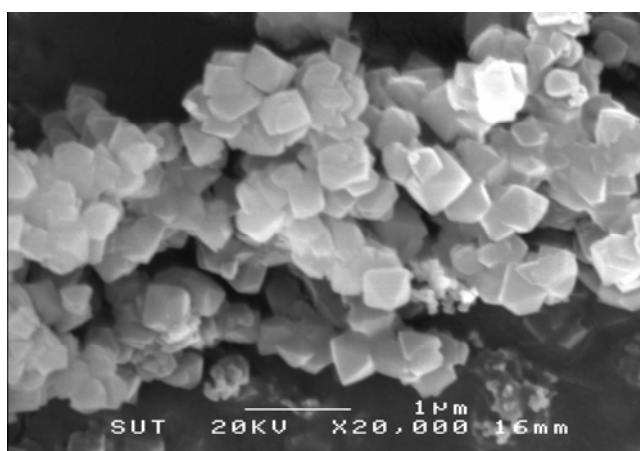


Figure 4.14 Plot of Si/Al ratio and HCl concentration.

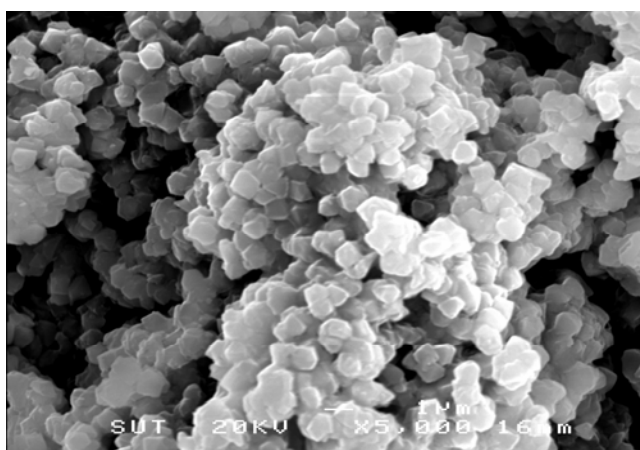
Table 4.4 showed the results of NaY before and after dealumination with HCl method. It was found that the particle size of dealuminated zeolite was larger than that of parent zeolite after dealumination due to a collapse of the structure which corresponding to the result of SEM shown in Fig. 4.15. It showed the morphology of zeolite NaY before and after dealumination with HCl. After dealumination the crystals of NaY are coagulated consequently, the larger average particle sizes are formed.

Table 4.4 The average particle size of zeolite NaY before and after dealumination with HCl method.

Sample	Average particle size
Parent zeolite Y	11.92 μm
HCl10	14.54 μm



(a)



(b)

Figure 4.15 Morphology of the zeolite NaY before (a) and after dealumination with HCl method (b).

Dealumination with HCl is found to be convenient to dealuminate zeolite Y. Nevertheless, it has the limitation that the yield from this method contains the maximum of Si/Al mole ratio in the range of 3.9 - 4.4 with %crystallinity from 64 - 16%. When the obtained dealuminated zeolite Y with Si/Al mole ratio was more than 4.4, its structure almost destroyed (%crystallinity obtained about 16%). In addition, we considered the steps of dealumination in this experiment to confirm the previous mechanism (Fitzgerald *et al.*, 1997; Zaika, Qingling, Chengfang, Jiaqing, and Yuhua, 2000). The proposed mechanism of dealumination by HCl in each step was summarized in this work (see Fig. 4.16). The mechanism consists of the following three steps. The first step Na-zeolite form was exchanged to NaNH_4 -zeolite by ion exchange with NH_4^+ . Then it was calcined at high temperature to remove NH_3 from zeolite framework and HY was occurred. Finally, HCl was used to dealuminate the framework of zeolite Y. They considered when zeolite was treated with HCl solution, the H^+ from electroionization of HCl was shifted to Al-O bond in the framework. It was broken via an attacked of that H^+ (Fitzgerald *et al.*, 1997; Zaika, Qingling, Chengfang, Jiaqing, and Yuhua, 2000). Al^{3+} specie was removed from the framework. The external Al^{3+} specie interacts with Cl^- to form AlCl_3 species, which were removed by washing several times with DI water. After that the Si-OH was formed. When aluminum leaves the framework, it leads to increase intensity at 3750 - 3400 cm^{-1} of the IR spectra as shown in Fig. 4.17. It was found that the intensity at 3412 and 906 cm^{-1} was increased. It may be due to increase in amount of Si-OH. However, the band around 3412 cm^{-1} attributed not only to Si-OH forming H-bond, but also to hydrate.

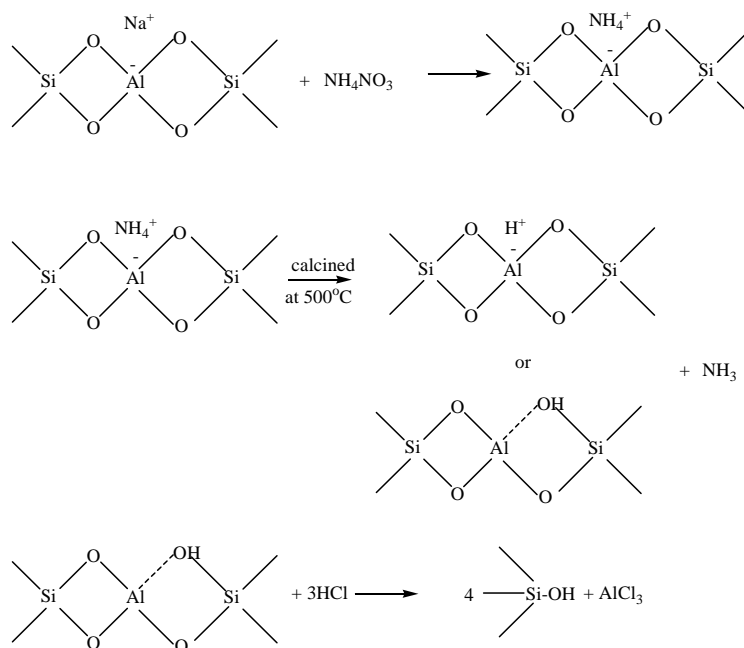


Figure 4.16 Mechanism of dealumination of zeolite by HCl (Fitzgerald *et al.*, 1997; Zaika, Qingling, Chengfang, Jiaqing, and Yuhua, 2000).

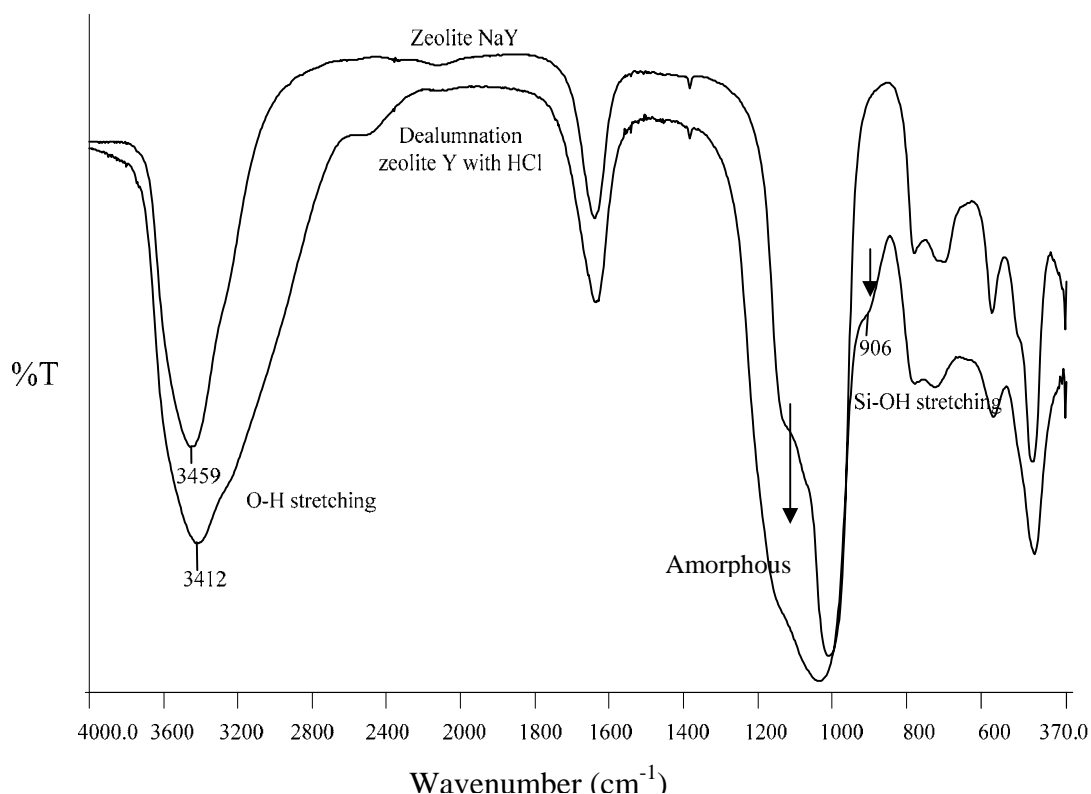


Figure 4.17 IR spectra of zeolite NaY and dealuminated NaY with HCl.

4.2.5 Comparison between organic and inorganic acid affecting dealumination

Figs. 4.18 and 4.19 showed the XRD patterns of HY after acetic and nitric acid treatments, respectively. The powder XRD diffractograms showed a progressive breakdown of the crystalline structure of the zeolite. It was found that dealumination with acetic acid to kept percent crystallinity more than the treatment with HNO₃ and HCl. It may be that acetic acid is a weak acid to remove aluminum slightly from the framework. Under more severe leaching conditions (> 0.1M HNO₃ and > 0.2M HCl), the diffraction peaks became weaker, indicating a collapse of the framework structure, while the broad peak due to the amorphous phase became more

obvious. These observations revealed that the formation of the amorphous phase was accompanied with the breakdown of the zeolite framework structure. Fig. 4.20 showed the relative amount of Si/Al mole ratio and %crystallinity of zeolite depending on the type of acid and its concentration. Acetic acid solution prevents the hydrolysis of the silicon bonds and also lacks the ability of chelating silicon ions (Giudici, Kouwenhaven, and Prins, 2000). The Si/Al ratio of CH_3COOH treatment was less than other acids, but the %crystallinity was higher. Compared HNO_3 and HCl treatment, it was found that the Si/Al ratio of both acid solutions was similar, but %crystallinity with HCl treatment was higher than that with HNO_3 treatment. Both of HCl and HNO_3 are strong acid and effective to remove the Al^{3+} from the framework and they produce same amount of Si/Al mole ratio. Consequently, the strong acid is suitable for dealumination more than weak acid.

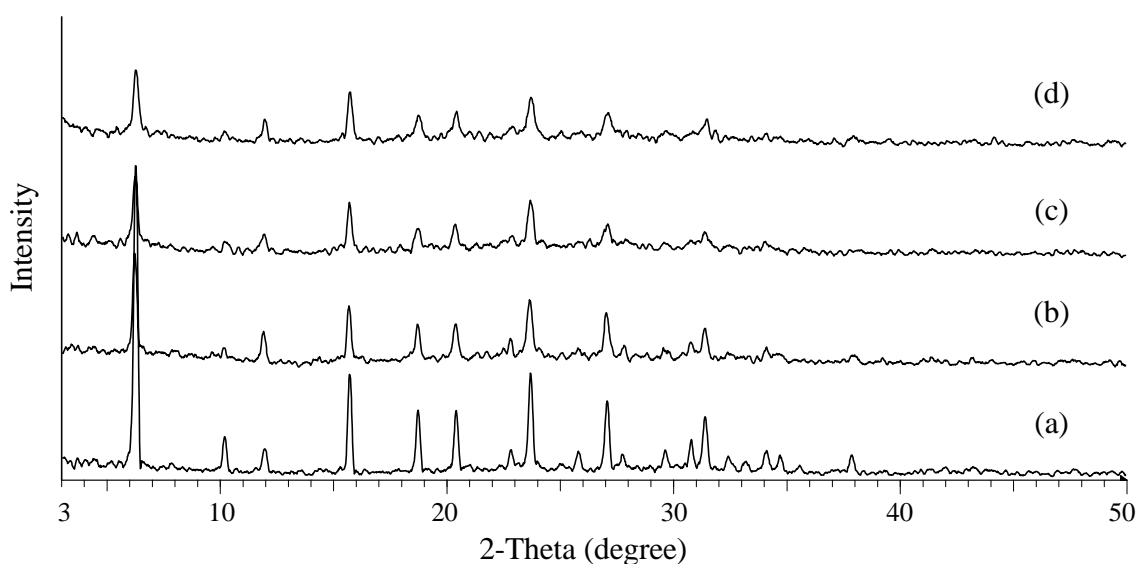


Figure 4.18 XRD patterns of HY dealuminated at various concentrations of acetic acid (CH_3COOH) at 60°C for 2 hours; (a) zeolite HY; (b) HY dealuminated at 0.1 M CH_3COOH ; (c) 0.2 M CH_3COOH ; (d) 0.3 M CH_3COOH .

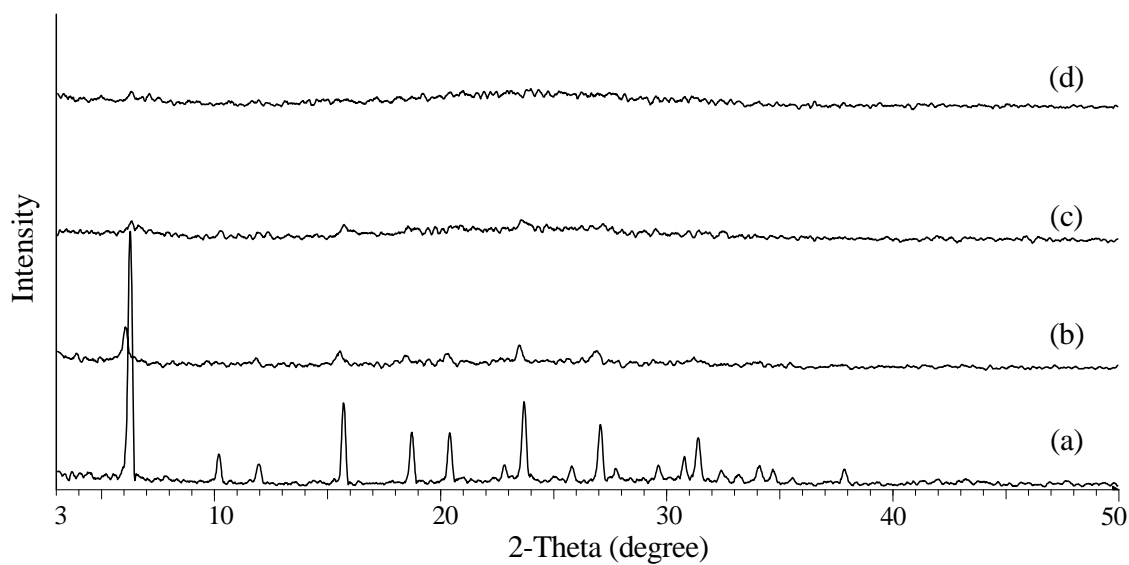


Figure 4.19 XRD patterns of HY dealuminated at various concentrations of nitric acid (HNO_3) at 60°C for 2 hours. (a) zeolite HY; (b) HY dealuminated at 0.1 M HNO_3 ; (c) 0.2 M HNO_3 ; (d) 0.3 M HNO_3 .

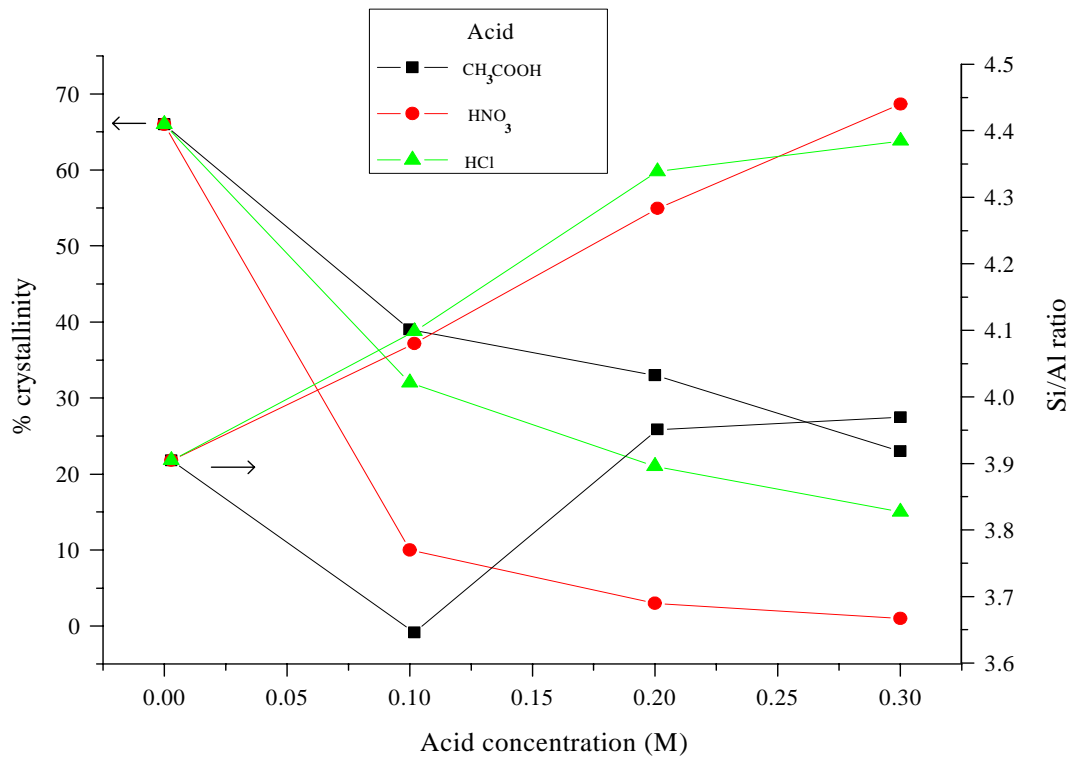


Figure 4.20 Plot of Si/Al ratio, %crystallinity and acid concentration.

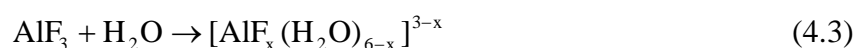
4.3 Dealumination with ammonium hexafluorosilicate (AHFS) treatment

The dealumination of zeolite NaY by AHFS treatment was performed under various concentrations of AHFS, in the presence and absence of buffer using ammonium acetate (NH₄OAc) and different mole ratio of AHFS/NH₄OAc.

4.3.1 Effect of the presence and absence of NH₄OAc on dealumination with AHFS

The experimental conditions of dealumination with AHFS treatment were shown in Table 4.5 and their results in Table 4.6. It was found that in the present of NH₄OAc (AHFS6) the %crystallinity was kept more than that in the absence of NH₄OAc (AHFS1) because of NH₄OAc used as buffer preventing the solution from becoming acidic. In the absence of NH₄OAc, the solution is more acidic to provide enough concentration of fluoride ion (F⁻) to remove aluminum from zeolite framework in form of AlF₆³⁻ and also F⁻ ions react with silanols at the surface. It maybe promotes the collapse of the zeolite framework. Thus, it is essential that the dealumination with AHFS has to contain NH₄OAc in the procedure, because NH₄OAc is able to extract Al³⁺ which reacts with F⁻ to form (NH₄)₃AlF₆ species as shown in eq. 4.1. One reported the proposed dealumination with AHFS as follows (Kao and Chen, 2003).

(a) In the presence of NH₄OAc



(b) In the absence of NH₄OAc

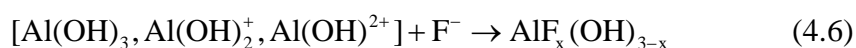
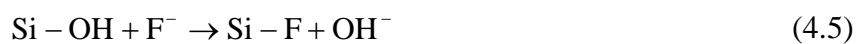
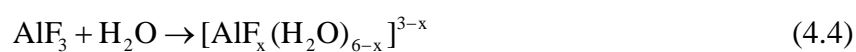


Table 4.5 The dealumination of zeolite NaY by AHFS treatment under various conditions.

Sample	Concentration of NH ₄ OAc (M)	Volume of NH ₄ OAc (ml)	Concentration of AHFS (M)	Volume of AHFS (ml)	AHFS/NH ₄ OAc mole ratio
AHFS1	-	-	0.05	15	-
AHFS2	1.0	50	0.05	15	0.015
AHFS3	1.0	50	0.25	15	0.075
AHFS4	1.0	50	0.5	15	0.15
AHFS5	1.0	100	-	-	0
AHFS6	1.0	100	0.05	15	0.0075
AHFS7	1.0	100	0.25	15	0.0375
AHFS8	1.0	100	0.5	15	0.075
AHFS9	1.0	100	0.75	15	0.1125
AHFS10	1.0	100	1.0	15	0.15
AHFS11	1.0	150	0.05	15	0.005

Table 4.5 (continued)

Sample	Concentration of NH₄OAc (M)	Volume of NH₄OAc (ml)	Concentration of AHFS (M)	Volume of AHFS (ml)	AHFS/NH₄OAc mole ratio
AHFS12	1.0	150	0.25	15	0.025
AHFS13	1.0	150	0.5	15	0.05
AHFS14	3.0	100	-	-	0
AHFS15	3.0	100	0.25	15	0.0125
AHFS16	3.0	100	0.5	15	0.025
AHFS17	3.0	100	0.75	15	0.0375
AHFS18	3.0	100	1.0	15	0.05

Notation of various concentrations of AHFS was described in Table 3.2 (see page 33)

4.3.2 Effect of AHFS and NH₄OAc concentration on AHFS dealumination

The results from dealumination in the presence and absence of AHFS were in Table 4.6. It was found that in the absence of AHFS (AHFS5) the percent crystallinity was kept more than that in the presence of AHFS (AHFS6), but the Si/Al ratio of absent AHFS was less than that of present AHFS. It indicated that the AHFS is important to increase Si/Al ratio because it removes the aluminum from the framework. In addition, the effect of AHFS concentration on dealumination was also considered. The percent crystallinity of the zeolite NaY was recorded before and after the dealumination treatment to determine the effect of the treatment on the zeolite structure (see Table 4.6). The loss of crystallinity increased with increasing the

concentration of AHFS. The AHFS-treated zeolite NaY had a Si/Al ratio about 4.9 - 11.3 and kept %crystallinity more than 50% (see Table. 4.6). On the other hand dealumination with HCl gave Si/Al ratio about 4 and %crystallinity was less than 50% (see Table 4.3). This may result from the silicon atoms of AHFS can directly replace the extract aluminium atoms, so the obtained dealuminated zeolite samples still maintain much of the crystallinity. FT-IR spectrum of O-T-O (T = Si or Al) asymmetric stretch shifted from 1006 to 1091 cm^{-1} ; symmetric stretch shifted from 780 and 730 to 808 and 732 cm^{-1} , respectively, and the intensity of double ring vibration decreased with increasing the concentration of AHFS. In IR spectra of AHFS18 showed the strong peak of O-Si-O symmetric stretch at 808 cm^{-1} (see Fig. 4.21). It was indicated that it gave a higher Si/Al ratio after dealuminated with AHFS. But the amorphous phase was occurring that showed in IR spectra. This result is consistent with the rules as mentioned in topic 4.2.

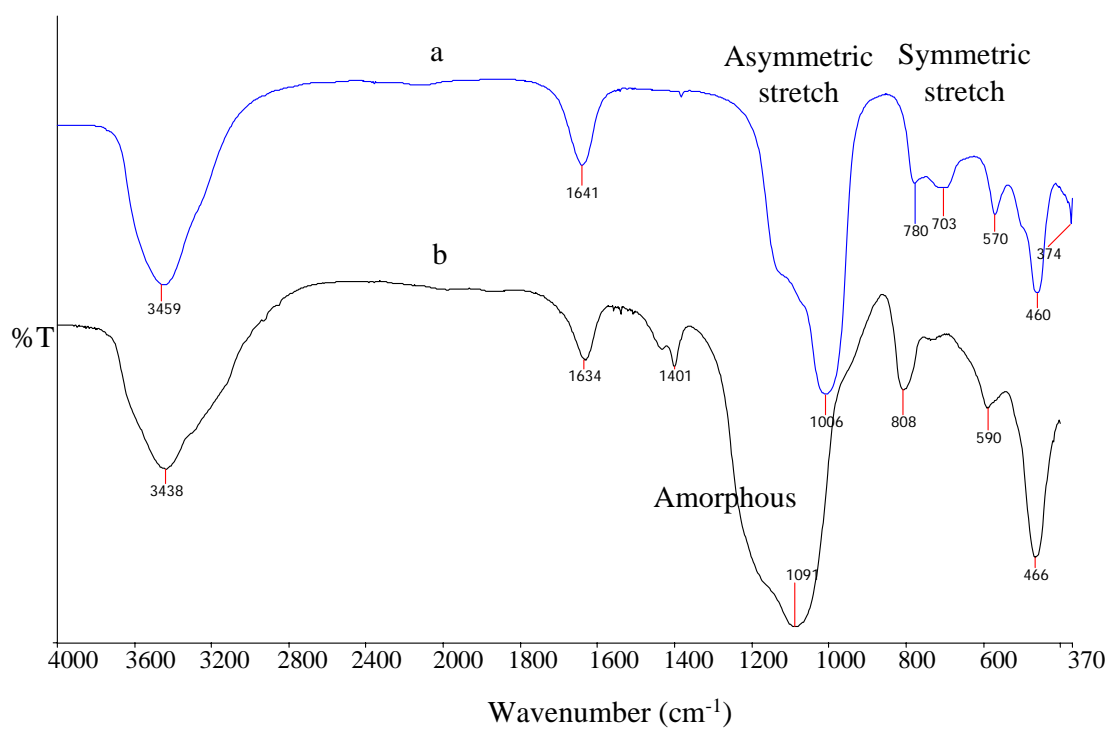


Figure 4.21 IR spectra of synthesized zeolite NaY (a) before and (b) after dealuminated of zeolite NaY with AHFS.

Table 4.6 The wave numbers, %crystallinity and Si/Al mole ratio of zeolite Y with AHFS dealumination.

Sample	Asymmetric stretch (1050 - 1150 cm ⁻¹)	Symmetric stretch (750 - 820 cm ⁻¹)	Double ring (~560 cm ⁻¹)	%Cry	Si/Al
NaY	1006 s	780 s, 703 m	570 s	100	3.7
AHFS1	1018 s	786 m, 713 m	573 w	79	4.9
AHFS2	1139mwsh, 1020s	785m,715m	573m	78	5.6
AHFS3	1170mwsh, 1060s	811s, 732mw	590m	66	9.3
AHFS4	1085s	811s, 712mw	590mw	20	10.6
AHFS5	1136 mwsh, 1006 s	777 m, 706 m	568 m	99	5.2
AHFS6	1136mwsh, 1012s	783m, 712m	570m	92	5.4
AHFS7	1159 mwsh, 1051 s	808 s, 729 mw	587 mw	82	6.7
AHFS8	1162 mwsh, 1071 s	814 s, 720 mw	590 mw	48	7.6
AHFS9	1168 mwsh, 1077 s	805 s, 723 mw	582 mw	41	7.9
AHFS10	1100s	800s, 718w	568mw	39	8.0
AHFS11	1135mwsh, 1009s	777m, 707m	567m	93	5.0
AHFS12	1153mwsh, 1046s	802s,726m	585m	81	6.4
AHFS13	1162mwsh, 1063s	811s, 720m	587mw	67	7.6
AHFS14	1136 mwsh, 1009 s	777 s, 709 m	568 m	98	5.5
AHFS15	1156 mwsh, 1032 s	797 s, 723 m	582 m	80	7.2
AHFS16	1170 mwsh, 1066 s	811 s, 729 m	590 m	49	8.1
AHFS17	1156 mwsh, 1057 s	805 s, 726 mw	577 m	48	9.2
AHFS18	1091 s	808 s, 732 w	590 w	21	11.3

Abbreviations: s, strong; ms, medium strong; m, medium; mw, medium weak; w, weak; sh, shoulder.

Fig. 4.22 showed the amount of Si/Al mole ratio of dealuminated zeolite NaY samples as a function of the amount of AHFS/NH₄OAc mole ratio. It was found that Si/Al ratio increased with increasing the AHFS/NH₄OAc mole ratio. The NH₄OAc at 0.3 mole at various concentrations of (NH₄)₂SiF₆ yielded the amount of Si/Al ratio very sharp from 5.5 - 11.3, whereas the amount of Si/Al mole ratio of the obtained 0.15, 0.1, and 0.05 mole of NH₄OAc were slightly increased with increasing concentration of (NH₄)₂SiF₆.

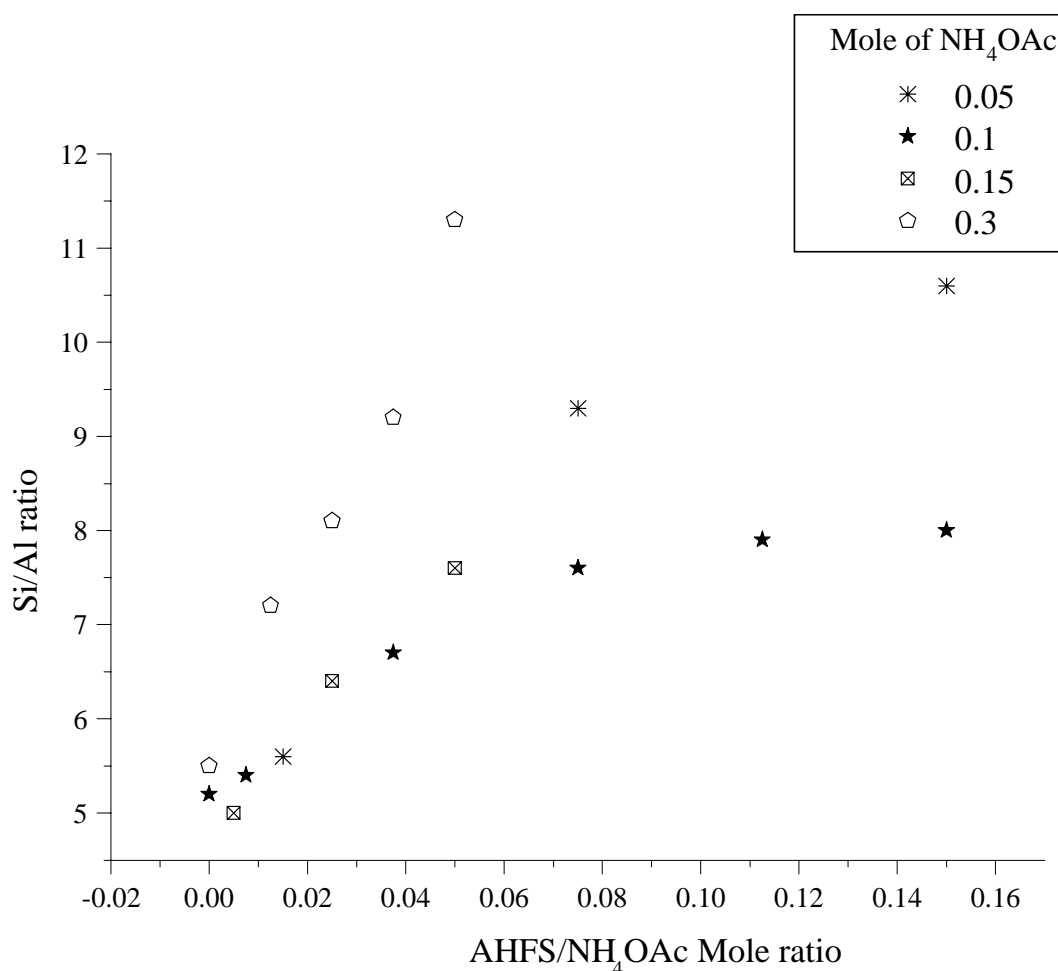


Figure 4.22 Plot of Si/Al ratio and AHFS/NH₄OAc mole ratio.

In addition, the %crystallinity decreased with increasing the AHFS/NH₄OAc mole ratio (see Fig. 4.23). It was very sharply decreased from 98 to 21% for the 0.3 mole of NH₄OAc more than that of 0.15, 0.1, and 0.05 mole of NH₄OAc. Therefore, the strong increase in Si/Al mole ratio affects the strong decrease in %crystallinity. When the obtained dealuminated zeolite Y with Si/Al mole ratio was more than 11.3, its structure was almost destroyed (%crystallinity obtained less than 21%).

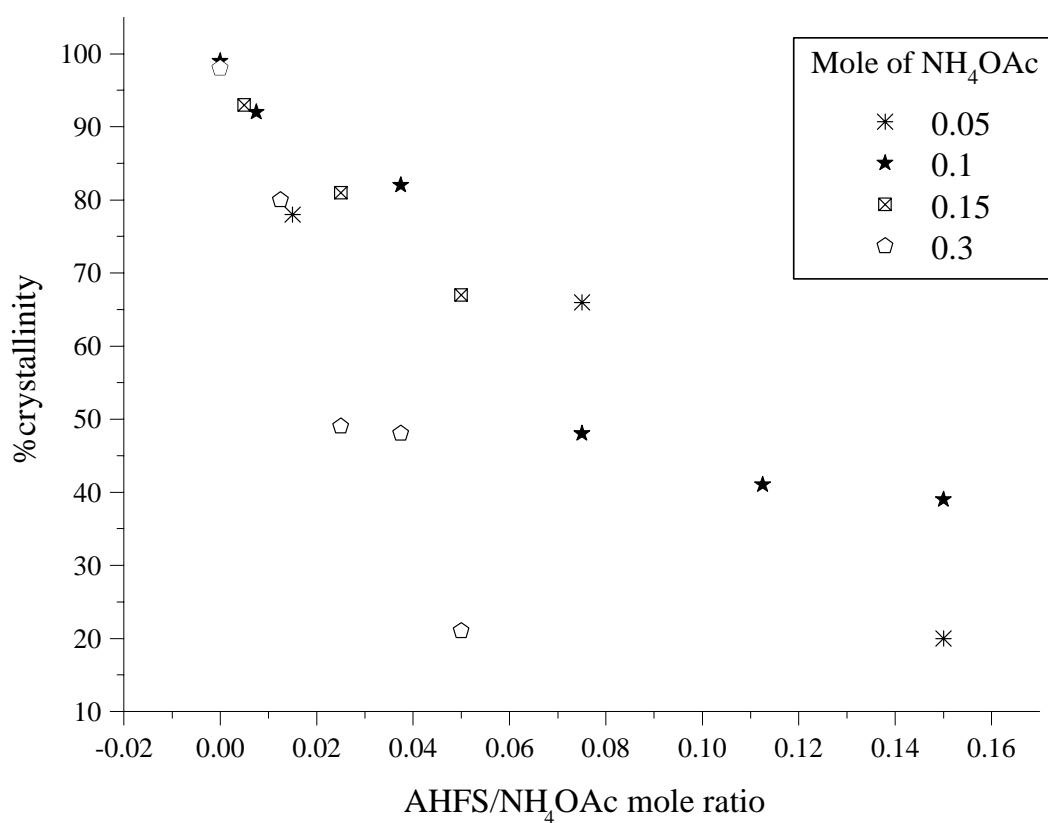
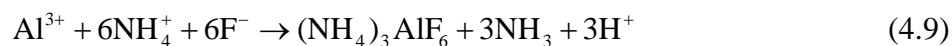


Figure 4.23 Plot of percent crystallinity and AHFS/NH₄OAc mole ratio.

Dealumination with AHFS is found to be convenient to dealuminate zeolite Y as HCl dealumination. However, AHFS dealumination method has more advantage that the yield from this method contains higher mole ratio of Si/Al (in the range of 3.9 - 11.3) and higher %crystallinity (in the range of 99 - 21%). The amount of Si/Al ratio and percent crystallinity for each sample was summarizing in Fig. 4.24. We show the previous mechanism as shown in eqs. 4.7 - 4.9 (Kao and Chen, 2003). The mechanism consists of the following steps. AHFS is very soluble in water (eq. 4.7), and SiF_6^{2-} undergoes hydrolysis as in eq. 4.8. Thus, AHFS can be used as the source for silicon fluoride. During AHFS dealumination in the presence of NH_4OAc , aluminum is first extracted from the framework leaving a vacancy in which silicon is inserted in a second step. It has been suggested that aluminum is removed in the form of AlF_6^{3-} ions (eq. 4.9).



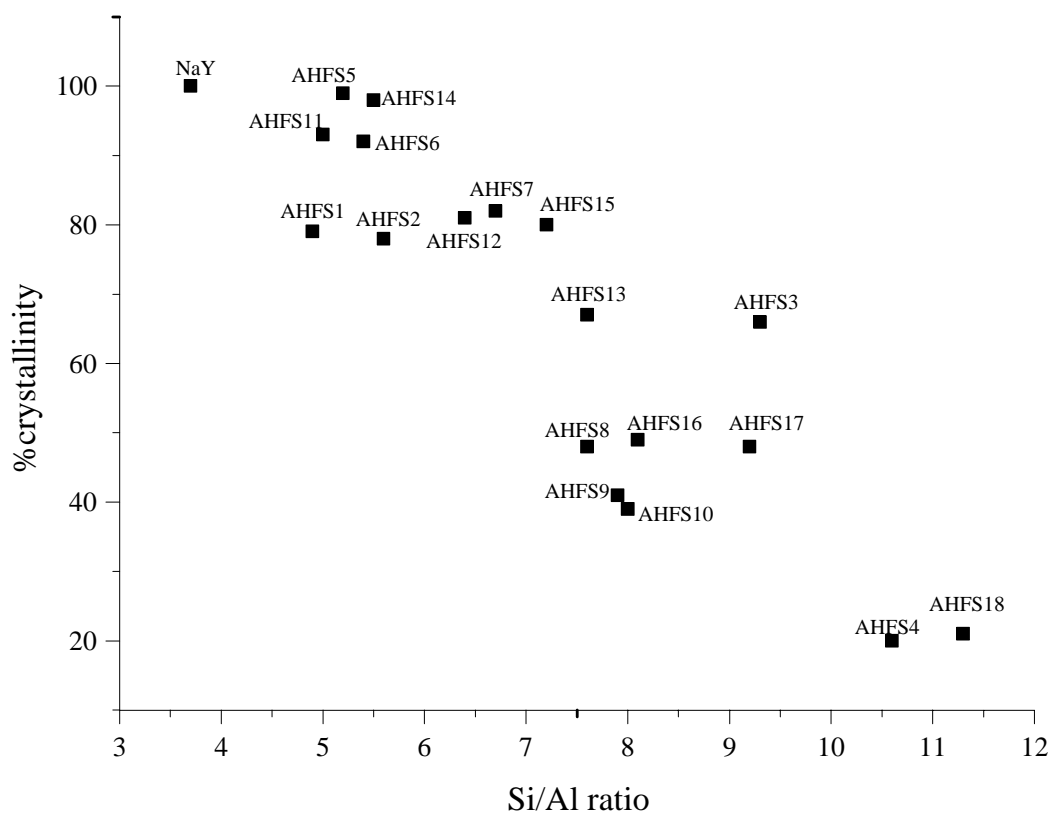


Figure 4.24 Relation of between %crystallinity and Si/Al ratio of dealuminated NaY by AHFS method.

4.4 The effect of cation and anion on dealumination with ammonium hexafluorosilicate (AHFS)

The samples of LiY, NaY and KY were exchanged with Li⁺, Na⁺ and K⁺, respectively, in the solution of chloride and nitrate salts. The degrees of dealumination of the three cations forms under several conditions were compared (see Table 3.4). The results in Table 4.7 showed the mole ratio of cation:Na⁺, percent crystallinity and Si/Al ratio. The step in ion exchange before dealuminating step was also considered. It found that ion exchange alone had slightly effect on the Si/Al ratio. But an exchange with K⁺ gave the %crystallinity (57 - 62%) less than that with Li⁺ and Na⁺ (77 - 88% and 78 - 86%). It may result from the size of cation. The bare ionic size of K⁺ (1.50Å) is larger than that of Li⁺ (0.76Å) and Na⁺ (1.02Å). The larger size can damage the structure of zeolite more than the small size.

In addition, the effect of anion on the loss of %crystallinity was considered. It was found that washing Cl⁻ and NO₃⁻ (LiY1, LiY3, NaY1, NaY3, KY1, and KY3) kept the %crystallinity more than without washing (LiY2, LiY4, NaY2, NaY4, KY2, and KY4) under the same conditions. It may be that Cl⁻ and NO₃⁻ diffuse in the structure of zeoliteY during cation exchanging. It may affect to collapse zeolite framework.

In the dealumination with AHFS (3M NH₄OAc 100ml, 0.5M AHFS) to produce the higher Si/Al ratio, It was found that the Na form could be dealuminated with higher degree of Si/Al ratio (8.1) and %crystallinity (49%). Therefore, the Na form in zeolite Y was suitable for dealumination than the others. This may be the size of Na⁺ suitable for dealumination.

Considering two cations (Li^+ and K^+) for dealumination (sample LiY1D and KY1D) it was found that LiY1D could produce higher Si/Al ratio of about 7.9 than KY1D (Si/Al ratio of about 7.1). Again Li form is clearly easier to dealuminate than the K form. This is probably due to the Li cation being smaller, leaving a wider free pore channel within which the AHFS molecule can diffuse more easily (Bartl *et al.*, 1996).

Table 4.7 The effect of mole ratio of cation: Na^+ on dealumination of zeolite NaY by AHFS treatment under various conditions.

Sample	$\text{Li}^+:\text{Na}^+$ mole ratio	$\text{K}^+:\text{Na}^+$ mole ratio	%Cry	Si/Al
Zeolite NaY			100	3.7
LiY1	1.5	0.7	86	3.7
LiY2	1.6	-	82	3.8
LiY3	1.6	-	88	3.8
LiY4	1.6	-	77	3.9
LiY1D	1.2	-	26	7.9
LiY2D	1.2	-	0	5.6

Table 4.7 (continued)

Sample	Li ⁺ :Na ⁺ mole ratio	K ⁺ :Na ⁺ mole		%Cry	Si/Al
		ratio			
NaY1	-	-	-	83	4.1
NaY2	0.02	-	-	80	4.0
NaY3	0.01	-	-	86	4.1
NaY4	0.01	-	-	78	4.0
NaY1D	-	-	-	49	8.1
NaY2D	0.01	-	-	35	5.3
KY1	0.01	2.4	2.4	57	4.0
KY2	0.01	2.4	2.4	49	4.0
KY3	-	2.4	2.4	67	3.9
KY4	-	2.5	2.5	62	3.8
KY1D	-	2.4	2.4	37	7.1
KY2D	-	2.4	2.4	0	5.5

Notation of various concentrations of AHFS was described in Table 3.4 (see page 37).

Table 4.8 The wavenumbers of zeolite Y with AHFS dealumination.

Sample	Asymmetric stretch (1050 - 1150 cm ⁻¹)	Symmetric stretch (750 - 820 cm ⁻¹)	Double ring (~560 cm ⁻¹)
LiY1	1130 sh, 1010 s	783 m, 703 s	571 s
LiY2	1130 sh, 1044 s	780 m, 702 s	568 s
LiY3	1136 sh, 1010 s	780 m, 703 s	571 s
LiY4	1130 sh, 1007 s	778 m, 702 s	572 s
LiY1D	1096 s	808 s, 730 w	587 mw
LiY2D	1099 s	800 s	557 wsh
NaY1D	1099 s	809 s, 736 mw	590 s
KY1D	1099 s	798 s, 725 w	579 m

Abbreviations: s, strong; ms, medium strong; m, medium; mw, medium weak; w, weak; sh, shoulder.

When we considered of Cl⁻ (LiY2D and KY2D) on dealumination the amorphous phase completely occurred. It may be that Cl⁻ affected the AHFS dealumination mechanism. Cl⁻ might be interfered F⁻ to form (NH₄)₃AlF₆ complex in AHFS dealumination. Therefore, Si/Al was only about 5.3 - 5.6. The Fig. 4.25 showed the relation of percent crystallinity and Si/Al ratio of cation and anion on AHFS dealumination.

From the IR results it also showed the structure collapsed by Cl^- (see Table 4.8). Symmetric stretch of double ring at 577 cm^{-1} which indicates the crystal phase showed very weak intensity in the case of sample containing Cl^- (LiY2D).

We have demonstrated the feasibility of dealuminated zeolite Y with AHFS after exchanging the original Na form into Li and K form. Higher degree of dealumination was preferred in Na form and remained essentially crystallite than Li and K form.

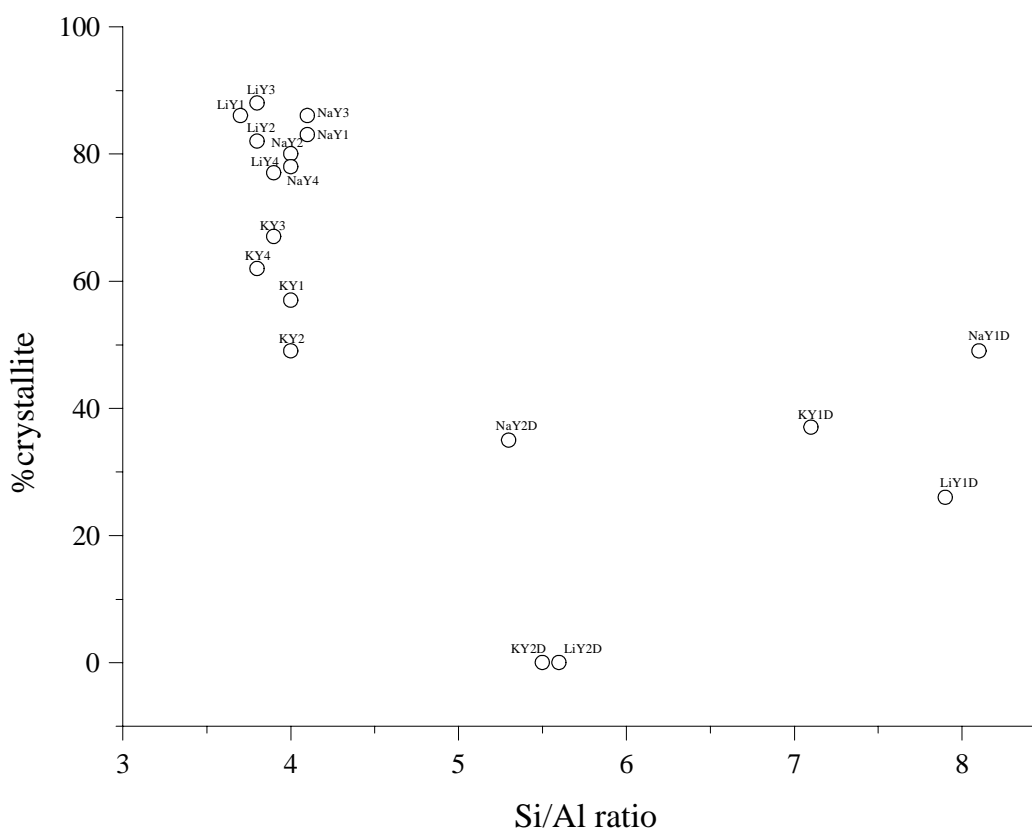


Figure 4.25 %crystallinity related to with Si/Al ratio for dealuminated LiY and KY by AHFS. Notation of various conditions was described in Table 3.4 (see page 37).

Fig. 4.26 showed %crystallinity relative to Si/Al ratio obtained from dealumination with AHFS and HCl. It was found that AHFS method (solid line) produced higher amount of Si/Al and percent crystallinity more than HCl method (dash line). Because of AHFS dealumination in the presence of NH_4OAc , aluminum is first extracted from the framework leaving a vacancy in which silicon is inserted in a second step. In addition, the effect of cation and anion on AHFS dealumination and ion exchange were also showed in Fig. 4.26.

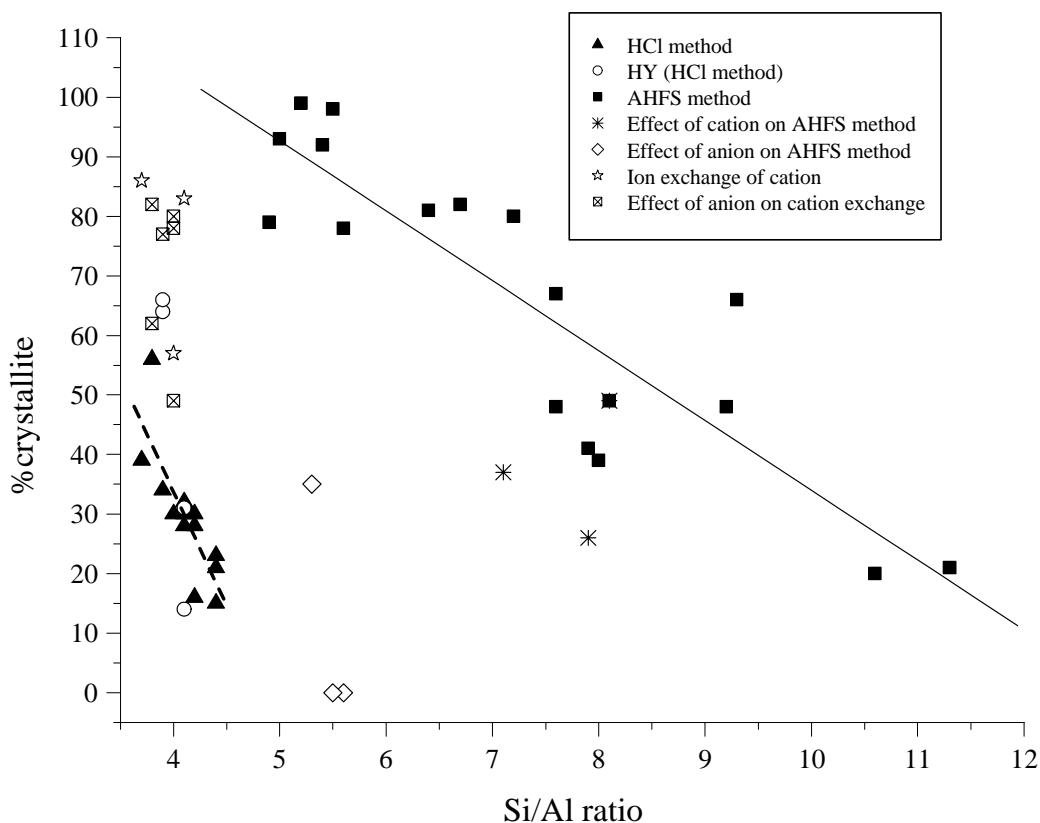


Figure 4.26 %crystallinity related to Si/Al ratio for dealumination of zeolite Y with AHFS and HCl, the effect of cation and anion on dealuminated zeolite Y by AHFS and ion exchange.

Table 4.9 The surface area, micropore volume and pore size were recorded before and after different dealuminations.

Sample	Si/Al ratio	%cry	BET surface (m²g⁻¹)	Micropore volume (cm³g⁻¹)	Average pore size (Å)
Zeolite NaY	3.7	100	916	0.40	19.2
HCl5	4.1	28	314	0.09	15.3
LiY1D	7.9	26	473	0.12	85.9
NaY1D	8.1	49	499	0.16	63.1
KY1D	7.1	37	122	0.04	63.5

The surface area, micropore volume and pore size were recorded before and after different dealuminations (see Table 4.9). It was found that surface area and micropore volume decreased whereas average pore size increased after dealumination. This may result from that Al atom was removed from the frameworks, then the structure collapsed. Consequently, the sample contained more amorphous phase. In the case of the effect of cation on dealumination, it showed that both the BET surface area and micropore volume decreased with increase in the cationic size of exchanged cation, excepted the Na form. It indicated that Na ion was suitable form for dealumination of zeolite Y.

4.5 Dealumination with Silicon tetrachloride (SiCl₄) treatment

The dealumination of zeolite NaY by SiCl₄ treatment carried out by dehydrated NaY under a nitrogen flow in reactor. Then, it was dealuminated with silicon tetrachloride vapor at various times and temperatures. The samples were treated further with a flow of dried nitrogen to remove residual SiCl₄. In this method was studied the effect of temperature, time and nitrogen flow rate on SiCl₄ dealumination. The experimental conditions of dealumination with SiCl₄ treatment were shown in Table 4.10

Table 4.10 The amount of Si/Al ratio and percent crystallinity of dealuminated zeolite Y by the SiCl₄ at various conditions.

Sample	Position of generated SiCl ₄		Temperature of generated SiCl ₄ (°C)	Reaction time (hours)	Reaction temperature (°C)	N ₂ Flow		Si/Al	%cry
	Inside	Outside				During reaction	After reaction		
	✓	-	✓	-					
S1	✓	-	25	24	25	-	-	4.3	24
S2	✓	-	25	96	25	✓	-	4.9	21
S3	✓	-	25	96	25	-	-	4.9	19
S4	-	✓	25	6	500	✓	-	5.7	46
S5	-	✓	25	4	500	✓	✓	5.5	70
S6	-	✓	40	4	500	✓	✓	5.8	73
S7	-	✓	40	4	500	✓	-	4.2	74
S8	-	✓	25	4	500	✓	-	4.1	76
S9	-	✓	25	4	25	✓	✓	4.1	67

Table 4.10 (continued)

Sample	Position of generated		Temperature of generated	Reaction time	Reaction temperature	N ₂ Flow		Si/Al	%cry
	SiCl ₄					SiCl ₄ (°C)	(hours)		
	Inside	Outside	reaction	reaction					
S10	-	✓	25	4	150	✓	✓	4.3	53
S11	-	✓	25	4	200	✓	✓	4.4	70
S12	-	✓	25	4	250	✓	✓	4.9	70
S13	-	✓	25	4	300	✓	✓	4.9	70
S14	-	✓	25	4	350	✓	✓	4.1	74
S15	-	✓	25	4	400	✓	✓	4.1	71
S16	-	✓	65	6	500	✓	✓	5.7	46
S17	-	✓	65	8	500	✓	✓	5.8	53
S18	-	✓	65	10	500	✓	✓	6.0	47

Notation of various conditions is described in Table3.3 (see page 36).

4.5.1 Effect of dehydration on SiCl₄ dealumination

The XRD pattern of a sample NaY and dehydrated NaY at 200°C for 2 hours was shown in Fig. 4.27. It was found that dehydrated NaY remained the crystallinity of 71%. It generally believes that the collapse of zeolite structure during dehydration is due to the presence of exchangeable cations (Bartl *et al.*, 1996). When removing the water molecule ligands, the cations must coordinate directly to the oxygen in the framework. Because of their high charge density, the cation can distort

the framework. The distortion in zeolite is so serious that some of the bonds connected to tetrahedral atoms (silicon or aluminium) are broken.

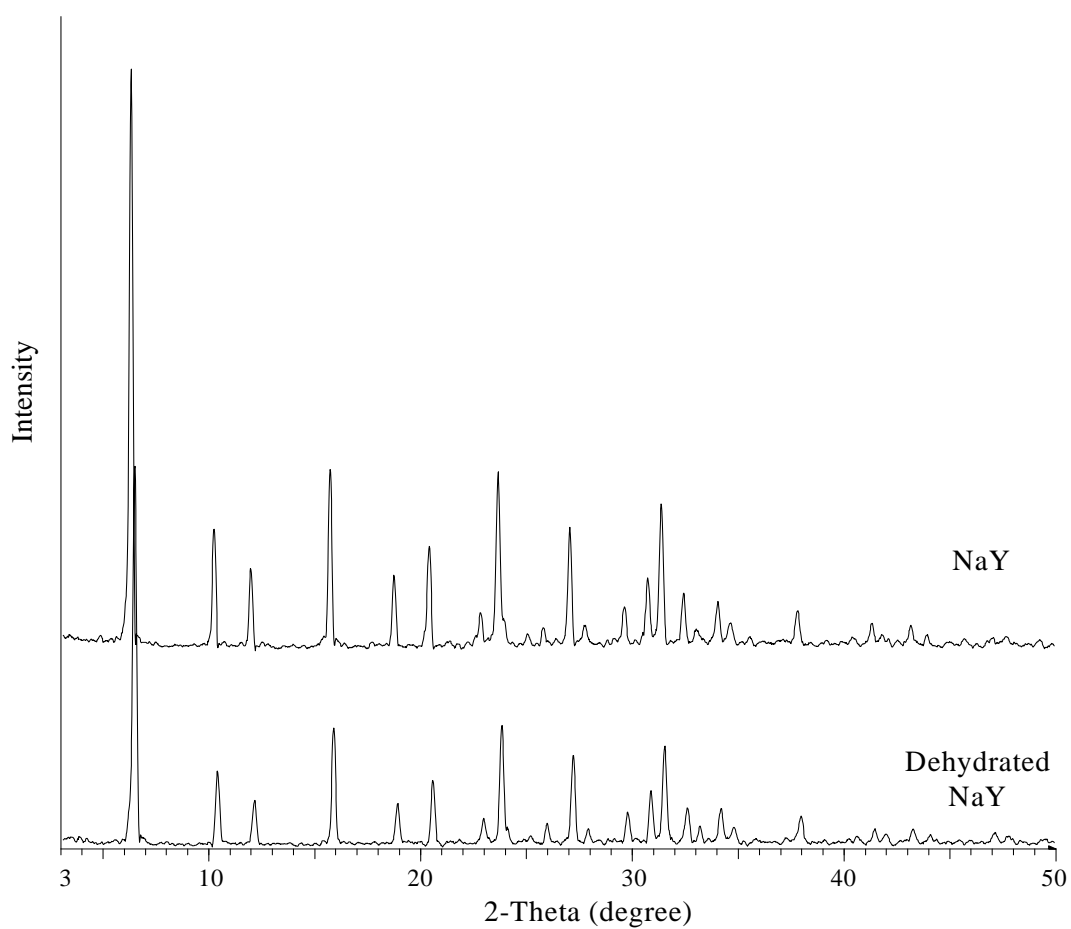


Figure 4.27 XRD patterns of NaY and dehydrated NaY at 200°C for 2 hours.

In this procedure the dehydrated NaY was used to dealuminate with SiCl_4 vapor. The XRD patterns of obtained dealuminated NaY and also dehydrated NaY were shown in Fig. 4.28. It was found that %crystallinity of dealuminated NaY and dehydrated NaY was slightly different. The %crystallinity of dealuminated NaY and dehydrated NaY was about 20% and 21%, respectively.

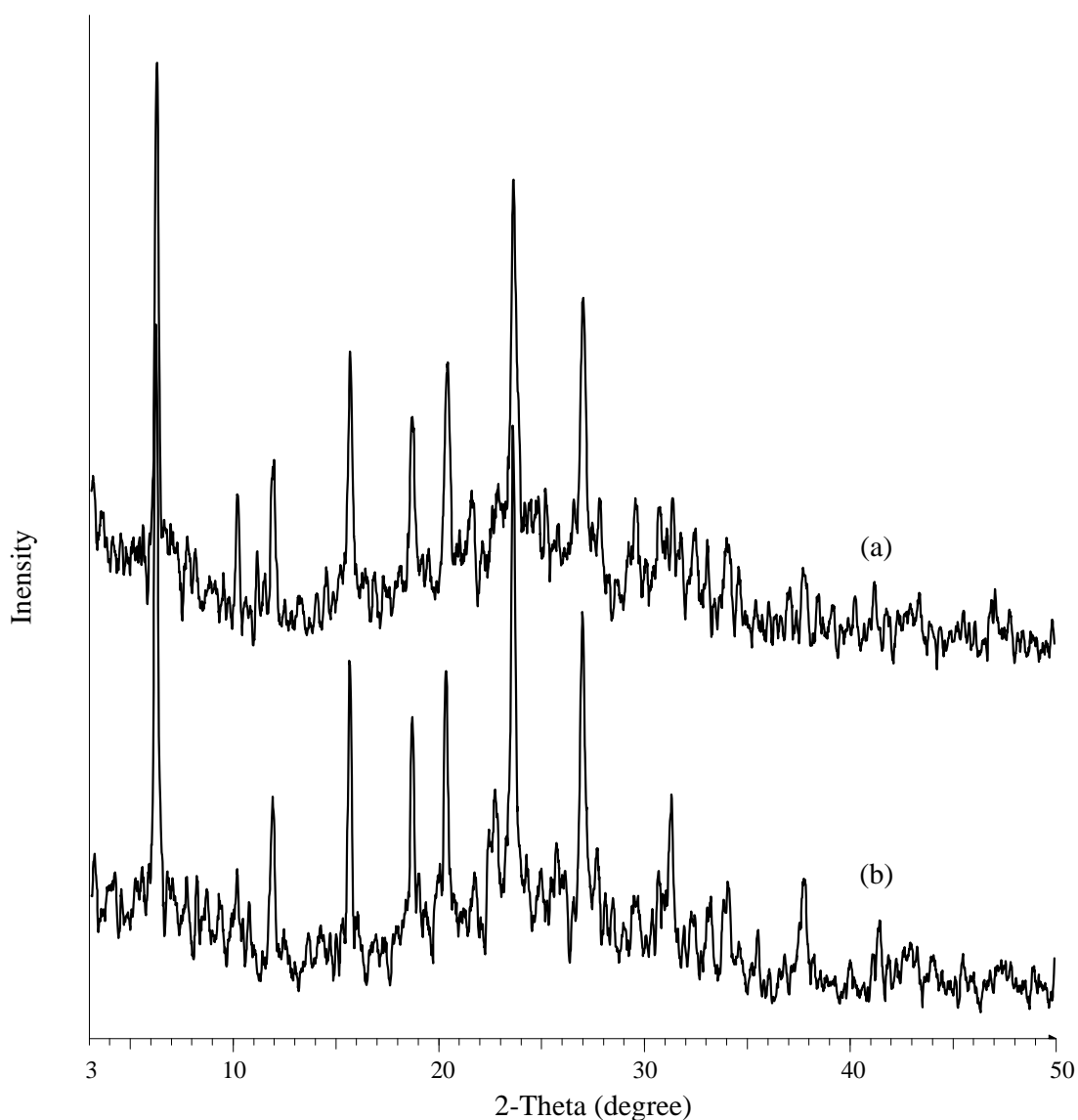


Figure 4.28 XRD patterns of dealuminated NaY with SiCl_4 (a) NaY dealuminated from hydrated zeolite NaY; (b) NaY dealuminated from dehydrated zeolite NaY.

4.5.2 Effect of concentration of SiCl₄ vapor and N₂ flowing on dealumination

Based on the experiment designed in some conditions dehydrated NaY samples were directly approached with saturated SiCl₄ vapor at 25°C in the reactor. The framework of obtained zeolite after treatment was severely destroyed. When reducing SiCl₄ vapor by generating it outside reactor, it was found that the obtained sample still contained %crystallinity about 46%. It indicated that concentration of SiCl₄ vapor is important because it can damage the zeolite framework. In addition, flowing N₂ (S2) in reactor kept the %crystallinity more than without flowing N₂ (S3) (see Fig. 4.29). It may be that SiCl₄ vapor was dilute to contact mildly at zeolite framework.

The Si/Al mole ratio results from ICP-MS were shown in the Table 4.11. In the case of S2 and S3 Si/Al mole ratio was the same. It indicates the flowing N₂ giving no effect on increasing Si/Al mole ratio in the reaction step. But the flowing N₂ after reaction ended can remove the residual phase. Therefore, it could be increased the Si/Al ratio (see Table 4.12). In addition, temperatures and times for dealumination in this method were considered in the next part.

Table 4.11 The %crystallinity and Si/Al mole ratio of dealuminated zeolite NaY with SiCl₄ vapor depending on the concentration of SiCl₄ and flowing N₂.

Sample	Concentration of SiCl₄	Flowing N₂ during reaction	%Cry	Si/Al mole ratio
S1	Inside	-	24	4.3
S2	Inside	✓	21	4.9
S3	Inside	-	19	4.9
S4	Outside	✓	46	5.7

Notation of various conditions was described in Table 3.3 (see page 36).

Table 4.12 The %crystallinity and Si/Al mole ratio of dealuminated zeolite NaY with SiCl₄ vapor depending on the flowing N₂ after reaction for removing residual.

Sample	Flowing N₂ after reaction	%Cry	Si/Al mole ratio
S5	✓	70	5.5
S6	✓	73	5.8
S7	-	74	4.2
S8	-	76	4.1

Notation of various conditions is described in Table 3.3 (see page 36).

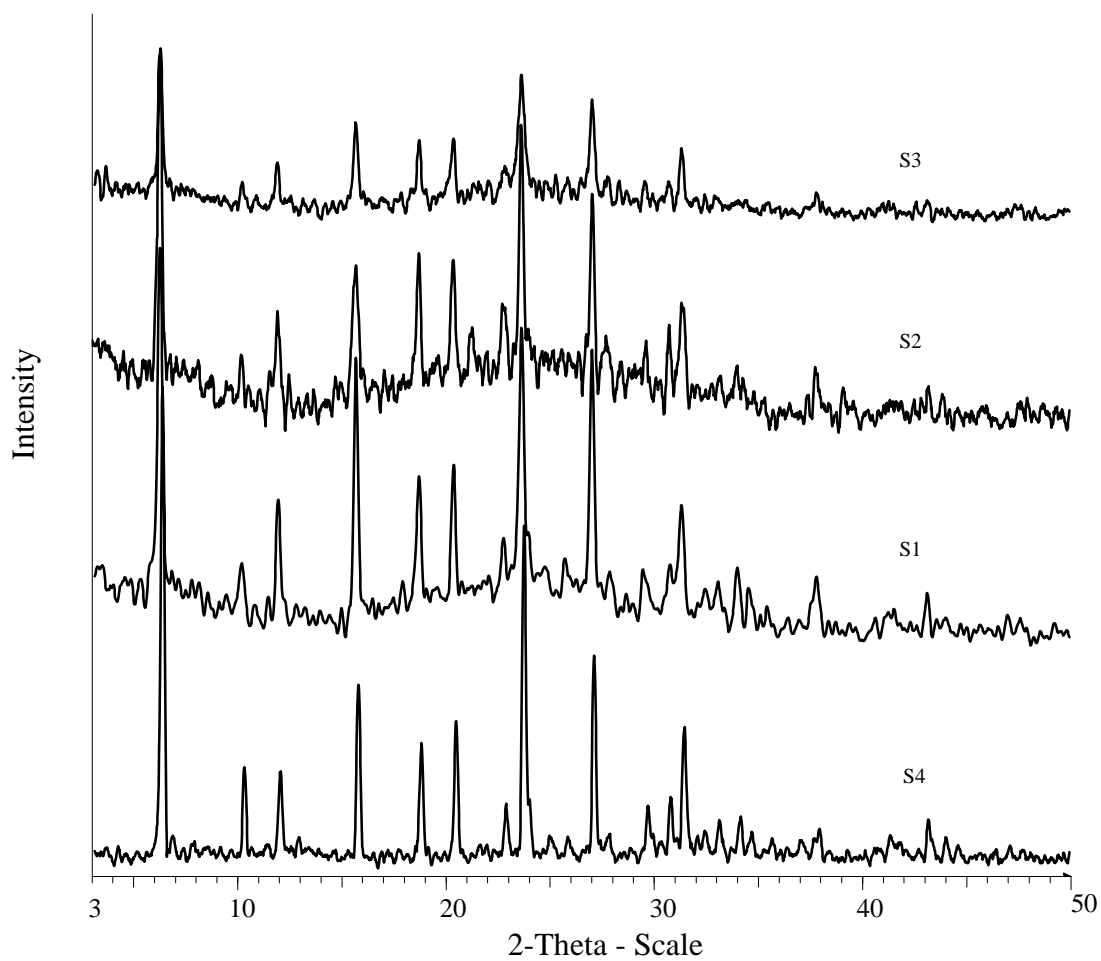


Figure 4.29 XRD patterns of dealumination of NaY with SiCl_4 vapor.

4.5.3 Effect of reaction temperatures on SiCl₄ dealumination

The dealumination at low temperatures ($\leq 200^\circ\text{C}$) Si/Al mole ratio was about 4.1-4.4, but higher temperatures ($\geq 200^\circ\text{C}$) Si/Al mole ratio was about 5, especially at 500°C Si/Al about 5.5 (see Table 4.13). Hence, reaction temperature at 500°C was selected for consideration further on the effect of reaction times.

Table 4.13 The %crystallinity and Si/Al mole ratio of dealuminated zeolite NaY with SiCl₄ vapor depending on temperatures.

Sample	Reaction temperature ($^\circ\text{C}$)	%Cry	Si/Al mole ratio
S9	25	67	4.1
S10	150	53	4.3
S11	200	70	4.4
S12	250	70	4.9
S13	300	70	4.9
S6	500	70	5.5

Notation of various conditions is described in Table 3.3 (see page 36).

4.5.4 Effect of reaction times on SiCl₄ dealumination

Table 4.14 The %crystallinity and Si/Al mole ratio of dealuminated zeolite NaY with SiCl₄ vapor depending on reaction times.

Sample	Reaction times	%Cry	Si/Al mole ratio
S7	4	73	5.8
S16	6	46	5.7
S17	8	53	5.8
S18	10	47	6.0

Notation of various conditions is described in Table 3.3 (see page 36).

The dealumination with SiCl₄ vapor depends on the reaction times (see Table 4.14). It was found that Si/Al ratio increased with increasing the reaction times, but the %crystallite decreased with increasing the reaction times. It indicated that more reaction time it took, more %crystallite was destroyed. The mechanism of SiCl₄ dealumination was proposed in eq. 4.10 (Beyer *et al.*, 1985). The aluminum is first extracted from the framework leaving a vacancy in which silicon is inserted in a second step.



In the previous literature reviews for SiCl₄ treatment it can produce the high Si/Al ratio (in the range of 10 - 100). However, in this work the obtained dealuminated NaY with this method was about 3.7 - 6.0. Because of that

dealumination with SiCl_4 was very difficult to perform when compared with the others. There are a lot of factors that were previously mentioned, affecting the dealumination. In addition, the equipment used in this study was not sufficiently appropriate to carry out the dealumination, because it has been just begun to set up. It has to take long times to develop the equipment. Therefore, the results in this study that will be used as guideline to provide some informations in the future study.

CHAPTER V

CONCLUSION

The dealumination of sodium Y zeolite by hydrochloric (HCl), ammonium hexafluorosilicate (AHFS) and silicon tetrachloride (SiCl_4) has been studied. The zeolite samples before and after dealumination in different methods were characterized by XRD, FT-IR, ICP-MS, DTA, SEM, BET and particle size analysis.

The dealumination with HCl was found to be convenient to dealuminate zeolite Y. It produced the Si/Al mole ratio in the range of 3.9 - 4.4 with %crystallinity from 64 - 16%. When the obtained dealuminated zeolite Y with Si/Al mole ratio was more than 4.4, its structure almost destroyed (%crystallinity obtained about 16%) with the HCl concentration more than 0.3 M. In the step of ion exchange process to transform NaY to NH_4Y , it was found that NH_4NO_3 solution kept percent crystallinity more than NH_4Cl solution due to Cl^- that can damage zeolite framework. The temperature at 500°C was suitable for changing NH_4Y into HY in calcination process. In addition, the effects of organic (CH_3COOH) and inorganic acid (HNO_3) on dealumination were also examined. The Si/Al ratio depending on CH_3COOH treatment was found to be less than that HNO_3 treatment, but the percent crystallinity obtained was higher. Compared HNO_3 and HCl treatment, it was found that the Si/Al mole ratio of both acid solutions was similar, but HCl treatment kept the percent crystallinity more than HNO_3 treatment.

Dealumination with AHFS was convenient to dealuminate zeolite Y as HCl dealumination. However, AHFS dealumination method has more efficiency to dealuminate. The yield from this method contains higher mole ratio of Si/Al (in the range of 5.2 - 11.3) and higher %crystallinity (in the range of 99 - 21%). In the presence of NH₄OAc the percent crystallite was kept more than that in the absence of NH₄OAc because of NH₄OAc working as a buffer preserving the pH of the solution. Therefore, the mole ratio of AHFS/NH₄OAc is considerable. It was found that Si/Al ratio increased with increasing AHFS/NH₄OAc. According to AHFS method, which produced the higher amount of Si/Al and higher percent crystallinity more than HCl method, it results from that aluminum atom is first extracted from the framework leaving a vacancy in which silicon is inserted in a second step. However, the Si/Al mole ratio was related with percent crystallinity by the way that Si/Al ratio increases whereas percent crystallinity decreases. In addition, after dealumination the surface area and micropore volume decrease whereas average pore sizes increase.

The effect of cation and anion on dealumination with AHFS was found that, higher degree of dealumination preferred in Na form more than in Li and K form and it still remained more crystallite phase, In addition, the surface area and micropore volume of Na form are higher than that of Li and K form. In the case of anion effect, it was found that, Cl⁻ influenced on the AHFS dealumination. It may interfere F⁻ to form (NH₄)₃AlF₆ complex in the machamism of AHFS dealumination.

In the results of SiCl₄ dealumination it showed the collapse of zeolite framework at higher concentration of SiCl₄ vapor. The Si/Al mole ratio increased with increasing reaction time and temperature. The reaction temperature at 500°C was selected for SiCl₄ dealumiantion. In addition, N₂ flowing in reactor kept the percent

crystallinity more than without N₂ flowing. It may be that SiCl₄ vapor was diluted to contact mildly at zeolite framework. Nevertheless, SiCl₄ treatment in this work gave mole ratio of Si/Al about 3.7 - 6.0 and kept %crystallinity about 70%. The results in this work contrasted with the previous literature review of SiCl₄ treatment (giving high Si/Al mole ratio about 10 - 100). Since, it was depended on a lot of factors such as reaction temperature, time and N₂ flowing. In addition, the equipment was not sufficiently appropriate to be used for dealumination.

REFERENCES

REFERENCES

- Anderson, M. W. and Klinowski, J. (1986). Zeolites treated with silicon tetrachloride vapour. **J. Chem. Soc., Faraday Trans. 1.** 82: 1449-1469.
- Bartl, P. and Hölderich, W. F. (2000). A study of the dealumination methods for zeolite L. **Micropor. Mesopor. Mater.** 38: 279-286.
- Bartl, P., Zibrowius, B., and Hoelderich, W. (1996). Dealumination of zeolite L with SiCl₄: influence of ion exchange. **Chem. Commun.** 6: 1611-1612.
- Barrer, R. M. and Makki, M. B. (1964). **Can. J. Chem.** 42: 1481.
- Belenkaya, I. M., Dubinin, M. M., and Krishtofom, I. I. (1967). **Izv. Akad. Nauk SSSR. Ser. Khim.** 10: 2164.
- Bell, R. G. (2001). **What are zeolites.** [on-line]. Available: <http://www.bza.org/zeolites.html>.
- Beyer, N. K., Belenykaya, M. I., and Hange, F. (1985). Preparation of high-silica faujasites with silicon tetrachloride. **Chem. Soc., Faraday Trans. 1.** 81: 2889-2901.
- Beyer, N. K. and Belenkaya, I. (1980). Catalysis by Zeolites. **Proc. Intern. Symposium.** 4: 481.
- Bhatia, S. (1990). **Zeolite Catalysis: Principles and Applications**, CRC Press, Inc., Boca Raton, Florida.
- Breck, D. W. (1974). **Zeolite Molecular Sieves**. New York: Wiley.
- Cheetham, A. K. and Day, P. (1992). **Solid State Chemistry Compounds**. Oxford. 226.

- Do, D. D. (1998). **Adsorption analysis: Equilibria and kinetics**. London: Imperial College.
- Dyer, A. (1988). **An Introduction to Zeolite Molecular Sieves**. New York: John Wiley & Sons.
- Ermolenko, N. F. and Shirinskaya, L. P. (1984). **Inorganic Ion Exchange Materials**. Lenin State Univ: Leningrad.
- Farrauto, R. J. (1997). **Fundamentals of Industrial Catalytic Processes**. London: Blackie Academic.
- Fejes, P., Kiricsi, I., Hannus, I., Kiss, A., and Schobel, G. (1980). **React. Kinet. Catal. Lett.** 14: 481.
- Fitzgerald, J. J., Hamza, A. I., Bronnimann, C. E., and Dec, S. F. (1997). Studies of the Solid/Solution "Interfacial" Dealumination of Kaolinite in HCl(aq) Using Solid-State ^1H CRAMPS and SP/MAS ^{29}Si NMR Spectroscopy. **J. Am. Chem. Soc.** 119: 7105-7113.
- Ginter, D. M., Bell, A. T., and Radke, C. J. (2005). **Synthesis zeolite** [online]. Available : <http://www.iza-online.org/synthesis/default.htm>.
- Giudici, R., Kouwenhoven, H. M., and Prins, R. (2000). Comparison of nitric and oxalic acid in the dealumination of mordenite. **Appl. Catal. A: Gen.** 203: 101-110.
- Grey, C. P., Poshni, F. I., Gualtieri, A. F., Norby, P., Hanson, J. C., and Corbin, D. R. (1997). Combined MAS NMR and X-ray Powder Diffraction Structural Characterization of Hydrofluorocarbon-134 Adsorbed on Zeolite Na-Y: Observation of Cation Migration and Strong Sorbate-Cation Interactions. **J. Amer. Chem. Soc.** 119: 1981-1989.

- Haines, P. J. (2002). **Principles of thermal analysis and calorimetry**. The Royal Society of Chemistry. UK. pp 166-168.
- Herreros, B. (2001). **The X-Ray Diffraction Zeolite Database**. [online]. Available : <http://suzy.unl.edu/bruno/zeodat.html>.
- Holmberg, B. A., Wang, H., and Yan, Y. (2004). High silicazeolite Y nanocrystals by dealumination and direct synthesis. **Micropor. Mesopor. Mater.** 74: 189-198.
- Jansen, J. C., Stöcker, M., Karge, H. G., and Weitkamp, J. (1994). **Studies in Surface Science and Catalysis, Vol. 85: Advanced Zeolite Science and Applications**. 85: 587-631.
- Kao, H. M. and Chen, Y. C. (2003). ^{27}Al and ^{19}F solid-state NMR studies of zeolite H- β dealuminated with ammonium hexafluorosilicate. **J. Phys. Chem. B.** 107: 3367-3375.
- Katada, N. *et al.* (2005). Standardization of catalyst: ion exchange of mordenite type zeolite 1. Remarkable dealumination accompanying ion exchange. **Appl. Catal. A: Gen.** 283: 63-74.
- Kerr, G. T. (1967). Intracrystalline rearrangement of constitutive water in hydrogen zeolite Y. **J. Phys. Chem.** 71: 4155.
- Larsen, E. M. and Vissers, D. R. (1960). The exchange of Li^+ , Na^+ and K^+ with H^+ on zirconium phosphate. **J. Phys. Chem.** 64: 1732.
- Lok, B.M. and Izod, T.P.J. (1982). **Zeolites**. 2: 66.
- Manahan, S. E. (1991). **Environmental Chemistry**. 5^{ed}. Lewis. USA. pp. 145-152.
- Meier, W. M. *et al.* (2001). **The Atlas of Zeolite Structure Types** [online]. Available : <http://www-iza-sc.csb.yale.edu/IZA-SC/Atlas/AtlasHome.html>.

- Ribeiro, F. R. *et al.* (1984). **Zeolites: Science and Technology**, Martinus Nijhoff Publishers: The Hague.
- Roland, E. and Kleinschmit, P. (1998). **Industrial inorganic chemical and products**. 6: 5169-5214.
- Shirinskaya, L. P., Ermolenko, N. F., and Nikolina, V. Y. (1971). **Dokl. Akad. Nauk BSSR**. 15: 35.
- Skeels, G. W. and Breck, D. W. (1983). **In proceedings of the sixth international zeolite conference** 19: 87.
- Szostak, R. (1998). **Molecular Sieves Principles of Synthesis and Identification**. New York: Van Nostrand Reinholds.
- Triantafillidis, C. S., Vlessidis, G., and Evmiridis, N. P. (2000). Dealuminated H-Y Zeolites: Influence of the Degree and the Type of Dealumination method on the Structural and Acidic Characteristics of H-Y Zeolites. **Ind. Eng. Chem. Res.** 39: 307-319.
- Vaughan, D. E. W. (1978). In Sand, L.B. and Mumpton, F.A. **Natural zeolite, Occurrence, properties, use**. New York: Pergamon.
- Weeks, T. J. and Bolton, A. P. (1975). Thermochemical Properties of Ammonium Exchanged Type L Zeolite. **J. Phys. Chem.** 79: 1924-1929.
- Zaika, X., Qingling, C., Chengfang, Z., Jiaqing, B., and Yuhua, C. (2000). Influence of citric acid treatment on the surface acid properties of zeolite beta. **J. Phys. Chem. B**. 104: 2853-2859.
- Zhang, W., Smirniotis, P. G., Gangoda, M., and Bose, R. N. (2000). Bronsted and Lewis acid sites in dealuminated ZSM-12 and β -zeolite characterized by NH_3 -

STPD, FT-IR, and MAS NMR spectroscopy. **J. Phys. Chem B.** 104: 4122-4129.

Zhdanov, S. P. and Novikov, B. G. (1966). **Dokl. Akad. Nauk SSSR.** 166: 1107.

APPENDICES

APPENDIX A

SIMULATED XRD POWDER PATTERNS FOR ZEOLTES

FAU

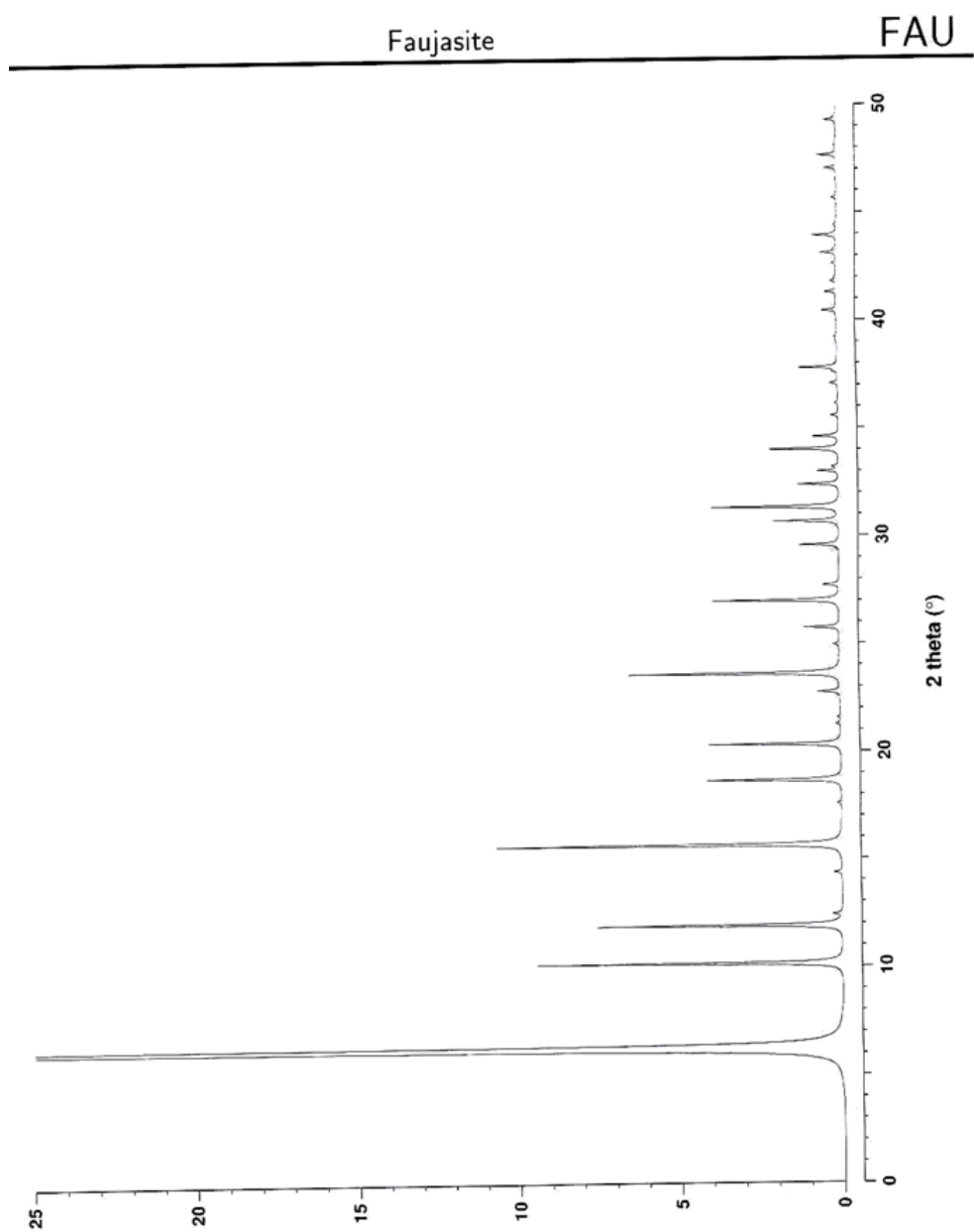
Faujasite

COMPOSITION: $(\text{Na}_{9.6}\text{Ca}_{4.8})(\text{Si}_{134.4}\text{Al}_{37.6}\text{O}_{384}) \cdot 263\text{H}_2\text{O}$
Kaiserstuhl, Germany.

CRYSTAL DATA: $Fd\bar{3}m$ (No. 227) origin at centre ($\bar{3}m$)
 $a = 24.74 \text{ \AA}$ $b = 24.74 \text{ \AA}$ $c = 24.74 \text{ \AA}$
 $\alpha = 90^\circ$ $\beta = 90^\circ$ $\gamma = 90^\circ$

REFERENCE: W. H. Baur,
Am. Miner. 49, 697-704 (1964).

<i>h</i>	<i>k</i>	<i>l</i>	2θ	<i>d</i>	<i>M</i>	I_{rel}	<i>h</i>	<i>k</i>	<i>l</i>	2θ	<i>d</i>	<i>M</i>	I_{rel}	<i>h</i>	<i>k</i>	<i>l</i>	2θ	<i>d</i>	<i>M</i>	I_{rel}
1	1	1	6.19	14.284	8	100.0	7	3	3	29.55	3.023	24	1.2	11	1	1	40.43	2.231	24	0.1
2	2	0	10.11	8.747	12	9.4	6	0	0	30.66	2.916	12	1.3	8	8	0	41.28	2.187	12	0.3
3	1	1	11.86	7.459	24	7.5	8	2	2	30.66	2.916	24	0.7	9	7	1	41.79	2.161	48	0.1
2	2	2	12.39	7.142	8	0.3	5	5	5	31.31	2.857	8	3.5	10	6	0	42.62	2.121	24	0.1
4	0	0	14.32	6.185	6	0.2	7	5	1	31.31	2.857	48	0.4	9	7	3	43.11	2.098	48	0.2
3	3	1	15.61	5.676	24	10.7	8	4	0	32.37	2.766	24	1.2	11	3	3	43.11	2.098	24	0.3
4	2	2	17.56	5.050	24	0.1	7	5	3	32.98	2.716	48	0.5	8	8	4	43.92	2.062	24	0.6
5	1	1	18.64	4.761	24	4.1	9	1	1	32.98	2.716	24	0.2	12	0	0	43.92	2.062	6	0.1
4	4	0	20.30	4.373	12	4.1	8	4	2	33.19	2.699	48	0.2	9	7	5	45.65	1.987	48	0.1
5	3	1	21.25	4.182	48	0.2	6	6	4	33.99	2.637	24	2.1	8	8	6	47.04	1.932	24	0.2
6	2	0	22.73	3.912	24	0.7	9	3	1	34.58	2.583	48	0.8	12	4	2	47.04	1.932	48	0.2
5	3	3	23.58	3.773	24	0.5	8	4	4	35.55	2.525	24	0.2	10	8	2	47.64	1.909	48	0.6
4	4	4	24.93	3.571	8	0.2	8	6	2	37.06	2.426	48	0.2	9	7	7	49.28	1.849	24	0.2
5	5	1	25.72	3.464	24	1.1	9	5	1	37.61	2.392	48	0.1	13	3	1	49.28	1.849	48	0.2
6	4	2	26.97	3.306	48	3.9	6	6	6	37.79	2.381	8	1.1							
7	3	1	27.70	3.221	48	0.4	7	7	5	40.43	2.231	24	0.3							

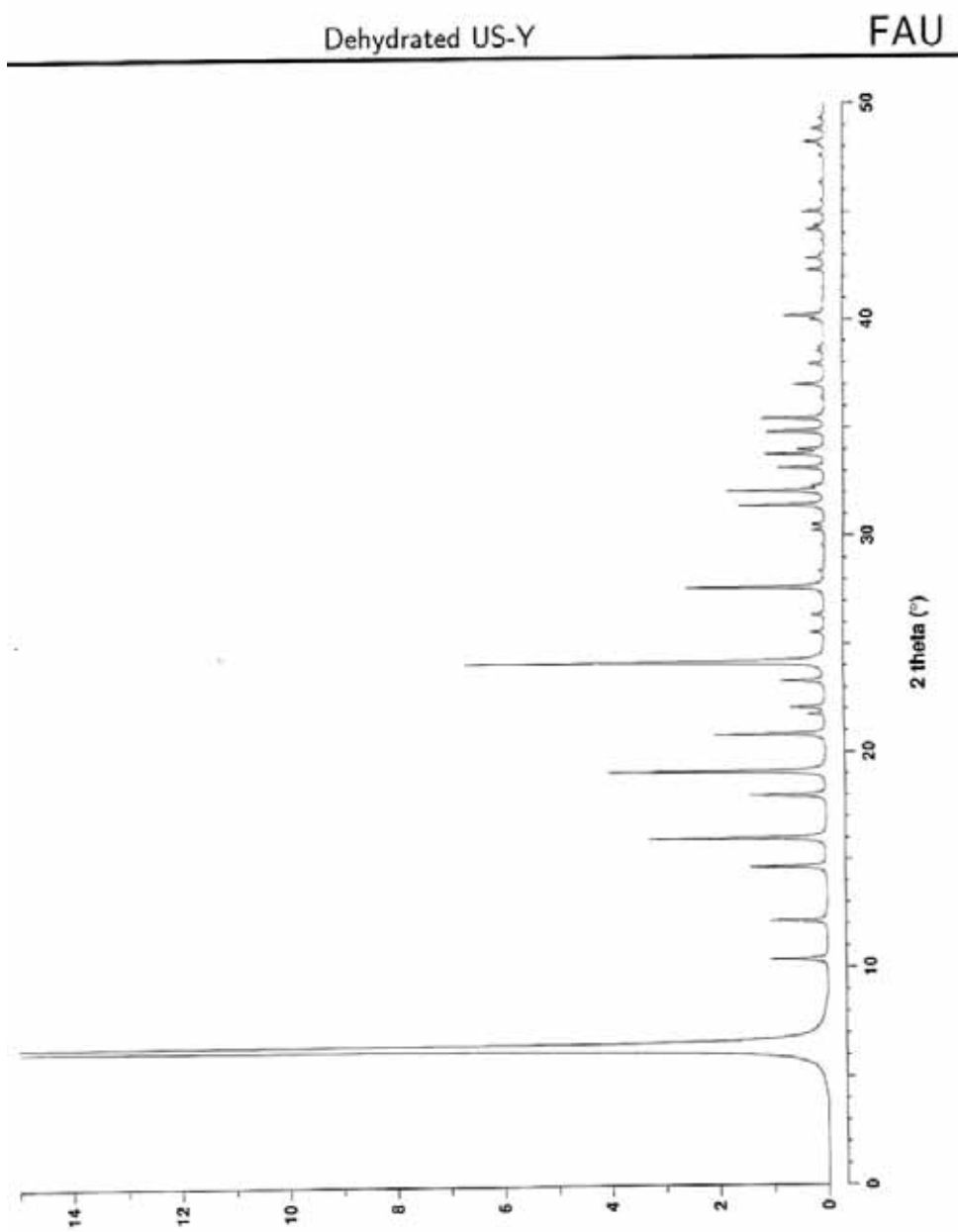


FAU

Dehydrated US-Y

COMPOSITION: $H_{18.9}(Si_{173.1}Al_{18.9}O_{384})$ CRYSTAL DATA: $Fd\bar{3}m$ (No. 227) origin at centre ($\bar{3}m$) $a = 24.171 \text{ \AA}$ $b = 24.171 \text{ \AA}$ $c = 24.171 \text{ \AA}$ $\alpha = 90^\circ$ $\beta = 90^\circ$ $\gamma = 90^\circ$ REFERENCE: J. B. Parise, D. R. Corbin, L. Abrams and D. E. Cox,
Acta Cryst. C40, 1493-1497 (1984).

h	k	l	2θ	d	M	I_{rel}	h	k	l	2θ	d	M	I_{rel}	h	k	l	2θ	d	M	I_{rel}	
1	1	1	6.33	13.955	8	100.0	5	5	1	26.33	3.385	24	0.2	9	3	1	35.43	2.534	48	1.2	
2	2	0	10.35	8.546	12	1.1	6	4	2	27.62	3.230	48	2.6	7	5	5	37.00	2.429	24	0.5	
3	1	1	12.14	7.288	24	1.1	7	3	3	30.27	2.953	24	0.2	10	2	0	37.96	2.370	24	0.2	
4	0	0	14.66	6.043	6	1.4	6	4	4	30.50	2.931	24	0.2	9	5	3	40.00	2.254	48	0.2	
3	3	1	15.98	5.545	24	3.3	6	6	0	31.40	2.849	12	0.9	8	6	4	40.18	2.244	48	0.7	
4	2	2	17.98	4.934	24	1.4	8	2	2	31.40	2.849	24	0.7	8	8	0	42.30	2.136	12	0.3	
3	3	3	19.08	4.652	8	0.2	5	5	5	32.07	2.791	8	1.2	9	5	5	42.82	2.112	24	0.1	
5	1	1	19.08	4.652	24	3.9	7	5	1	32.07	2.791	48	0.6	11	3	1	42.82	2.112	48	0.2	
4	4	0	20.79	4.273	12	2.1	6	6	2	32.29	2.773	24	0.2	9	7	3	44.17	2.050	48	0.3	
5	3	1	21.75	4.086	48	0.3	8	4	0	33.15	2.702	24	0.8	10	6	2	44.34	2.043	48	0.2	
4	4	2	22.06	4.029	24	0.6	7	5	3	33.78	2.653	48	0.9	8	8	4	45.00	2.014	24	0.4	
6	2	0	23.27	3.822	24	0.8	9	1	1	33.78	2.653	24	0.2	8	8	6	48.21	1.887	24	0.3	
5	3	3	24.14	3.686	24	6.7	8	4	2	33.99	2.637	48	0.5	10	8	2	48.84	1.865	48	0.2	
4	4	4	25.53	3.489	8	0.2	6	6	4	34.82	2.577	24	1.1								



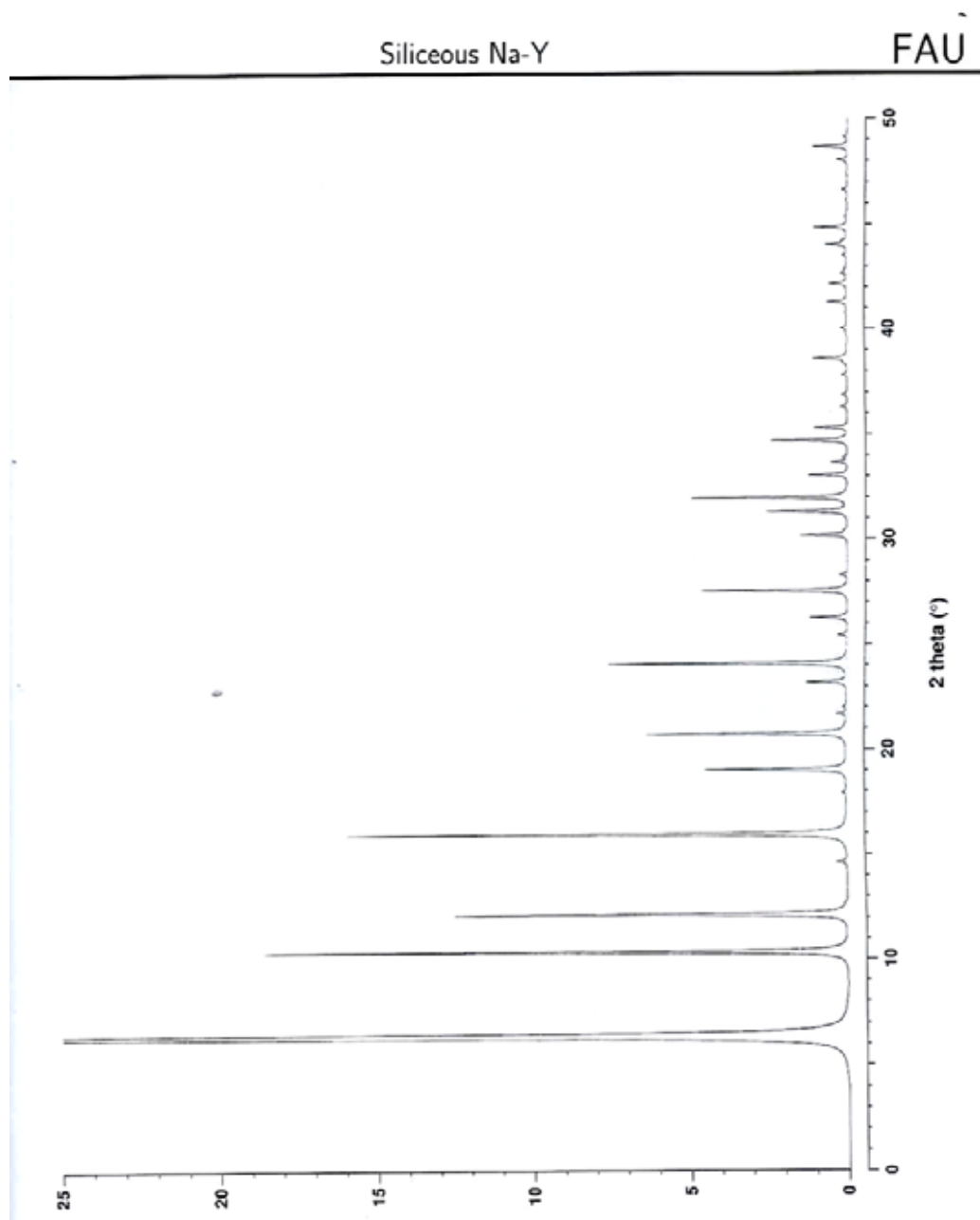
FAU

Siliceous Na-Y

COMPOSITION: $\text{Si}_{192}\text{O}_{384}$ CRYSTAL DATA: $Fd\bar{3}m$ (No. 227) origin at centre ($\bar{3}m$) $a = 24.703 \text{ \AA}$ $b = 24.703 \text{ \AA}$ $c = 24.703 \text{ \AA}$ $\alpha = 90^\circ$ $\beta = 90^\circ$ $\gamma = 90^\circ$

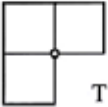
REFERENCE: J. J. Hriljac, M. M. Eddy, A. K. Cheetham, J. A. Donohue and G. J. Ray, J. Solid State Chem. 106, 66-72 (1993).

<i>h</i>	<i>k</i>	<i>l</i>	2θ	<i>d</i>	<i>M</i>	<i>I</i> _{rel}	<i>h</i>	<i>k</i>	<i>l</i>	2θ	<i>d</i>	<i>M</i>	<i>I</i> _{rel}	<i>h</i>	<i>k</i>	<i>l</i>	2θ	<i>d</i>	<i>M</i>	<i>I</i> _{rel}
1	1	1	6.31	14.005	8	100.0	7	3	1	28.26	3.158	48	0.2	8	6	4	40.03	2.252	48	0.2
2	2	0	10.31	8.576	12	18.6	7	3	3	30.16	2.964	24	1.5	7	7	5	41.28	2.187	24	0.2
3	1	1	12.10	7.314	24	12.5	6	6	0	31.29	2.859	12	1.9	11	1	1	41.28	2.187	24	0.4
4	0	0	14.61	6.064	6	0.3	8	2	2	31.29	2.859	24	0.7	8	8	0	42.14	2.144	12	0.6
3	3	1	15.93	5.565	24	16.0	5	5	5	31.95	2.801	8	4.4	9	7	1	42.66	2.119	48	0.1
4	2	2	17.91	4.952	24	0.1	7	5	1	31.95	2.801	48	0.5	10	6	0	43.51	2.080	24	0.1
3	3	3	19.01	4.668	8	0.2	8	4	0	33.03	2.712	24	1.2	9	7	3	44.01	2.057	48	0.1
5	1	1	19.01	4.668	24	4.3	7	5	3	33.66	2.663	48	0.5	11	3	3	44.01	2.057	24	0.5
4	4	0	20.71	4.288	12	6.4	8	4	2	33.87	2.647	48	0.1	10	6	2	44.18	2.050	48	0.2
5	3	1	21.67	4.100	48	0.3	6	6	4	34.69	2.586	24	2.4	8	8	4	44.84	2.022	24	0.7
4	4	2	21.98	4.043	24	0.1	9	3	1	35.29	2.543	48	1.0	12	0	0	44.84	2.022	6	0.3
6	2	0	23.19	3.836	24	1.3	8	4	4	36.28	2.476	24	0.3	9	7	5	46.61	1.948	48	0.1
5	3	3	24.06	3.699	24	7.6	7	5	5	36.87	2.438	24	0.2	8	8	6	48.03	1.894	24	0.2
4	4	4	25.44	3.501	8	0.3	8	6	2	37.82	2.379	48	0.2	12	4	2	48.03	1.894	48	0.1
5	5	1	26.24	3.397	24	1.2	9	5	1	38.38	2.345	48	0.1	10	8	2	48.65	1.872	48	1.1
6	4	2	27.52	3.242	48	4.6	6	6	6	38.57	2.334	8	1.1							



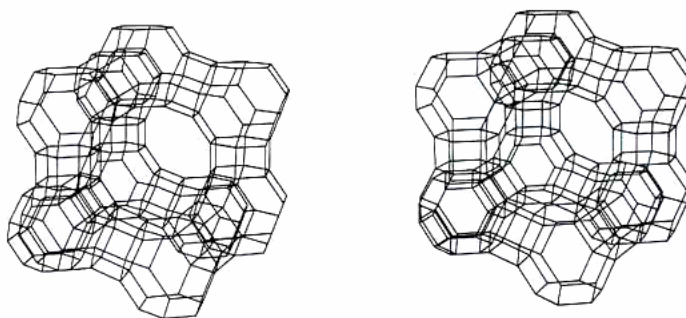
APPENDIX B

ATLAS OF ZEOLITE STRUCTURE TYPES

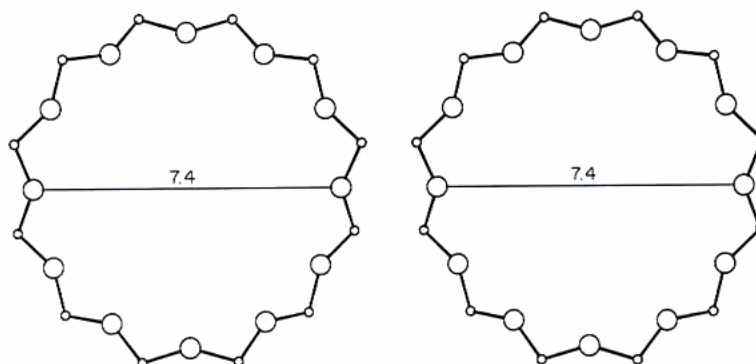
FAU	FAUJASITE	Fd $\bar{3}m$
Framework density:	12.7 T/1000 Å ³	
Loop configuration of T-atoms:		
Coordination sequences:	T(192) 4 9 16 25 37 53 73 96 120 145	
Channels:	<111> 12 7,4***	
Type material:	Faujasite (Na ₂ ,Ca,Mg) ₂₉ [Al ₅₈ Si ₁₃₄ O ₃₈₄] · 240 H ₂ O cubic, Fd $\bar{3}m$, a=24.7 Å ^(1,2)	
Isotypic framework structures:	Beryllophosphate X ⁽³⁾ CSZ-1 (EMT-FAU structural intermediate) ⁽⁴⁾ ECR-30 (EMT-FAU structural intermediate) ⁽⁵⁾ Linde X ^(6,7) Linde Y ^(8,9) LZ-210 ⁽¹⁰⁾ SAPO-37 ⁽¹¹⁾ Zincophosphate X ⁽³⁾ ZSM-20 (EMT-FAU structural intermediate) ⁽¹²⁾ ZSM-3 (EMT-FAU structural intermediate) ⁽¹³⁾ and numerous other compositional variants	

References:

- (1) G. Bergerhoff, W. H. Baur and W. Nowacki, N. Jb. Miner. Mh. **1958**, 193 (1958)
- (2) W. H. Baur, Am. Mineral. **49**, 697 (1964)
- (3) T. E. Gier and G. D. Stucky, Zeolites **12**, 770 (1992).
- (4) M. G. Barrett and D. E. W. Vaughan, UK Patent GB 2,076, 793 A (1981).



framework viewed along [111]



12-ring viewed along [111]

- (5) D. W. Breck, U.S. Patent 3,130,007 (1964).
- (6) M. L. Costenoble, W. J. Mortier and J. B. Uytterhoeven, *J.C.S. Faraday Trans. I*, **72**, 1877 (1976).
- (7) B. M. Lok, C. A. Messina, R. L. Patton, R. T. Gajek, T. R. Cannan and E. M. Flanigen, *J. Am. Chem. Soc.* **106**, 6092 (1984).
- (8) T. E. Gier and G. D. Stucky, *Nature* **349**, 508 (1991).
- (9) D. W. Breck and G. W. Skeels, US Patent 4,503,023 (1985).
- (10) D. E. W. Vaughan, E Patent, 0,351,461 (1989).
- (11) J. M. Newsam, M. M. J. Treacy, D. E. W. Vaughan, K. G. Strohmaier and W. J. Mortier, *J. Chem. Soc., Chem. Commun.* **1989**, 493 (1989).
- (12) G. T. Kokotailo and J. Ciric, *Advances in Chemistry Series*, **101**, 109 (1971).
- (13) M. G. Barrett and D. E. W. Vaughan, UK Patent GB 2,076, 793 A (1981).

APPENDIX C

ADSORPTION ISOTHERMS

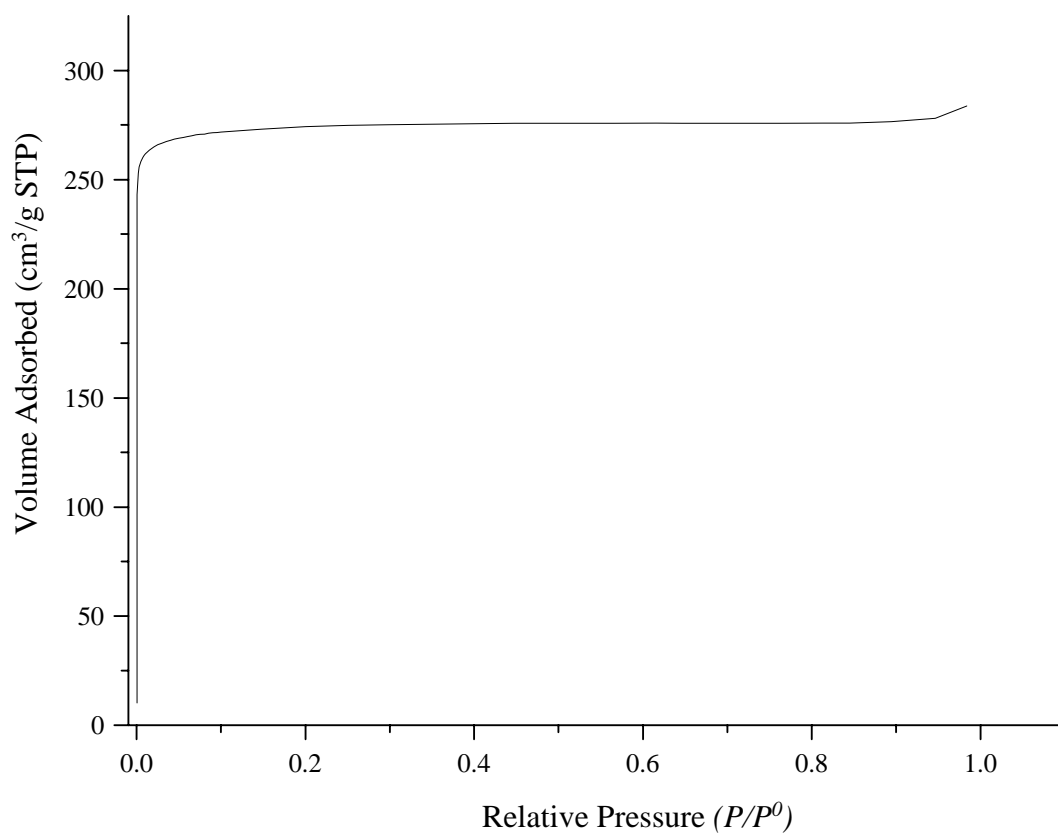


Figure A1 Nitrogen adsorption isotherms of synthesized zeolite NaY.

BET Surface Area: 915.5828 m²/g

Micropore Volume: 0.401419 cm³/g

Average Pore Diameter (4V/A by BET): 19.1737 Å

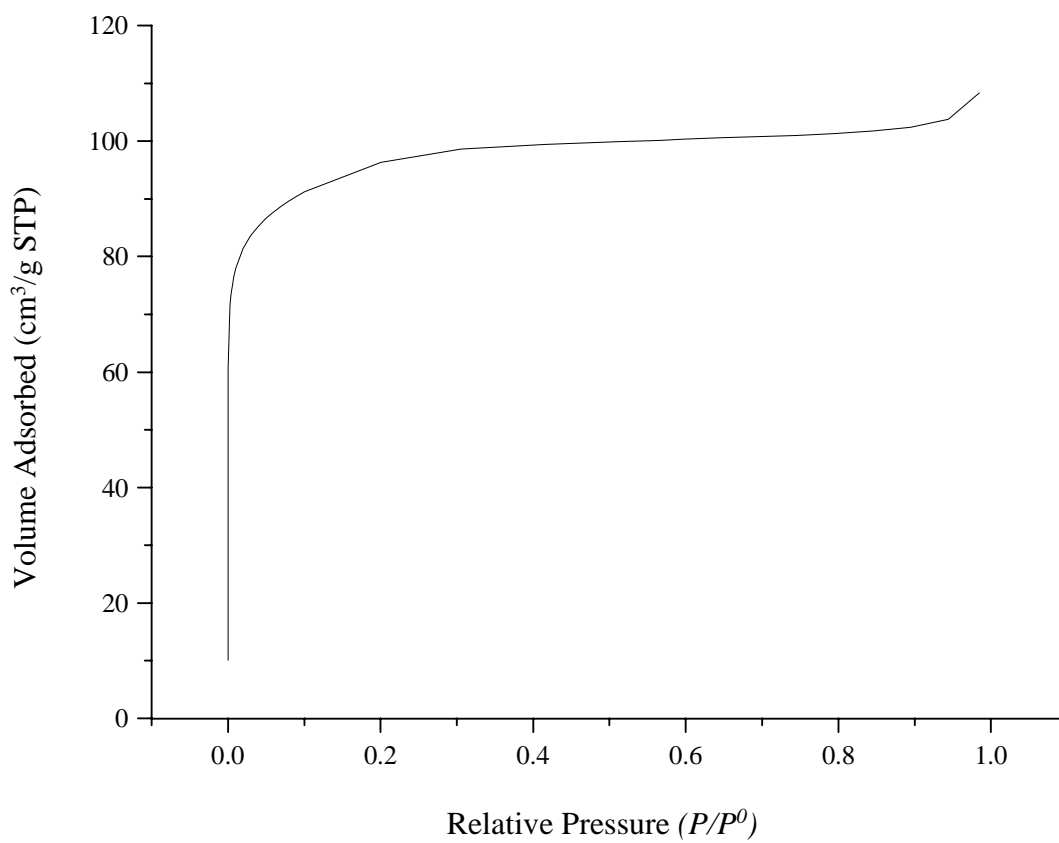


Figure A2 Nitrogen adsorption isotherms of dealuminated zeolite NaY by HCl method (HCl15).

BET Surface Area: 314.5624 m^2/g

Micropore Volume: 0.09125 cm^3/g

Average Pore Diameter (4V/A by BET): 15.3148 \AA

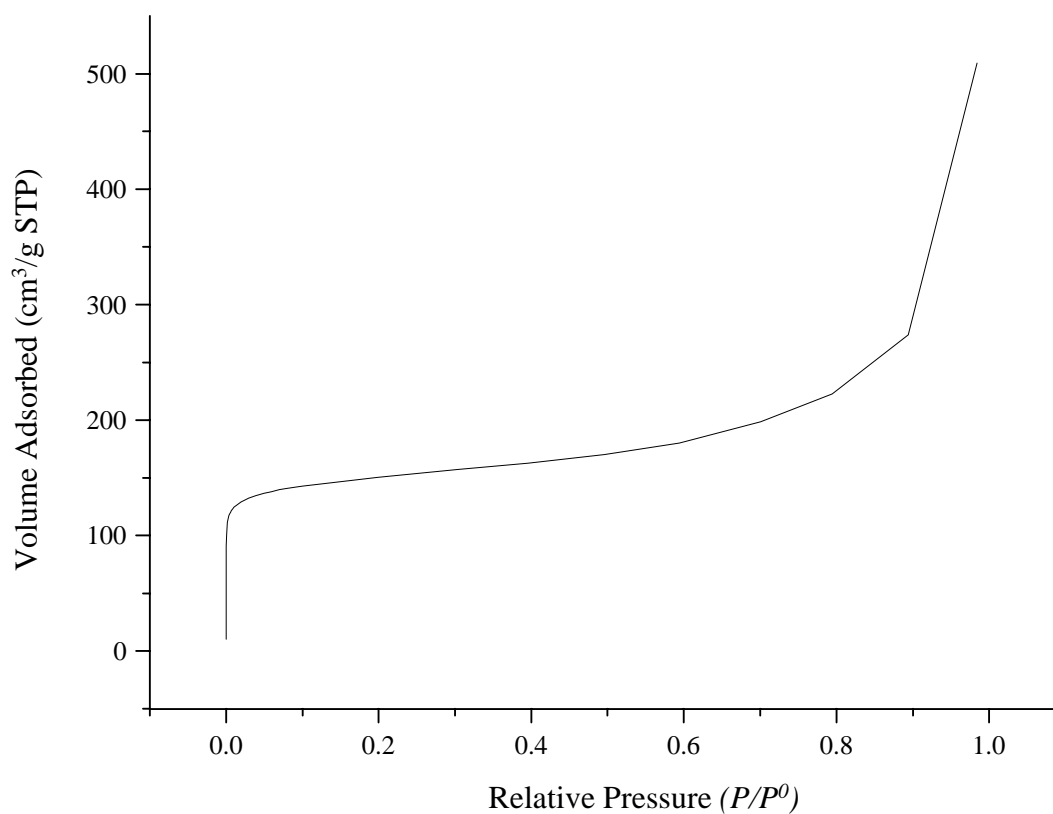


Figure A3 Nitrogen adsorption isotherms of dealuminated zeolite NaY by AHFS method (NaY1D).

BET Surface Area: 499.4007 m^2/g

Micropore Volume: 0.155921 cm^3/g

Average Pore Diameter (4V/A by BET): 63.0872 \AA

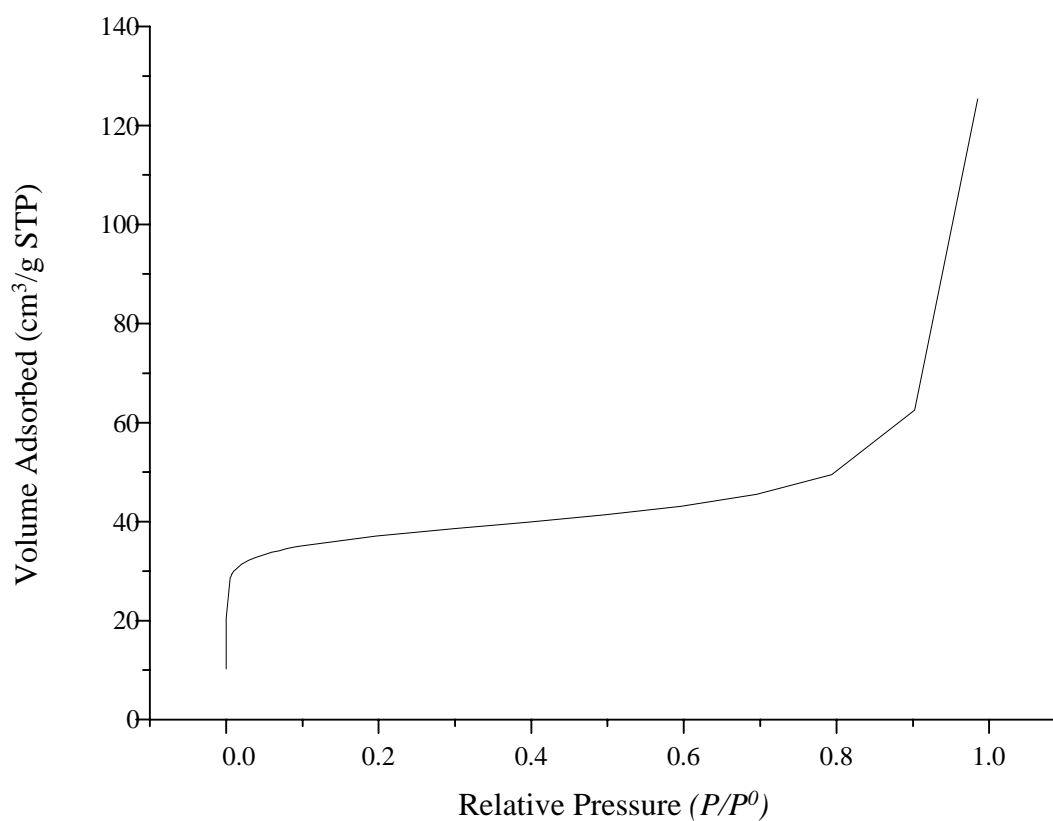


Figure A4 Nitrogen adsorption isotherms of dealuminated zeolite KY by AHFS method (KY1D).

BET Surface Area:	122.0681 m ² /g
Micropore Volume:	0.036865 cm ³ /g
Average Pore Diameter (4V/A by BET):	63.5459 Å

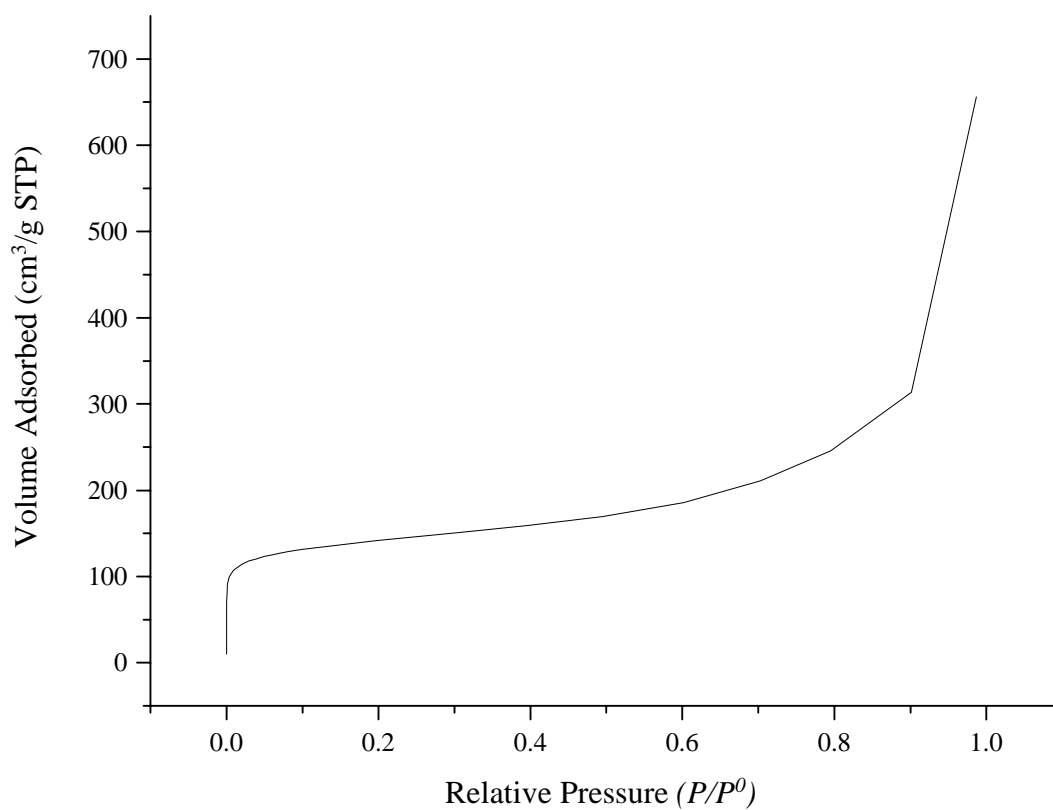


Figure A5 Nitrogen adsorption isotherms of dealuminated zeolite LiY by AHFS method (LiY1D).

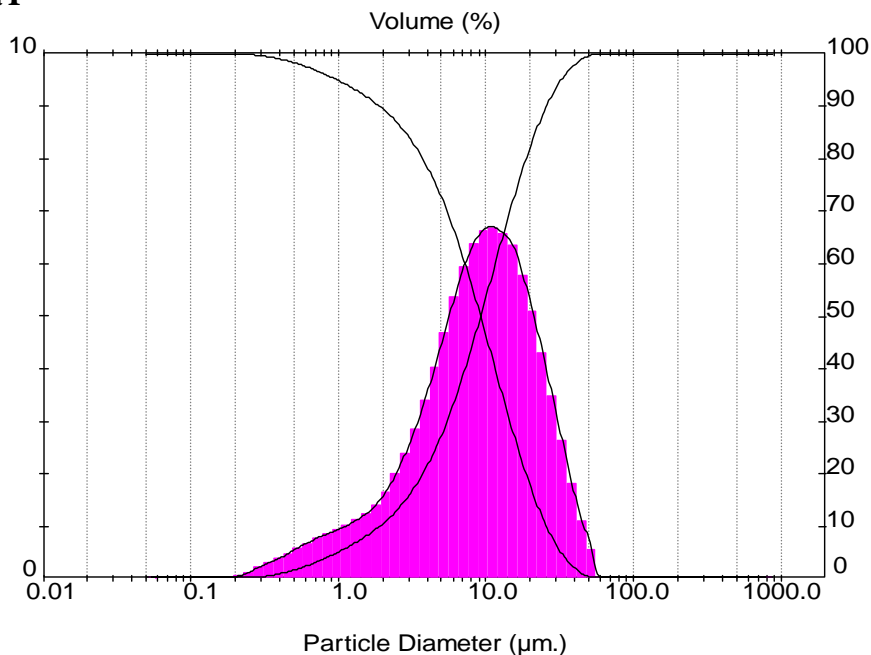
BET Surface Area: 472.8449 m^2/g

Micropore Volume: 0.115960 cm^3/g

Average Pore Diameter (4V/A by BET): 85.868 \AA

APPENDIX D
PARTICLE SIZE ANALYSIS

Zeolite NaY



Result: Histogram Table

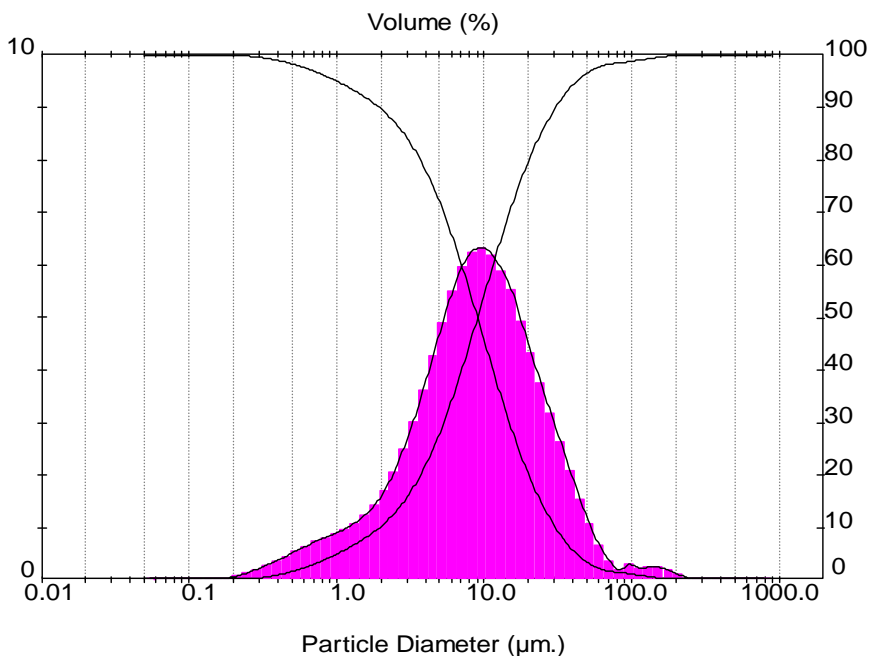
ID: zy001	Run No: 3	Measured: 25/8/105 9:56PM
File: CHUTIMA	Rec. No: 3	Analysed: 25/8/105 9:56PM
Path: C:\SIZERS\DATA\		Source: Analysed

Range: 300RF mm	Beam: 2.40 mm	Sampler: MS17	Obs': 10.9 %
Presentation: 3OHD	Analysis: Poly disperse		Residual: 0.411 %
Modifications: None			

Conc. = 0.0074 %Vol	Density = 1.000 g/cm ³	S.S.A.= 1.5045 m ² /g
Distribution: Volume	D[4, 3] = 11.92 µm	D[3, 2] = 3.99 µm
D(v, 0.1) = 1.90 µm	D(v, 0.5) = 9.20 µm	D(v, 0.9) = 25.80 µm
Span = 2.597E+00	Uniformity = 7.964E-01	

Size (µm)	Volume Under %						
0.055	0.00	0.635	2.67	7.31	40.44	84.15	100.00
0.061	0.00	0.700	3.14	8.06	44.39	92.79	100.00
0.067	0.00	0.772	3.65	8.89	48.50	102.3	100.00
0.074	0.00	0.851	4.18	9.80	52.72	112.8	100.00
0.082	0.00	0.938	4.74	10.81	56.99	124.4	100.00
0.090	0.00	1.03	5.34	11.91	61.27	137.2	100.00
0.099	0.00	1.14	5.97	13.14	65.50	151.3	100.00
0.109	0.00	1.26	6.64	14.49	69.67	166.8	100.00
0.121	0.00	1.39	7.36	15.97	73.75	183.9	100.00
0.133	0.00	1.53	8.12	17.62	77.62	202.8	100.00
0.147	0.01	1.69	8.94	19.42	81.22	223.6	100.00
0.162	0.02	1.86	9.82	21.42	84.55	246.6	100.00
0.178	0.03	2.05	10.80	23.62	87.56	271.9	100.00
0.196	0.05	2.26	11.89	26.04	90.25	299.8	100.00
0.217	0.09	2.49	13.11	28.72	92.59	330.6	100.00
0.239	0.14	2.75	14.49	31.66	94.58	364.6	100.00
0.263	0.23	3.03	16.04	34.92	96.23	402.0	100.00
0.290	0.35	3.34	17.77	38.50	97.55	443.3	100.00
0.320	0.51	3.69	19.71	42.45	98.54	488.8	100.00
0.353	0.71	4.07	21.89	46.81	99.26	539.0	100.00
0.389	0.94	4.48	24.31	51.62	99.78	594.3	100.00
0.429	1.20	4.94	26.99	56.92	100.00	655.4	100.00
0.473	1.50	5.45	29.95	62.76	100.00	722.7	100.00
0.522	1.85	6.01	33.19	69.21	100.00	796.9	100.00
0.576	2.25	6.63	36.70	76.32	100.00	878.7	100.00

Dealuminated zeolite NaY with HCl method



Result: Histogram Table

ID: cal500	Run No: 21	Measured: 25/8/105 11:26PM
File: CHUTIMA	Rec. No: 21	Analysed: 25/8/105 11:26PM
Path: C:\SIZERS\DATA\		Source: Analysed

Range: 300RF mm	Beam: 2.40 mm	Sampler: MS17	Obs': 11.5 %
Presentation: 3OHD	Analysis: Poly disperse		Residual: 0.503 %
Modifications: None			

Conc. = 0.0079 %Vol	Density = 1.000 g/cm ³	S.S.A.= 1.5053 m ² /g
Distribution: Volume	D[4, 3] = 14.54 µm	D[3, 2] = 3.99 µm
D(v, 0.1) = 1.94 µm	D(v, 0.5) = 9.02 µm	D(v, 0.9) = 30.52 µm
Span = 3.167E+00	Unif ormity = 1.112E+00	

Size (µm)	Volume Under %						
0.055	0.00	0.635	2.64	7.31	41.44	84.15	98.50
0.061	0.00	0.700	3.08	8.06	45.36	92.79	98.65
0.067	0.00	0.772	3.56	8.89	49.38	102.3	98.86
0.074	0.00	0.851	4.07	9.80	53.42	112.8	99.02
0.082	0.00	0.938	4.61	10.81	57.45	124.4	99.17
0.090	0.00	1.03	5.18	11.91	61.41	137.2	99.34
0.099	0.00	1.14	5.79	13.14	65.25	151.3	99.50
0.109	0.00	1.26	6.44	14.49	68.97	166.8	99.65
0.121	0.01	1.39	7.13	15.97	72.53	183.9	99.78
0.133	0.01	1.53	7.88	17.62	75.85	202.8	99.87
0.147	0.02	1.69	8.69	19.42	78.92	223.6	99.94
0.162	0.03	1.86	9.58	21.42	81.74	246.6	99.98
0.178	0.06	2.05	10.57	23.62	84.33	271.9	99.99
0.196	0.09	2.26	11.68	26.04	86.67	299.8	100.00
0.217	0.14	2.49	12.94	28.72	88.79	330.6	100.00
0.239	0.20	2.75	14.38	31.66	90.69	364.6	100.00
0.263	0.30	3.03	16.00	34.92	92.35	402.0	100.00
0.290	0.43	3.34	17.83	38.50	93.79	443.3	100.00
0.320	0.58	3.69	19.89	42.45	95.01	488.8	100.00
0.353	0.77	4.07	22.20	46.81	96.00	539.0	100.00
0.389	0.99	4.48	24.77	51.62	96.80	594.3	100.00
0.429	1.24	4.94	27.61	56.92	97.41	655.4	100.00
0.473	1.53	5.45	30.72	62.76	97.85	722.7	100.00
0.522	1.86	6.01	34.08	69.21	98.17	796.9	100.00
0.576	2.23	6.63	37.67	76.32	98.38	878.7	100.00

CURRICULUM VITAE

NAME: Miss Chutima Thongkasam

DATE OF BIRTH: October 08, 1976

PLACE OF BIRTH: Nakhon Ratchasima, Thailand

CITIZENSHIP: Thailand

EDUCATIONAL BACKGROUND:

1999 Bachelor of Science (Chemistry), B.Sc. (Chemistry)

Kasetsart University, Bangkok, Thailand

WORK EXPERIENCE:

2000-2003 Technician, Center of Scientific, Nakhon Ratchasima Rajabhat
University, Nakhon Ratchasima, Thailand

2003 Teaching Assistance, School of Chemistry, Institute of Science,
Suranaree University of Technology, Nakhon Ratchasima.

PRESENTATION:

- 2006
1. Oral presentation "The Comparison of Dealumination Method of zeolite Y" The 13th Tri-University International Joint Seminar & Symposium 2006 October 29th to November 2nd 2006, Mie University, Japan
 2. Poster presentation "Dealumination zeolite Y by HCl method" The 32nd Congress on Science and Technology of Thailand (STT32.) October 10-12, 2006 Venus : Queen Sirikit National Convention Center (QSNCC), Thailand